

A Facsimile Report

Reproduced by

**United States
Department of Energy**
Office of Scientific and Technical Information

LOS ALAMOS NATIONAL LABORATORY
3 9338 00347 7618

Post Office Box 62 Oak Ridge, Tennessee 37831



Please return to CIC-14 Report
Collection when no longer
needed.

UNCLASSIFIED

-1-

AECD-3840

Subject Category: PHYSICS AND MATHEMATICS

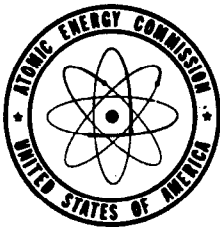
UNITED STATES ATOMIC ENERGY COMMISSION

**TRANSIENT AND STEADY STATE
CHARACTERISTICS OF A BOILING REACTOR.
THE BORAX EXPERIMENTS, 1953**

By
J. R. Dietrich
D. C. Layman

February 1954

**Argonne National Laboratory
Lemont, Illinois**



Technical Information Service, Oak Ridge, Tennessee

UNCLASSIFIED

2

Date Declassified: December 9, 1955.

This report was prepared as a scientific account of Government-sponsored work. Neither the United States, nor the Commission, nor any person acting on behalf of the Commission makes any warranty or representation, express or implied, with respect to the accuracy, completeness, or usefulness of the information contained in this report, or that the use of any information, apparatus, method, or process disclosed in this report may not infringe privately owned rights. The Commission assumes no liability with respect to the use of, or from damages resulting from the use of, any information, apparatus, method, or process disclosed in this report.

This report has been reproduced directly from the best available copy.

Issuance of this document does not constitute authority for declassification of classified material of the same or similar content and title by the same authors.

Since nontechnical and nonessential prefatory material has been deleted, the first page of the report is page 7.

Printed in USA, Price 65 cents. Available from the Office of Technical Services, Department of Commerce, Washington 25, D. C.

ARGONNE NATIONAL LABORATORY
P. O. Box 299
Lemont, Illinois

TRANSIENT AND STEADY STATE CHARACTERISTICS
OF A BOILING REACTOR

The Borax Experiments, 1953

Experiments by W. H. Zinn, D. C. Layman,
H. V. Lichtenberger, S. Untermyer,
J. R. Dietrich, W. C. Lipinski,
R. E. Cote,* and C. C. Bigelow*

Reported by
J. R. Dietrich and D. C. Layman

Acknowledgement

From time to time, the Borax Experiment received valuable assistance from the following individuals whose efforts are hereby gratefully acknowledged: N. L. Krisberg, Reactor Development Division, AEC Washington, M. Novick, B. C. Cerutti, R. A. Cameron, R. O. Haroldsen, G. H. Stonehocker of the EBR Staff, and also T. Brill, W. C. Redman, J. A. DeShong, A. J. Ulrich, J. R. Schiltz in the design and preparation of instruments, and O. A. Schulze in the analysis of results.

*Loaned Employees from Pratt & Whitney Aircraft

February 1954

Operated by The University of Chicago
under
Contract W-31-109-eng-38

TABLE OF CONTENTS

	Page
ABSTRACT	11
I. INTRODUCTION	12
II. REACTOR AND ASSOCIATED EQUIPMENT	14
A. Reactor	14
B. Control Drive Mechanism	16
C. Shielding	17
D. Reactor Controls and Operating Instrumentation	17
1. Control Rod Drives and Reactor Shutdown	17
2. Water Controls	18
3. Pressure Control	19
4. Nuclear Instrumentation	19
5. Miscellaneous	20
III. NUCLEAR CHARACTERISTICS OF THE REACTOR	21
A. Criticality	21
B. Power Distribution	21
C. Control Rod Calibrations and Neutron Lifetime	22
D. Temperature and Density Coefficient	23
IV. EXPERIMENTS ON SELF LIMITATION OF POWER EXCURSIONS	24
A. Method and Special Instrumentation	24
B. General Characteristics of Power Excursions	26
C. Subcooled Excursions and Power Calibration	28
D. Effect of Initial Period, or Excess Reactivity, on Power Excursion	30
E. Pressure Generated During Excursions	32
F. Photographs of Excursions	34
G. Discussion of Results of Excursions	34
V. STEADY BOILING AT ATMOSPHERIC PRESSURE	38

TABLE OF CONTENTS

	Page
VI. STEADY BOILING AT ELEVATED PRESSURE	40
A. General Characteristics	40
B. Records of Pressurized Boiling Runs.	41
C. Rapid Fluctuations of Reactor Period.	43
D. Operation with Fixed Orifice	44
E. Operation in Closed Vessel	44
F. Discussion of Boiling Operation	44
VII. SUMMARY OF RESULTS	46
REFERENCES	48
APPENDICES	49
APPENDIX A Detailed Composition and Calculated Nuclear Constant of Borax Reactor.	49
APPENDIX B Transient Instrumentation.	53
APPENDIX C Power Calibration of Ion Chambers	56
APPENDIX D Measurement of Steam Flow through an Orifice at Critical Pressure	65
FIGURES	67

TRANSIENT AND STEADY STATE CHARACTERISTICS OF A BOILING REACTOR

The Borax Experiment, 1953

ABSTRACT

The characteristics of transient and steady state boiling in a water-cooled, water-moderated reactor have been investigated in a reactor which was set up and operated at the Reactor Testing Station during the Summer and Fall of 1953.

In a series of about 70 intentional "runaway" type tests it was demonstrated that the formation of steam and consequent ejection of water from the reactor core can provide inherent protection against the runaway hazard in suitably designed reactors of the water-cooled, water-moderated (H_2O or D_2O) type. Power excursions of periods as short as 0.005 second (2.1% excess reactivity in the experimental reactor) were terminated by this process. Although the maximum power in the excursions went as high as 2600 megawatts, fuel plate temperature never exceeded 640F. Maximum power, total energy liberation, and fuel plate temperatures were investigated at atmospheric pressure as functions of excess reactivity in the excursion and initial reactor temperature.

Operation of the reactor in steady boiling at pressures up to 130 psig and powers up to 1200 kw demonstrated that quite smooth operation is attainable up to the point where the steam content of the reactor represents about -2% k_{eff} in reactivity. At higher steam contents characteristic power fluctuations were observed. The reactor steam power was shown to be self-regulating. The effects of various operating conditions and system variables on reactor power and operating characteristics were investigated.

Results of the investigation are believed to point the way toward more economical power reactors through minimization of the hazard problem, simplification of reactor design, and reduction of the temperature demands on reactor materials.

I. INTRODUCTION

At the present stage of reactor development the technical feasibility of reactors for power production as well as for materials production has been demonstrated. The development of economically competitive power reactors remains, however, to be achieved, and only as that development is achieved will the major potentialities of nuclear energy be realized. Economic feasibility involves both operating costs and initial cost of the reactor, its site, and associated equipment. An important fraction of both costs in conventional reactor designs stems from the hazards, both proven and hypothetical, of the reactors. These hazards affect the initial cost if they necessitate large exclusion areas, remote locations, specialized building designs, or excessively large safety factors. They affect operating cost if they lead to high insurance rates, involved safety procedures, or inconvenient reactor locations.

Utilization of the boiling process gives promise of leading to designs for water-cooled, water-moderated reactors (either H_2O or D_2O) which make important reductions in both initial and operating costs by simplifying reactor design and minimizing or eliminating the hazard problem. The same principles, when applied to production reactors, should lead to economic improvement, and when applied to research reactors, to wider usefulness.

Utilization of the boiling process in water-moderated reactors depends upon the fact that such reactors can be designed to have a negative steam coefficient of reactivity; i.e., the formation of steam and consequent displacement of water from the reactor causes a net decrease in reactivity as a result of increased neutron leakage and, in reactors containing U^{238} , increased resonance absorption. The achievement of this negative coefficient does not usually impose important design limitations. All practical designs which are both cooled and moderated by D_2O will automatically have negative coefficients. All small reactors which are both cooled and moderated by H_2O will have a negative coefficient, and it is not difficult to attain a negative coefficient in larger reactors by appropriate adjustment of the lattice constants. In fact, it is possible to attain almost any desired magnitude of the coefficient in H_2O reactors by adjustment of the buckling and the lattice constants. A negative steam coefficient can be achieved in H_2O -cooled reactors which employ other materials as the principal moderator, but only through rather specialized design; the reactors of this type which have been built to date have positive coefficients.

The reactivity decrease caused by steam formation in reactors with negative coefficients constitutes an inherent, ever present power-limiting mechanism which, by suitable reactor design, can be utilized to eliminate the hazard of reactor runaway provided it can be shown that steam formation occurs fast enough to limit reactor power to safe values in the fastest power transients which may be imposed on the reactor.

Further, the negative steam coefficient represents a regulating tendency which could make possible the stable operation of a reactor in steady boiling in spite of the manifest irregularities of the boiling process. The extent to which boiling operation can be utilized depends upon the degree of boiling which can be employed without exceeding the tolerable limits of power fluctuation. The applications range from the employment of surface boiling in reactors of conventional design for improvement of heat transfer rates, to the design of boiler reactors which generate useable steam directly. A reactor of the latter type, if stable at all, would be self-regulating. It would make possible a power reactor system which approached the ultimate in simplicity, consisting, in essence, simply of a reactor and shield, a turbine, a condenser, and a feed pump. The steam would, furthermore, be delivered to the turbine at full reactor pressure, and the temperatures imposed on reactor materials for a given steam pressure would be at the absolute possible minimum.

The possibility of boiling reactors has been a subject of speculation from time to time since the early days of reactor development (ref. 1), and, more recently, the LITR has been operated for short periods in subcooled boiling (ref. 2, 3). The self-limiting tendency of reactors with negative steam coefficients of reactivity has also been widely recognized and has been the subject of laboratory investigations (ref. 4).

In 1952, at the instigation of S. Untermyer, serious plans were first made for determining, in an experimental reactor, the self-limiting characteristics of water-cooled reactors and the operating characteristics of boiling reactors (ref. 5). The reactor was set up at the Argonne site at the Reactor Testing Station in Idaho in the early Summer of 1953. Through the remainder of the Summer and early Fall, the reactor was put through a series of intentional "runaway" excursions and periods of steady boiling operation, the latter covering operating pressures up to 130 psig. Quite evidently it was not possible to determine all the characteristics of boiling in such a short time. Conclusive proof was, however, obtained that steam formation is a most effective, reliable, and rapid power-limiting process, capable of protecting properly designed reactors against reactivity excursions which produce reactor periods shorter than 5 milliseconds. Steady boiling operation demonstrated that some of the applications of boiling operation are certainly feasible, and that the prospect for a true boiler reactor is promising. The detailed results of the experiments are described in the following Sections of this report. The group of experiments has been given the code name Borax, and the experimental reactor used has generally been referred to as the Borax reactor.

Simultaneously with the planning and execution of the Borax program, similar questions relating to boiling and self-regulation in homogeneous reactors have been under investigation by Oak Ridge National Laboratory (ref. 6). Reference 7 describes a recent proposal for a low power boiling reactor plant by the Bendix Aviation Corporation.

II. REACTOR AND ASSOCIATED EQUIPMENT

The reactor was located at the Argonne site at the National Reactor Testing Station, Arco, Idaho. The reactor proper was located 2730 feet northwest of the Experimental Breeder Reactor entrance. It was controlled from a trailer placed just outside the EBR entrance; during reactor operation an exclusion radius of one-half mile was maintained around the reactor. This system of remote operation made possible experiments of the "runaway" type without hazard to personnel and, by minimizing shielding requirements, resulted in low construction cost and easy access to the reactor for instrumentation and experimental changes.

Since the reactor was not housed, the program was conducted during the summer months only. Instrumentation and controls were located in three trailers pre-assembled at Argonne during early 1953 and hauled to the Reactor Testing Station Site. Figures 1 and 2 show the physical plant.

A short description of the various components follows.

A. Reactor

Figure 3 is a vertical section of the reactor installation, showing the relative locations of the reactor, the control drive mechanism, and the shielding arrangements. A cut-away view of the reactor installation is shown in Figure 75.

The reactor tank was made of carbon steel, plastic lined for corrosion resistance, and contained 120 cu ft water at operating level. When operating at atmospheric pressure, an open top section was used which, in conjunction with a control rod drive locating spider, permitted visual inspection of the core after runs and photographic records of the water surface during runs. When pressurized runs were in progress the open top section was replaced with a spool piece and a blind flange. The control rod drive mechanism pierced the top flange through packing glands. System pressure could be controlled either manually or automatically through conventional but rapid response pressure control instrumentation. The system design pressure was 125 psig, and runs up to 138 psig were made. Figure 4 shows the reactor in vertical section; Figures 5 and 6, respectively, show the open and closed (pressurized) reactor top details. In Figure 6 the control extension rods have been disconnected from the control rod drive mechanism.

The core was built up from a lower grid into which 36 fuel assemblies or dummy plugs were placed. This could provide about 7% clean cold excess reactivity. Criticality was reached with 26 fuel assemblies. Dummy plugs were used to fill out the core grid to permit relatively constant geometry for water flow considerations. The plugs were the same

length as the fuel assemblies, but were made up of short aluminum end pieces connected by a length of thin-walled aluminum tubing. The end pieces were identical in shape and dimensions with the corresponding sections of the fuel assemblies. The plugs thus filled out the vacant core spaces at top and bottom, but left an almost pure water reflector adjacent to the active core over most of its length. Fuel assemblies were located at their upper ends by a spider and clamping arrangements, Figure 7.

The fuel assemblies were made of curved fuel plates containing a U^{235} -aluminum alloy core, clad with aluminum. Each assembly contained 18 fuel plates brazed into aluminum side plates to form units roughly three inches square (Figure 8). The length of the fueled portion of the fuel plates was two feet.¹ Appendix A gives details of the fuel assembly composition.

A special removable fuel plate subassembly contained plates to which thermocouples were affixed (Figure 9). These thermocouples recorded surface and center temperatures during transient operation. The removable fuel plates were identical with the standard ones except for lack of curvature.

The core was divided into quadrants (Figure 7), and control rods were located in the openings so obtained. An outer group of four blades (shim rods) was moved as a gang, while the central rod was moved independently. The four blades were raised to increase reactivity and could be shot rapidly downward by springs for reactor shutdown. The central rod was moved downward to increase reactivity and could be spring ejected downward for rapid reactivity increases during the investigation of transient phenomena.

Each of the four blades (shim rods) was about 7 inches wide and consisted of a cadmium insert, nickel-plated for corrosion resistance, in an aluminum supporting structure. These absorbing blades were rigidly attached to extension pieces which extended upwards through the dashpot spider and terminated in magnetic armatures. The armatures also served as dashpot plates and engaged dashpots to absorb the impact energy when the rods were scrambled. Figure 5 shows the magnet assemblies and related details.

The central control rod was a flat blade of aluminum containing cadmium inserts in the form of 30-mil strips of adjustable width.

The rod was slightly longer than twice the core length, and contained the cadmium inserts only in the lower half. Cadmium was inserted in the core, therefore, when the rod was in the fully raised position, and was removed when the rod was ejected downward. Since the amount of cadmium in the central rod was adjustable, a wide range of reactivity changes was permissible.

¹The fuel assemblies were actually MTR assemblies of the original "unsweetened" (130 grams U^{235} per assembly) type, with the inlet and outlet ends modified to adapt them to Borax requirements.

An antimony-beryllium neutron source was built into the connecting tube of one of the dummy plugs, at mid-core level. It remained in the reactor throughout operation.

Water flow under natural convection during boiling runs was vertically upward through the reactor core, returning downward through the reflector. During severe transients water was, no doubt, expelled both upwards and downwards from the core.

The reactor could be electrically pre-heated to the desired operating temperature by an external heating system consisting of a circulating pump and immersion heaters. Another pump was used to transfer water between the deionized water storage tank and the reactor. A third pumping system was used to fill and empty the shielding tank. These details are shown in Figures 10 and 11.

B. Control Drive Mechanism

The control rods were moved and positioned by an external drive mechanism (Figures 12, 13 and 14) with magnetic attachment to armatures on the control rod extensions. Magnet assemblies (Figure 5) were attached to hollow shafts through which the magnet power lines were carried, and these shafts were directly coupled to the drive mechanism proper. Since the drive mechanism pierced the pressure vessel head through packing glands when the reactor was pressurized, it was necessary to effect magnetic disengagement inside the reactor tank. Spring loaded ejection plates were incorporated in the magnet assemblies to increase rod velocity during scrams or the initiation of transients.

The four blade (shim) rods were ganged to a common ball nut and lead screw drive. This was driven by a conventional gear-motor and speed reducer. The central rod was positioned by a rack and pinion drive, also driven by a conventional gear-motor and speed reducer. Since it was necessary to provide sufficient force on the descending magnets to compress the ejection springs and promote metal-to-metal contact between the magnets and control rod armatures for engagement, it was desirable to limit the torque by stalling the motors. Voltage control was therefore used to reduce the locked rotor torque to the desired value. Since a failure of the magnetic engagement of the central control rod to its drive would instigate a reactor transient, a mechanical safety latch was built into the system which required manual setting, control-air pressure, and instrument power for release. By this method unplanned transients were avoided. A magnetic clutch was placed in the central control rod driving system, and the control rod externally counter-weighted. De-energizing this clutch allowed the rod to be rapidly returned to its full upward (black) position and was of value in rod calibrations, as well as serving as a secondary rapid shutdown device.

C. Shielding

As has been pointed out, all personnel were removed from the reactor area during operations, and the reactor was remotely controlled. The shielding requirements, therefore, were based upon long-lived decay radioactivity. Since the duration of individual runs was of the order of an hour, the buildup of fission products was not excessive, and shielding requirements were satisfied by the use of sand and/or water.

The reactor was placed in a shield tank twenty feet deep, sitting on a concrete slab ten feet below ground level. Sand and gravel were piled up around the shield tank at about a 45° angle. The reactor core was located approximately three feet below ground level, and personnel at ground level were shielded by at least eleven feet of sand and gravel. This arrangement permitted area access at all times immediately after termination of a run. At times when it was necessary for personnel to work on the reactor the shield tank was filled with water, and sub-tolerance radiation levels were reached with a few hours decay.

The location of the reactor in the shield tank required several pumps and other accessories to be located in a pit immediately adjacent to the shield tank (Figure 10). A concrete block wall was built across this pit just outside the shield tank, making it possible for personnel to work in the pit for extended periods of time within a few hours after a run was terminated.

D. Reactor Controls and Operating Instrumentation

The reactor control boards and nuclear indicators necessary for reactor control were located in a trailer just outside the EBR fence, and one-half mile southeast of the reactor (Figure 15). Electrical switchgear and nuclear signal amplifiers were located in a trailer adjacent to the reactor (Figure 16). These two trailers were interconnected with half-mile lengths of multi-conductor cables and coaxial cables as required. A third trailer located near the EBR fence contained a photographic dark room and auxiliary equipment. All electric motors except the control rod drives were powered through magnetic contactors in the reactor trailer with 110 volt, three-wire pushbutton controls on the control boards in the control trailer.

A brief description of each major control system is given.

1. Control Rod Drives and Reactor Shutdown

Three-phase, 220 volt motors were used to power the control rod drive mechanism. Total speed reduction was about 400 to 1 making it necessary to reduce the voltage to these motors so that the locked rotor torque was limited to a reasonable value. This was accomplished by power-stats

(adjustable autotransformers) in the power leads. Three-phase motors were used because of their reversing characteristics. These motors were controlled by spring return toggle switches located on the control boards.

Magnet current was supplied by full wave bridge rectifiers with voltage control on the a-c side. The change in impedance of the magnet coil when the armature was engaged was utilized to indicate when the control rod was held by its magnet. Contact switches were used to signal, through pilot lights, when the control rod armature was in the dashpot. Selsyns were used to indicate the location of the control rod drive mechanism, and, indirectly, through the indication of the control rod armature-magnet engagement, the position of the control rod in relation to the core.

During tests of the runaway type, transients were started by manually activating the release latch (to permit the rod to drop from the magnet) and then manually de-energizing the magnet of the central rod. At a preset time following the central rod ejection a timer automatically de-energized the shim rod magnets to inject the shim rods and terminate the experiment.

Fast reactor shutdown (scram) was effected by de-energizing relays in the magnet current power leads through push buttons located on the control board. Any or all of the four shims could be de-energized manually, with the scram signal de-energizing all four. Scram could be initiated by the transient timer, manually through push buttons located on the control boards and in the reactor trailer, and, when consistent with the experiments being performed, by the reactor period meter and the linear power meter. Fast reactor shutdown could also be effected by interrupting the shim rod magnet energizing current directly at a telephone jack connection located on the control board. A six-inch water dump valve could be opened by means of push buttons on the control board. This valve dumped the water from the reactor into the pump pit constituting a slower but positive shutdown process.

2. Water Controls

Electric pressure transducers were used to telemeter the water levels in the reactor tank and the shield tank to an indicator on the control board. Eight thermocouple circuits were available to transmit water temperatures and some key machinery temperatures. The reactor was filled and emptied by a pump located in the pump pit and controlled from the control board. Remote flow control was built into this system, but was abandoned in favor of fixed orifice control.

The electrical pre-heating system operated by circulating the reactor water through a side loop over immersion heaters of 150 kw rating. The circulating pump and the heaters could be turned on or off from the control board, and further instrumentation automatically cut off the

heaters in case of loss of water flow, as might result from pump failure or steam binding. Signal lights indicated when the pump was on and when flow existed.

3. Pressure Control

During pressurized operations the reactor was operated on both six-inch and two-inch pressure control valves, and under various combinations of automatic pressure control (at the reactor) and manual pressure control (from the control trailer). In all cases, a push button on the control board led to quick opening of the six-inch valve for over-pressure protection. Reactor pressure was telemetered to the control board, and recorded. A limit switch in this recorder also activated the quick valve opening in case of over-pressure. The reactor vessel was further protected by a rupture disc and spring loaded pressure relief valves.

4. Nuclear Instrumentation

Only the operating instrumentation is described here; special instrumentation for power excursion tests is described in Section IV and in Appendix B. The operating instrumentation is shown schematically in Figure 17.

To eliminate the necessity of water-proofing detectors and leads, three 8-inch diameter vertical thimbles were located against the shield tank wall, extending the full depth of the tank. A void introduced in the reactor reflector was aligned with the thimble closest to the reactor; this increased neutron leakage to some extent so as to improve detection at low levels. The location of these thimbles relative to the reactor is shown in Figure 18. During the initial approach to criticality, a temporary thimble was installed nearer the core to improve the counting rate.

Channels 1 and 2 (Figure 17) were counter channels, differing only in the type of neutron sensitive detector used and in their locations. The detectors used included BF_3 counters and U^{235} fission chambers. The detector signals were amplified in pre-amplifiers attached to the detectors, then carried to the reactor trailer where they were further amplified and transmitted to the control trailer. The pulse amplifiers were fitted with stepwise gain control, and with audio sensitivity and volume controls for a loudspeaker located on the reactor control drive platform. Each amplifier had its individual high voltage supply.

Each signal transmitted to the control trailer was re-amplified to correct for attenuation in the transmission cable, fed through a discriminator and a shaping circuit to a count-rate meter and to a scaling register. A 1000 cycle oscillator provided a calibrating signal for the count-rate meter.

Channel 3 received a current signal from a compensated ion chamber. The ion chamber shared a common high voltage supply (plus and minus) with the ion chamber of Channel 4. The current signal so obtained was fed through a logarithmic amplifier with a built-in calibrating current of 10^{-6} amp, and the logarithmic output voltage transmitted to the control trailer. This signal was indicated at the control trailer on a panel mounted meter, recorded on a Brown Electronik strip chart recorder, and fed into a differentiating circuit. The output of the differentiating circuit was fed into a panel-mounted period meter, a Brown Electronik strip chart recorder.

Channel 4 received a current signal from an ion chamber, amplified this signal on a linear amplifier in the reactor trailer, transmitted the linear power signal to the control trailer where it was indicated by a panel mounted linear power meter, recorded on a Brown Electronik strip chart recorder, and fed into a Brush amplifier driving a Brush recorder. The Brush record was introduced to provide a record of power fluctuations during boiling runs. Since this channel was to operate over a wide range of neutron fluxes, range selections varying by a total factor of 3×10^7 were built into the channel. Range selection could be controlled at either the control trailer or the reactor trailer.

Channel 5 was designed to transmit the gamma background at the top of the reactor to the control trailer. The signal was generated by an "Argonne Plastic Scintillator," detected and amplified by a photomultiplier, and fed to a logarithmic amplifier. This signal was transmitted to the control trailer and indicated by a panel mounted meter.

5. Miscellaneous

Microphones were used to record the sound of control rod ejection and boiling, and also to telemeter reactor sounds to the control trailer for operator guidance and recording.

A warning klaxon and flashing light served as personnel warning when the blade control rods were lifted from the fully inserted position.

III. NUCLEAR CHARACTERISTICS OF THE REACTOR

A. Criticality

The reactor reached criticality when the core had been built to twenty-six fuel elements (3.60 kilograms of U^{235}) in the pattern diagrammed in Figure 18. With this loading the reactor had 0.23% excess reactivity at 94°F. As the program progressed and more excess reactivity was required, further fuel elements were added in the sequence indicated in Table I. The worth of the added fuel elements in reactivity is also indicated in the table for those cases in which it was measured.

The detailed composition and the nuclear constants for the reactor are given in Appendix A.

Table I

PROGRAM OF FUEL ADDITIONS

Addition number	Grid space	Worth of addition (% k_{eff})	Total number assemblies	Core volume (liters)
1	13	1.22	27	103
2	18	0.94	28	107
3	24	1.00	29	111
4	12	--	30	115
5	7 and 30	1.29	32	122

B. Power Distribution

The thermal neutron flux distribution was roughly mapped over the volume of the core with gold foils at a low power level (a few watts) and with cobalt foils during steady boiling operation at a power of about 600 kw. Figure 19 shows the axial power distribution (with all control rods out) derived from the two measurements. Comparable agreements were obtained in measurements of distributions in the radial plane. The distributions measured in three representative traverses in the radial plane were combined to give the power distribution from fuel assembly to fuel assembly, as indicated in Figure 19. This distribution would, of course, change slightly as more fuel assemblies were added, but not significantly for the purposes of the Borax experiment.

C. Control Rod Calibrations and Neutron Lifetime

Cadmium inserts of two different widths -- 1.17 in. and 2.34 in. were used in the central control rod during the program. Calibrations of the rod were obtained with both insert widths.

A differential worth calibration of the rod containing the narrower strip was made by the usual method of withdrawing the rod a short distance from its critical position and measuring the resulting asymptotic reactor period. In order to extend this calibration over the entire length of the rod, sufficient excess reactivity was added (one fuel element) to require almost full insertion of the rod for criticality at ambient temperature. The reactor water was then heated slowly, and the strong negative temperature coefficient required that the rod be continuously withdrawn to maintain criticality. Differential calibrations were made at appropriate intervals to provide a complete calibration curve. The total worth of the rod and the worth of several large segments of the rod were also measured by the "rod drop" method.* It was also shown by such measurements that, to within experimental error, the worth of the rod did not change with temperature up to temperatures of 200F.

The measurements described above provided a preliminary calibration curve for use in the early operations. During the later experiments, in which the central control rod was ejected from the reactor for the purpose of studying reactor behavior under rapid transients, the resulting reactor periods provided a much more precise calibration. To convert the periods into reactivity changes, a knowledge of the neutron lifetime is necessary, since in many cases the reactivity involved was greater than prompt critical.

Although the effective neutron lifetime was not known independently, it could be set within fairly close limits by adjusting it to give what appeared to be consistent shapes for the calibration curves for both the 1.17 in. cadmium strip and the 2.34 in. strip. The value arrived at for the effective lifetime was 6.5×10^{-5} second. It is believed to be correct to within $\pm 0.5 \times 10^{-5}$ second. The computed infinite thermal lifetime in the reactor is 5.8×10^{-5} second. The resulting calibration curve for the 1.17 in. cadmium strip is shown in Figure 20, which includes both the points from the fast excursions and from the "rod drop" measurements. Figure 21 is the derivative of this curve with the points obtained during the differential calibration of the rod included.

*An inappropriate name for these particular experiments, since the rod could not be dropped into the reactor, but was instead jerked rapidly upward into the reactor by the counterweight previously described.

The calibration of the central rod containing the 2.34 in. cadmium strip is shown in Figure 22. This calibration was arrived at from the fast excursion experiments, using the effective neutron lifetime of 6.5×10^{-5} second. Two points near the top of the curve were obtained by long period differential calibrations. During the sequence of experiments from which the curve was derived, the critical position for the central rod was varied as necessary by adjustment of the degree of insertion of the shim rods. The curve represents, therefore, a calibration of the central rod for the case in which the shim rods are inserted to some variable depth, which ranged from about three inches to six inches.

For the case in which the shim rods were entirely withdrawn a calibration curve for the rod with the 2.34 in. cadmium strip was arrived at by measuring the total worth of the rod, and assuming that the shape of the curve was the same as that for the rod containing the 1.17 in. cadmium strip. The resulting curve is shown in Figure 23.

The shim rods were never inserted more than about 6 in. into the core during operation; the remainder of the length was utilized only for shutdown. The rods were, therefore, calibrated over only about 6-1/2 in. of insertion. The calibration curve up to 5 in. of insertion was obtained by calibration against the central rod. The two higher points were evaluated from the change in shim rod position when fuel elements were added to the core. (Fig. 24)

D. Temperature and Density Coefficient

The measured change of reactivity with temperature is shown in Figure 25. The portion of the curve up to 205F was obtained simultaneously with the calibration of the central rod containing the 1.17 in. cadmium strip, as described in Section C above. The points at higher temperatures were derived from measurements of critical rod positions (central rod and shim rods) incidental to other experiments in the pressurized reactor.

Under conditions of boiling operation, the reactivity of the reactor is dependent upon the quantity of steam contained in the core. For reactivity purposes this steam can be considered simply as a void in the water moderator. It was not possible to measure the steam or void coefficient of reactivity experimentally. This coefficient was calculated by the two-group approximation, for uniform distribution of void in the reactor core, and no void in the reflector. At 200F the calculated average coefficient, up to 10% void, is -0.235% k per % void in the core water. Up to 20% void the coefficient is -0.272% k per % void in the core water. The coefficient is evidently nearly constant from zero to 20% void, the maximum range of interest in the experiments. The calculated average coefficient up to 10% void at 350F is -0.250% k per % void in the core water.

IV. EXPERIMENTS ON SELF LIMITATION OF POWER EXCURSIONS

A. Method and Special Instrumentation

The objective of these experiments was to determine the extent to which the reactor, by the formation of sufficient steam to render the reactor subcritical, would protect itself against the effects of sudden large externally caused reactivity increases. It has been mentioned that the central control rod was a rod having a length double that of the core and containing neutron absorbing material (cadmium) in the bottom half of its length. If the reactor were initially critical with the bottom (absorbing) part of the rod partially inserted in the core, ejection of the rod downward under the force of gravity plus the force of the ejection springs would impose upon the reactor a sudden reactivity increase equal to the reactivity worth of that portion of the rod which was initially in the core. Thus, although the absorbing portion of the rod was always completely ejected from the core, the magnitude of the reactivity jump could be adjusted to any desired value by adjusting the amount of rod insertion required for criticality. This was accomplished by appropriate choice of fuel loading plus partial insertion of the shim rods. The time interval during which the reactor was subjected to the applied excess reactivity could be adjusted to any desired value by a timer mechanism which initiated injection of the shim rods at an adjustable interval after ejection of the center rod.

The self-limitation performance of the reactor was explored cautiously by making the initial experiments with a short pulse of excess reactivity which produced a reactor period of about 0.2 second, and gradually increasing the time duration of the excess reactivity pulse in a series of experiments until it was evident that the reactor would limit the power excursion to a safe value, and in fact, bring the power back from its peak value to a relatively low value. After this self-limitation had been established, the timer was set to apply the excess reactivity pulse for an interval definitely longer than that required for the reactor to terminate the power excursion, and the severity of the excursions was gradually increased by increasing the amplitude of the reactivity pulse.

Figure 26 shows the asymptotic period reached by the reactor as a function of excess reactivity. The curve is quite steep in the vicinity of prompt criticality, an increase of about 25 inhours in reactivity sufficing to reduce the period by a factor of 2. Careful adjustment of the reactivity pulse was necessary in this region in order to progress by increments which represented safe extrapolations from previous experiments.

To simplify the interpretation of the experimental results it was desirable that the reactivity pulse applied be effectively a "square wave." This was accomplished by starting each excursion from a very low power level (about one watt) and utilizing a relatively fast rod ejection. Figure 27

shows the rate of ejection of the central rod as measured in three different experimental ejections. As indicated, the rod entered its dashpot about 2-1/2 in. before ejection was completed. The worth of this last 2-1/2 in. of rod was too low (Figure 22) to affect the reactor period appreciably. Figure 28, derived from Figures 22 and 27, shows the rate of addition of reactivity during the fastest excursion made (5 millisecond period). This excursion started from a power of 1.5 watts. Figure 29 shows the power rise resulting from the reactivity addition of Figure 28, as computed by numerical integration of the reactor kinetic equations by O. A. Schulze. By the time the rod enters the dashpot the power has risen only to about 5 megawatts, and the period is essentially constant at 5 milliseconds for all powers greater than 0.1 megawatt. Inasmuch as the reactor power eventually exceeded 2,000 megawatts before shutting itself down, it is evident that for purposes of this experiment, the injection of reactivity could be considered instantaneous. This conclusion was verified by the excursion records themselves, which showed a constant period maintained for at least 5 periods prior to the beginning of shutdown in all excursions.

The three major types of information recorded during the power excursion were reactor power, total energy of the excursion, and temperature of selected fuel plates. Reactor power and fuel plate temperature were recorded on a single strip of photographic paper by a Heiland magnetic oscillograph employing high speed galvanometers. Power was measured by three different boron-coated ion chambers, located as indicated in the table below, feeding the Heiland galvanometers through logarithmic amplifiers.

Type Chamber	Thimble Number (see Fig. 18)	Position of Record on Chart (see Fig. 30)
Gamma Compensated	2*	Top
Uncompensated	3	Bottom
Uncompensated	1	Middle

*During the more energetic excursions this chamber, which was more sensitive than the others, was taken out of the thimble and moved to a position about 20 feet from the reactor.

The function of the multiplicity of ion chambers was to record power from positions of various neutron flux densities (at different heights in the thimbles), and thus insure that at least one record would be obtained within the useful current range of the ion chamber. Actually all three of the chambers gave useful readings on most excursions. In such cases the reactor period as measured by the three chambers agreed to within 10% or better. The ion chamber readings were converted to absolute powers as described in Section C below.

Two special fuel plates were installed in the core during the power excursion experiments. Each plate had a thermocouple installed on its surface at the midpoint of its length and width, and a second thermocouple installed at about the mid-thickness of its aluminum-uranium alloy core, in roughly the same location with respect to length and width. Of these four thermocouples only three were used for recording data, because of a shortage of the proper galvanometers. The thermocouple fuel plates were installed, along with a sufficient number of other fuel plates to fill out the assembly, in the special fuel assembly (Figure 9). The special fuel assembly was installed in the core in position 21 (Figure 18). Locations of the thermocoupled plates in the assembly are indicated in a later Section along with the results of the measurements.

A detailed discussion of the instrumentation for the power excursions, covering time responses of the instruments, is contained in Appendix B.

The total energy of power excursions was measured by foils, calibrated for total energy as described in Section D below. In some cases cobalt foils were installed in the reactor core for this purpose. As a matter of convenience, however, most of the excursions were recorded by gold foils located externally just outside the reactor tank. The internal foils gave more consistent data because they were not subjected to the variations associated with leakage of neutrons through the thick water reflector and the reactor tank.

B. General Characteristics of Power Excursions

Figure 30 is a reproduction of the record of a typical power excursion in which, at the beginning of the excursion, the reactor water had been heated to saturation temperature by electric heaters. Ejection of the central control rod produced about 1.4% excess reactivity, resulting in a period of about 0.01 second. That the reactor power was rising on the asymptotic period is evident from the long straight portion of each of the power (ion chamber) curves. The power rise was checked at a value of 330 megawatts by the formation of steam in the core, and further steam generation rendered the core subcritical and resulted in a rapid power decrease to a value of about 0.2 megawatt. Typical behavior of the power after the minimum value was reached is discussed further below. The fuel plate temperatures reach the maximum values at a time slightly after peak power. This behavior is to be expected as the fuel plates store a large fraction of the energy of the excursion up to the time when vigorous boiling begins. The fuel plate temperature thus represents an integral of reactor power, modified by a time variable heat loss to the reactor water.

Once the initial power excursion has been checked by boiling in the reactor, the subsequent power variation depends both qualitatively and quantitatively upon the amount of excess reactivity to which the reactor was

subjected. Several excursions were made in which the applied excess reactivity was maintained for periods of from 4 to 20 seconds to investigate this behavior. Figure 31, in which the curves are tracings from excursion records similar to that of Figure 30, summarizes these results. When the excess reactivity applied is low, corresponding to reactor periods of about 0.03 second or longer, the reactor power after the initial surge settles down to a relatively steady value in the neighborhood of half a megawatt. This steady boiling behavior is typified by the top trace of Figure 31. For higher excess reactivities than that which resulted in this trace, the power after the first surge goes through a series of damped oscillations before settling down to a steady value.

If the excess reactivity applied exceeds that corresponding to a period of 0.02 or 0.03 second, the initial power excursion is followed by a series of qualitatively similar excursions of smaller amplitude, occurring at intervals of about one second. Operation of this type was observed for periods as long as 20 seconds. The amplitudes of the successive excursions, although they varied in an irregular manner, showed no sustained tendency to increase or decrease and it was assumed that they would continue indefinitely if water was supplied to replace that lost by steam generation and splashing. This type of operation was called chugging, and will be so referred to throughout this report.

When the excess reactivity applied was increased to that corresponding to a period of about 0.01 second, the chugging was no longer observed, although the excess reactivity was applied for intervals as long as 4 seconds. The power after the first surge decreased to a low value (0.2 megawatt or less) and did not again increase. By the ion chamber indications, this low value was about 0.2 megawatt. However, for excursions of this type the effects of the initial power surge were rather violent, and a large quantity of water was expelled from the reactor with each excursion. The fractional neutron leakage from the reactor core to the ion chambers therefore may have increased drastically after the initial power surge, resulting in a power indication which was much too high. The chambers would, of course, also begin to respond to gamma radiation after sudden very large power decreases. It was therefore not determined whether the initial power surge expelled enough water to render the reactor permanently subcritical or whether the power indicated after the initial surge was actually produced in steady boiling operation. The exact water level in the reactor tank after a violent excursion was not determined as the water level indicator after such an excursion, did not read accurately and it was not possible to approach the reactor for visual observation without first adding water for shielding purposes. Evidently the transition from chugging type excursions to those which gave permanent shutdown depends upon the design of the reactor, and it is presumed that, if the reactor tank did not permit permanent expulsion of the water, chugging operation would continue at the higher excess reactivities.

When the excess reactivity applied was increased to about 2% to give periods in the 0.005 second range, the qualitative behavior of reactor power remained the same, but the fuel plate temperature did not drop immediately after the power surge. This behavior is shown in the bottom trace of Figure 31. Fuel plate temperature remained high for almost a second after the power surge and then decreased by small jumps, as though the plate had been blanketed by steam for some time after the power excursion.

If excess reactivity is applied to the reactor when its temperature is below the saturation temperature of the water, sufficient energy must be generated to raise the temperature of the fuel plates and that of, at least, a thin film of water adjacent to the fuel plates to the boiling point before steam can be formed to check the power rise. Thus one expects that, for excursions of the same period, those occurring in the cool reactor will be the more energetic. A number of excursions were made under this condition, which will be referred to hereafter as the subcooled condition. Figure 32 shows records of two excursions with comparable amounts of subcooling but with two different periods. The most noticeable difference between the subcooled runs and those at saturation temperature is the shorter time interval between the initial power surge and the peak of the secondary surge, which follows in 0.3 to 0.5 second, in contrast to the interval of about 1 second between chugs in the saturated condition. This decrease in the time interval is not surprising inasmuch as steam can disappear from the core by condensation as well as by the inflow of water. The low peak values of these secondary surges are, however, surprising. They may be related to the fact that the fuel plate temperatures do not decrease rapidly to the initial value, and in fact appear to remain above the saturation temperature for a relatively long time. Durations of the pulse of applied excess reactivity greater than 1.0 to 1.5 seconds were not investigated under subcooled conditions.

The quantitative characteristics of the power excursions both from the subcooled and saturated condition are discussed in detail in the following Sections.

C. Subcooled Excursions and Power Calibration

It can be demonstrated theoretically that a fuel plate, immersed in stagnant water and heated by an exponentially increasing power excursion of short period, does not lose an appreciable fraction of its heat to the surrounding water until boiling begins. The Borax power excursions confirm this prediction inasmuch as the measured fuel plate temperature rises are quite closely exponential up to the time when the power rise itself breaks away from the exponential. This situation can be utilized to obtain an absolute power calibration for the ion chambers from the subcooled power excursions. Thus, up to any time before the fuel plates reach the saturation temperature, the time integral of the power generated in the fuel plates will

be very nearly equal to the temperature rise of the average fuel plate times the total heat capacity of all the fuel plates in the core. This principle was used to calibrate the ion chambers used in the excursion experiments from the averaged results of six subcooled runs made with two different values of applied excess reactivity. As water temperature was changed it was necessary to make a correction for the variation in neutron leakage through the thick (approximately 14 in.) water reflector. The calculated leakage at 200F was higher by a factor of 1.35 than the leakage at 76F, the lowest temperature used.

In Figures 33 and 34 the power calibrations have been applied to show the power, energy, and temperature relationships for the six runs utilized in deriving the calibrations, as well as for two additional runs made with the same periods, but with little or no subcooling. In each case, curve (b) is the power variation as seen by the ion chamber, and curve (a) is an extrapolation of the original exponential portion of this power curve. Curve (c) is the integral of the power curve, and curve (d) is the total heat content of all the fuel plates, obtained by multiplying the measured fuel plate temperature (corrected for galvanometer lag) by the ratio of the power density at the thermocouple to the average power density over the core (0.54) and by the total heat capacity of all the fuel plates. The degree to which curves (c) and (d) fail to coincide at the time when saturation temperature is reached is a measure of the degree of internal inconsistency of the power calibration data.

Note that the energy values plotted represent only the energy converted to heat within the fuel plates during the excursion. Since this is the only energy recognized as playing a significant part in determining the characteristics of the power excursions, it is convenient always to consider it alone as the energy of the excursion. This terminology has been adopted throughout the Section of this report which deals with power excursions. Whenever power or energy is mentioned in this Section, it is to be understood that reference is made only to that which appears as heat in the fuel plates. To arrive at the true total energy, these values should be increased by about 15% to account for prompt heat generated elsewhere (7%) and for delayed energy emission (8%).

If allowance is made for the fact that the power calibration does not fit all of the records of Figures 33 and 34 equally well, it is evident that the heat stored in the fuel plates does constitute very nearly all of the energy generated until a plate temperature is reached which is well above that corresponding to saturation at ambient pressure. In fact, the two curves (c) and (d) diverge, in most cases, just before the power curve (b) reaches its maximum, as would be expected if the divergence indicates the formation of steam in appreciable quantities.

In Figure 33 the ratio of the total energy generated to the maximum energy stored in the fuel plates is considerably lower for the excursion with two degrees subcooling. The shorter period runs of Figure 34 do not

show this behavior as subcooling is decreased. In this connection it should be remembered that the rapid ejection of water from the core cannot be accomplished without building up an accelerating pressure, and that the saturation temperature in the core during the shutdown process is higher than that corresponding to ambient pressure by a considerable amount which increases as the period is shortened.

Evidently, a heat flux from fuel plate to water can be derived from the difference between curves (c) and (d). The highest flux occurs in the run with 43 degrees subcooling and 0.013 second period, and amounts to about 10^6 BTU per ft^2 hr for the average fuel plate.

It can be seen in Figures 33 and 34 that the reactor power curve begins to deviate slightly from the exponential well before the power rise is finally stopped. Although the records do not give this early deviation accurately it seems to be a characteristic feature of all the power excursions, whether or not they were run from the subcooled condition. At least part, and perhaps all, of the early deviation can be attributed to the small reactivity decrease resulting from fuel plate expansion. The early stages of boiling at a few of the very hottest fuel plates may also contribute to the phenomenon.

Figure 35 is a plot of total energy of the power excursions of Figures 33 and 34 as a function of subcooling. Since the energy required to raise the fuel plates to saturation temperature cannot contribute to the shutdown process, but is nevertheless an appreciable fraction of the total energy when subcooling is large, this energy has been subtracted from the total, and the difference plotted in Figure 36. The significance of this operation is somewhat ambiguous, since it is not evident whether the appropriate energy to subtract is that required to raise the hottest plate to saturation or that required to raise the average plate to saturation. The average plate was used in Figure 36.

Figure 37 shows the maximum fuel plate temperatures reached as functions of degree of subcooling. The special fuel assembly with the thermocoupled plates (plates 1 and 4) was installed in position 21 of the core grid (Figure 18). The reason for the lower temperatures in plate 1 than in plate 4 is not known. The temperatures of plate 4 were used in establishing the power calibration.

D. Effect of Initial Period, or Excess Reactivity, on Power Excursion

The relation between period and excess reactivity is a constant one for a given reactor, but varies among reactors with different effective neutron lifetimes. For reasons discussed in Section G below, it is believed that the period is the more important variable in determining the severity of a reactor excursion. Consequently, in the following Sections, the power excursions will be characterized by their periods rather than by the excess

reactivity applied. It is to be understood that by period is meant the asymptotic exponential period which is reached after the control rod is fully ejected, and which is maintained until the shutdown process begins to be effective. The period may be converted to the corresponding excess reactivity by the curve of Figure 26.

The effect of period on power excursions was investigated by a series of experiments run with the reactor water initially at saturation temperature. Fuel plate temperatures were measured on plates 1 and 11 (see Figure 37 for plate locations). Again the special fuel assembly containing the thermocoupled plates was installed in position 21 of the core grid (Figure 18). The results of the temperature measurements are plotted against the reciprocal of the period in Figure 38. Note that maximum plate temperature rise, rather than plate temperature, is plotted. The actual plate temperature is higher by about 200F, the initial reactor temperature. The fastest reactor period, 0.005 second, which corresponds to 2.1% excess k_{eff} , resulted in a maximum plate temperature of less than 650F. The temperatures were measured at what is believed to be very nearly the hottest spot in the reactor.

The total energy of the power excursion is plotted as a function of reciprocal period in Figure 39. The relative energy variation was determined by foils, as indicated. The absolute energy scale for the curve was determined by fitting it to three points, indicated by solid circles, for which absolute energy values had been established by integration of their power (ion chamber) curves. The two lower points are from the two excursions of negligible subcooling in Figures 33 and 34.

The similarity of shape between the total energy and maximum plate temperature curves is striking, and, indeed, if maximum temperature rise is plotted against total energy the curve can be fit by a straight line over most of its length (Figure 40). The total heat capacity of the fuel plates in the core is 0.05 megawatt second per degree F. If the factor 0.54 is applied to take account of the ratio of average power density to power density at the thermocouple, a fuel plate temperature rise of 400F corresponds to a total energy content of $(400)(0.54)(0.05) = 11$ megawatt seconds. Thus, for short period excursions, about half the total energy of the excursion appears to be stored in the fuel plates when they reach their maximum temperature. The fraction seems to be appreciably larger for excursions of relatively long period.

As might be expected, the maximum power reached during excursions shows considerably more scatter than the total energy of the excursions. The maximum power in the most energetic excursion (0.005 second period) was 2600 megawatts. It is instructive to plot, for excursions of various periods, the product of the maximum power times the period as a function of the total energy of the excursion. Such a plot is shown in Figure 41.

Although, on the basis of evidence described in the paragraph below, a curve with slightly increasing slope has been drawn through the points, it is roughly correct to say that the curve is fit by a straight line through the origin with a slope equal to approximately two. That is to say, the total energy liberated in the excursion is roughly the same as that which would have been liberated if the power had been maintained at its maximum value for two periods. An alternate statement is that, roughly, the total energy of the excursion is that which would have been produced if the power had risen to maximum value with an exponential increase, and then immediately decayed on a decreasing exponential of the same period.

Since the initial part of the power excursion is known to be nearly exponential over a large fraction of its rise, the near constancy of slope in Figure 41 implies strongly that the shape of the entire power transient remains nearly constant as period is varied, provided time is measured in the non-dimensional units of period rather than in seconds. Figure 42 demonstrates that this supposition is indeed true. The ion chamber records of excursions of three different periods have been plotted, normalizing all peak powers to the same arbitrary value, and using period as the unit of time. Although it is true that the long period excursion (curve (c)) definitely cuts off more sharply than the shorter period excursions (curves (a) and (b)) on this time scale, the curves are remarkably similar when it is considered that the period has been shortened by a factor of 45 between curves (c) and (b). Evidently there is an appreciable variation in shape of the power excursion from run to run at the same period, inasmuch as curve (b), in comparison with (a), represents a reversal of the trend indicated from either (c) to (b) or (c) to (a). The scatter of points in Figure 41 is no doubt a reflection of this type of variation. That there should be some variation from run to run is hardly surprising - indeed when one considers the rapidity with which power is varying during the excursion it is surprising that the variations are not greater.

E. Pressure Generated During Excursions

The speed with which water must be ejected from the reactor core to terminate the short period power excursions can only be attained if an accelerating pressure is built up within the reactor core. This pressure is, of course, produced by the generation of steam at the fuel plates. Provision was made for measuring the pressure in the core by means of electrical strain gauge pressure transducers. Reliable pressure records were obtained, however, only on a few excursions of relatively long period. Splashing of water which occurred with shorter period excursions resulted in wetting of the transducer wiring at unanticipated points, and perhaps did some mechanical damage to the transducers themselves which led to inconsistent results. The limited time available for the experiments did not permit the correction of these difficulties. Figure 43 is a record of a power excursion including pressure records from two transducers of different

sensitivities. The shape of the pressure curve is consistent with the interpretations previously put upon the ion chamber and thermocouple records; the pressure begins to rise at about the time reactor power breaks sharply away from the exponential, and reaches its maximum value when the power is dropping off rapidly.

The pressure records which were obtained at shorter periods recorded a maximum pressure of about 70 psig for the excursion of 0.005 second period. Within the very wide scatter of the records it appeared that pressure might increase approximately linearly with reciprocal period. It is believed, however, that these recorded pressures are considerably too low. In fact, photographic records indicate that virtually all of the water was expelled from the core during the shorter period excursions. Since the ion chamber records indicate that expulsion was completed in, at most, about 4 reactor periods (cf. Figure 42), it is difficult to see how such rapid water expulsion could be achieved without considerably higher pressures. It may be possible through further analysis of the ion chamber records to arrive at rough values of the pressure during the excursions through considerations of the reactivity variation and the void coefficient of reactivity.

The pressures generated during the fast excursions did some mechanical damage to the reactor core. During the sequence of excursions with periods between about 0.01 and 0.005 seconds, the outermost plates in many of the fuel assemblies (Figure 8), which are normally concave outward, were permanently reversed in curvature, giving an assembly which was convex on both sides. After these experiments the core was disassembled, and the bent plates were pounded roughly back into shape, but they were no longer very strong. The subcooled excursion tests were made after this repair of the initial damage. As the subcooled tests with 0.013 second period progressed, it was evident from slight permanent changes in reactivity that the deformation was again occurring. This deformation proceeded to the point where the innermost fuel assemblies began to be pushed into the control rod channels. At this point the excursion tests were discontinued, the fuel assemblies were again straightened, and the investigation of steady boiling was begun. It was because of this deformation that the subcooled excursions were not run at shorter periods. There is no reason to believe that the subcooled experiments would have deformed the assemblies if they had not been already weakened by the previous bending, since visual and photographic observations showed that the water agitation associated with the subcooled experiments was far less than that which had occurred previously with shorter period excursions at saturation temperature. It should be emphasized that this damage to the reactor core was purely a function of its particular mechanical design and was caused by pressure alone. The necessary differential pressure across the end fuel plate for reversal of its curvature at room temperature has been shown to be between 18 and 25 psi (ref. 7). The total pressures generated in the core during the transient runs were at least several times this value.

F. Photographs of Excursions

Figures 45 through 51 are enlargements of individual frames of 16 millimeter motion picture records which were taken of some of the excursions. For the less violent excursions (Figures 47 through 51) the camera was located just outside the earth shield and looked down upon the open top of the reactor, where the control rod magnets and the surface of the reactor water were visible. The core itself was not visible. Figure 12 is a photograph of the reactor showing the location of the mirrors for these movies. For the more violent shorter period excursions (Figure 44), the moving picture camera was set up at some distance from the reactor to record the expulsion of steam and water. Figures 45 and 46 are records of such excursions. The approximate times indicated on the photographs are measured from the time of release of the central control rod. These excursions were made with the reactor water initially at saturation temperature, and are in fact two of the excursions whose power records are reproduced in Figure 42. It is interesting to note that in the frames of Figure 45 marked 840 millisecond and 1180 milliseconds, the pressure inside the control rod housing has lifted the corner of the top of the housing an observable amount.

Figures 47, 48 and 49 depict some subcooled excursions with periods in the 20 millisecond range. In each of these figures the flash of light produced by the reactor as it went through its power surge can be seen in the photograph in the upper right hand corner of the page. Most of the agitation of the water surface occurs after this light flash disappears, i.e., after reactor power has dropped back to a relatively low value. This is no doubt a result of the fact that much of the total steam formed during the excursion is produced by heat stored in the fuel plates after reactor power has decreased. A further striking characteristic is the relatively mild effect of these excursions in so far as the agitation of the water surface is concerned.

Figures 50 and 51 were made with a double mirror rather than the single one which was used for the previous photographs. Figure 50 represents an excursion of about the same period as those of Figures 47 through 49 but with no subcooling. Agitation of the water surface is considerably more violent, and a little water is spilled over the edge of the tank. In Figure 51 the period of the excursion has been decreased to 13.6 milliseconds, with no subcooling. A considerable quantity of water was expelled from the reactor tank, and some impinged on the surface of the mirror itself.

G. Discussion of Results of Excursions

Inasmuch as the Borax reactor employed MTR fuel elements, the results are directly applicable to a number of reactors employing the same type of fuel element, particularly to reactors of "swimming pool" type and

the Argonne CP-5 type. In reactors such as MTR itself, which employ high-velocity coolant circulation to attain relatively high heat transfer rates, some modification of the behavior might be anticipated. Further analysis of the Borax data may indicate the type of modification to be expected. From the standpoint of safety information for reactors which operate at temperatures below saturation, more subcooled experiments at shorter periods would have been desirable. In the case of dilute D_2O -moderated reactors, however, the range covered seems quite adequate since, because of the long effective neutron lifetime, short periods can only be achieved by very large excess reactivities. In CP-5, for example, about 8% excess reactivity would be required to reach a period as short as 0.013 second.

In considering the safety of water-cooled reactors which have core and fuel plate designs quite different from that used in Borax, the Borax experiments can no longer be considered as specific safety demonstrations, but only as giving information which can be applied in safety analysis. Aside from the specific quantitative data which may be extracted from the results to fit the particular problem at hand, a few generalizations can be made which have a bearing on all water-cooled reactors.

Perhaps the most fundamental observation is that the self-limitation of power by the formation of steam and ejection of water in water-cooled reactors is a consistent and repeatable phenomenon, and one which in a sequence of some 70 experiments showed no anomalies other than those attributable to instrumental errors. Thus, it is evident that the transient behavior of reactors of this type can be established by appropriate experiments, with reasonable assurance that the results will not be invalidated for safety analyses by occasional exceptions of an irrational type.

Before considering further general results of the Borax excursions, it is worthwhile to note briefly some of the thermal characteristics of the reactor. One of the significant quantities is the heat required to form important amounts of steam in the reactor. At atmospheric pressure the heat of vaporization of a volume of steam sufficient to fill all the fuel passages in the core is 0.087 megawatt second. Since the void coefficient of reactivity in the reactor is about 0.25% k_{eff} per per cent steam, less than 10% of the coolant channel volume must be filled with steam to remove the excess reactivity injected in the fastest Borax excursion. Thus, even if the pressure in the core becomes momentarily quite high during the excursion, the energy required for actual vaporization of the steam is still a very small fraction of the total energy of the excursion (cf. Figure 39). It is this simple consideration which leads one to believe that the quantity of excess reactivity injected into the reactor is per se a relatively unimportant consideration: only as the excess reactivity determines the reactor period does it become an important variable.

The quantity of heat required to raise the temperature of all the fuel plates in the reactor core 1°F is 0.05 megawatt second, and the quantity of heat required to raise the temperature of all the water in the coolant channels of the core 1°F is 0.15 megawatt second. Thus the quantity of heat necessary to raise the water temperature 1°F , if utilized entirely for vaporization of water, is more than enough to fill the entire core with steam at atmospheric pressure. If one considers these relative quantities without emphasis on the part played by dynamic pressurization of the water in the core, one is led to expect, qualitatively, the following type of excursion behavior. Having reached the asymptotic exponential, the reactor power continues to rise exponentially until sufficient heat is stored in the fuel plates to raise their temperature to the saturation point, and to some further point if any (hypothetical) time lag exists in the formation of steam. Once steam begins to form, the further power generation necessary to make enough steam for shutdown would be quite negligible, and the power decrease would be extremely rapid unless some inherent limitation existed in the rate at which steam could be formed.

When one considers, however, the consequences of the pressure build-up in the core by water acceleration, the situation is considerably modified. In the first place, it is now evident that there is really no sharp distinction between excursions from the subcooled condition and excursions from temperatures which correspond to saturation at ambient pressure. Since now the water will, in all excursions, be at a temperature below the instantaneous saturation temperature, the heat capacity of the water represents a heat sink of important magnitude. Until boiling starts its effect is negligible, since there is no effective means of heat transfer from the fuel plate surface to the body of the water. The evidence of the Borax experiments is that this heat sink becomes important after surface boiling begins inasmuch as about half of the total energy of the excursion can not be accounted for either by heat storage in the fuel plates or by immediate vaporization of water (Section D above). It is presumed that the formation of steam at the fuel plate surfaces results in an effective mechanism for heat transfer from the fuel plate to the bulk liquid water. This consideration is of importance when reactors are considered which employ fuel elements or fuel element cladding of poor conductivity. With the relatively thin aluminum fuel plates used in Borax, very large heat output could be supported without a large temperature drop between the center and the surface of the fuel plate. The rate at which heat must be transferred out of the fuel plate during the excursion will, of course, have a large effect on the center temperature of fuel elements of poorer conductivity.

With respect to a hypothetical time lag in initiation of the boiling process, it must be said that if one exists its effect is obscured by the complexity of the situation described above. If a time lag does exist, its magnitude is so strongly dependent upon fuel plate temperature that the time lag concept does not appear to be a very useful one at this time. A more

applicable method of describing the speed of shutdown is to say that the length of time required for the power to rise from 10% of its peak value to the peak value and to return again to 10% of peak value lies between 3 and 4.5 periods (Figure 42). The shape of the power excursion is further characterized by the relation that the total energy of the excursion is roughly equal to the maximum power multiplied by twice the period.

V. STEADY BOILING AT ATMOSPHERIC PRESSURE

The reactor was operated as a boiling reactor, at steady power, with the lid of the reactor tank removed (Figure 5). Figure 12 shows the reactor boiling at about 700 kw. Power was indicated by the ion chamber in thimble 1 (Figure 18) and could be recorded simultaneously on a Brown Electronik recorder and a fast Brush recorder. The chamber was calibrated for absolute power by heating the reactor under its own power at temperatures below saturation, as described in Appendix C. Inasmuch as these calibrations were made with a non-boiling reactor, and the neutron leakage to the ion chamber is a function of the water density in the reactor core and, particularly, of the density in the reflector, these calibrations contained some uncertainties. Theoretical corrections for the effects of steam voids in the core have been estimated, as described in Appendix C, but an uncertainty of 10 to 15% exists in the calibration.

The usual history of a boiling run was roughly as follows. The reactor water was heated to the boiling point by the electric heaters, the heaters and circulated pump were turned off, and the reactor made critical at a low power by withdrawal of control rods. A control rod was then further withdrawn to put the reactor on a period between 5 and 30 seconds; the power was allowed to rise on this period until the boiling began and steam in the reactor compensated the excess reactivity, causing the power to level off of its own accord to some steady value. The power was then increased in steps by incremental withdrawals of the control rod. The reactivity added to the reactor by control rod motion after initial criticality will hereafter be referred to as the reactivity compensated by steam. When this quantity was relatively low, the power output of the reactor was subject to fluctuations of ± 10 to 20%. These fluctuations did not occur with any noticeable regularity, but had the appearance that one might expect from the irregular bubbling in a boiling system. After the reactivity compensated by steam was increased above 1.5 or 1.6% k_{eff} the variations began to appear as oscillations of definite frequency, the frequency ranging from about 1.2 to 1.8 cycles per second. These oscillations occurred in pulses containing several complete oscillation periods. The pulses were separated from one another by periods of irregular variation similar to those seen at the lower reactivities. As the reactivity compensated by steam was increased further, the amplitude of these oscillations increased, the number of oscillations per pulse increased, and the interval between pulses decreased, until finally the oscillation was practically continuous, but with varying amplitude. These characteristics of boiling operation are illustrated by Figure 52, which is a reproduction of sections of the Brown Electronik chart. It is evident from the chart that the reactor is under tight automatic power control. That is to say, whenever the control rod is moved (i.e., Δk is changed), the average power very quickly adjusts to the appropriate value and maintains that value as long as the rod position remains unchanged. Figure 53 is a replot of a similar but different boiling run, showing a curve of reactivity compensated by steam along with the

corresponding power curve. Also plotted on this curve are points which show the maximum and minimum values of the power fluctuation. Figure 54 is a curve showing average power as a function of reactivity compensated by steam for a number of steady boiling runs. The points from various runs are reasonably consistent with one another. The variations that do exist may be the result of differences in core configuration, as indicated on the figure. The decrease in slope of the curve as more reactivity is added is striking. This behavior may be connected with the occurrence of the oscillations in the power. In the reactivity range where oscillations were present only intermittently, however, little or no difference in average power could be measured between the oscillating and nonoscillating phases of operation. Figure 55 is a plot of the amplitude of power fluctuation, expressed as the ratio of maximum to minimum power, as a function of reactivity compensated by steam, for several runs. No curve has been drawn through these points as there is a wide scatter from run to run. A discussion of the detailed characteristics of the power oscillations at elevated pressure is contained in Section VI. Those at atmospheric pressure were not sufficiently different to warrant separate discussion. The main difference observed was greater fluctuation in the amplitude of the oscillation at atmospheric pressure, and somewhat less regularity in wave shape.

In the run plotted in Figure 53, after the last increase in reactivity, which increased the reactivity compensated by steam to 2.6%, the reactor operated for about half a minute with power oscillations of amplitude which varied from almost zero to the maximum shown in Figure 55. It then went through a series of oscillations of rapidly increasing amplitude which in the space of a few oscillations took on the characteristics of chugging operation of the type previously described in connection with the power excursions. Figure 56 is a record of this transition from oscillatory boiling to chugging. The record is from the fast Heiland oscillograph, and the powers are recorded on a logarithmic scale. As can be seen in the figure, maximum powers of 50 to 60 megawatts were reached. If the ion chamber calibration can be assumed to remain constant during this operation, the average power of the reactor increased by a factor of 2 or 3 over that just prior to the onset of chugging. It is possible, however, that the water agitation resulting from the chugging changed the average leakage of neutrons from the reactor to the ion chamber. The reactor was shut down at the end of the record by insertion of the shim rods. The chugging operation caused no damage to the reactor. Actually, more violent chugging operation had been experienced for periods up to 20 seconds in previous runs of the excursion type. The maximum period attained by the chug which reached the highest power was 0.017 seconds. This represents an excess reactivity of about 1.2% k_{eff} , only about half the total (2.6%) which had been added and was previously compensated by steam.

VI. STEADY BOILING AT ELEVATED PRESSURE

A. General Characteristics

Operation at elevated pressure demonstrates some additional characteristics of the boiling reactor beyond those observed at atmospheric pressure. These characteristics have to do primarily with the effects of the various system variables upon reactor operation. They become apparent under pressurized operation because, in the first place, a pressure regulator must be added to the system, and in the second place, the heat capacity of the reactor and its water represents a more important heat reservoir as a result of the higher operating temperature. The behavior of the reactor can best be understood if it is remembered that, roughly speaking, the reactor will regulate itself to produce steam at a constant rate so long as the positions of control rods are not changed. Since all the heat produced by the reactor need not necessarily go into the vaporization of water, the reactor will not necessarily regulate itself to a constant power output. Thus, for example, if cooled make-up water is injected during operation, heat will be required to raise the temperature of the water to the saturation point, and reactor power may be expected to increase if control rod positions are held constant. Again, if during reactor operation the pressure control valve allows reactor pressure to increase, extra energy will be produced by the reactor to heat the reactor water to the correspondingly higher saturation temperature. Variations of these kinds were observed during reactor operation. The pressure regulating valve was used with a wide proportional band, and the pressure maintained by the valve was, therefore, a (slowly varying) function of steam flow. Cold make-up water was injected as required to replace that boiled off. The injection was at a relatively fast rate, higher than the rate of evaporation attained in any of the runs; during any given run, therefore, water was injected either too rapidly or not at all, and neither process could be continued for long without running the reactor water level either too high or too low. Since the heat capacity of the reactor system was high, a relatively long time was required to attain thermal equilibrium. These circumstances, plus the desire to explore the effects of all system variables and to find any that might conceivably lead to instability, resulted in few runs at equilibrium conditions. It is, therefore, not possible to plot a curve giving power output as a function of reactivity, such as that which was obtained in the atmospheric pressure runs (Figure 54). It can be said, however, that the shape of such a curve for pressurized operation is qualitatively similar to that of Figure 54, and that the curve reaches a value of about 1200 kilowatts when the reactivity compensated by steam is about 2.8% k_{eff} . Further characteristics of the operation under pressurized conditions can best be demonstrated by showing detailed records of runs which were made under various operating conditions.

B. Records of Pressurized Boiling Runs

Figure 57 is a replotted record of a typical run. Saturation temperature of the reactor water, reactor power, and the reactivity compensated by steam are plotted as functions of time. The temperature is the saturation temperature corresponding to the pressure indicated by the reactor pressure recorder. The reactivity compensated by steam (Δk_s) was evaluated by taking the algebraic sum of the reactivity change due to control rod motions after initial criticality and the reactivity change caused by change in reactor temperature (Figure 25). The reactor power is that indicated by the ion chamber, calibrated as described in Appendix C. The power calibration should be more reliable for these runs than for the ones at atmospheric pressure, since the calibrations were made with the reactor actually boiling. As in the atmospheric case, rapid power oscillations, of frequency about 1.4 per second, occurred under certain operating conditions. These oscillations are not indicated in Figure 57 or in the following Figures 58 and 59; only the average power is plotted. The characteristic of the oscillations will be discussed in a later Section.

The record of Figure 57 begins after the reactor has been brought up to a power of about 150 kw. As reactor power was raised, the pressure maintained by the steam control valve increased, as shown by the increasing saturation temperature. During this interval, power was being used to raise the temperature of the reactor and its water, as well as to produce net steam, and a high total power was produced for relatively little reactivity compensated by steam. As an equilibrium pressure was established across the control valve, and the rate of reactor temperature rise decreased, it was necessary to increase the reactivity compensated by steam (by removing control rod) higher and higher to maintain the total power level. As equilibrium was established, a power level of about 900 kw was maintained with a reactivity of about 1.5% compensated by steam. During the latter part of the run, cold feed water was injected and the control rods were withdrawn further. A power level of about 1200 kw was established with 2.2% reactivity compensated by steam.

The steam dome of the reactor was provided with both a 2-inch and a 6-inch pressure control valve. Normal operation was on the 2-inch valve, with the 6-inch valve closed and set to open at some higher pressure for over-pressure relief. During the run shown in Figure 58, however, the 2-inch control valve was in operation and the 6-inch valve was under (remote) manual control. It was left closed until about 2:58 PM when it was opened slightly by the manual control and then closed again. The effect was a decrease in reactor pressure and the release, as steam, of some of the heat stored in the reactor water. The reactor total power, of course, decreased. During the interval from 2:58 to 3:11 PM some difficulty was experienced in getting the 6-inch valve completely closed, and it leaked a variable amount, as observed visually and as indicated by the variations in the

saturation temperature curve. These variations are reflected in reactor power. At 3:11 PM the 6-inch valve was opened wide momentarily, and both reactor pressure and power decreased sharply. The operation of opening and shutting the valve covered an interval of about half a minute. The power overshoot its equilibrium value by about 30% after reclosure of the valve. The energy involved in the overshoot was not enough to give any detectable increase in reactor pressure.

Figure 58 also shows (at 2:44 PM) the effect of turning off the electric immersion heaters and their associated circulating pump while the reactor was in operation. The sharp rise in power immediately after the heaters were turned off no doubt represented partially the assumption by the reactor of the heat load previously carried by the heaters, but it was also probably partially due to the fact that the heaters and pump had been feeding some steam directly into the inlet end of the reactor core. The heaters and pump were normally off during the reactor operation.

The effect of injection of cold make-up water was not completely consistent from run to run. In general it resulted in reactor power increase if control rod positions were maintained constant. But in some cases the effects appeared very shortly after the beginning of injection, whereas in other cases the increase in power built up gradually and reached its full value only after three or four minutes. It seems reasonable that these variations may be due to variations in the natural circulation flow pattern within the reactor at the time injection is begun. Thus, if the cold water is carried directly up through the center of the core, it should have a larger and more nearly immediate effect than if it mixes first with a large fraction of the water in the reactor tank. Figure 59 is a record of a run in which the effects of injection were particularly apparent. It seems probable that the metering orifice for the injection water may have, on this run, permitted larger injection flow than normal, because the effect of injection on reactor pressure is quite marked, whereas usually this effect was small. Figure 59 should, therefore, be considered as a qualitative demonstration only. In Figure 59 each period of injection caused an almost immediate rise in reactor power in all cases except the last (at 4:40 PM). The difference between the effects of the last injection and previous injections may be attributable to the fact that, contrary to usual practice, the circulating pump for the immersion heaters was being operated during the early part of the run (the heaters, however, were off). It seems reasonable that the operation of this pump did tend to channel the incoming injection water up through the center of the core. Just before the last period of water injection, the water level in the reactor had been allowed to become quite low -- lower in fact than the lower limit of the level indicator. This low water level probably accounts for the gradual decrease in power during the last part of the run.

The decreases in reactivity held by steam at 4:03 and 4:16 PM were made (by rod insertion) because power oscillations of rather large

amplitude had built up. During this run the injection of make-up water appeared to intensify power oscillations. This tendency was observed also in other runs, but to a lesser degree.

C. Rapid Fluctuations of Reactor Power

As in the case of boiling at atmospheric pressure, the fluctuations in reactor power were of two kinds: an irregular fluctuation of small amplitude when reactivity compensated by steam was less than about 2% k_{eff} , and an oscillation of definite frequency and higher amplitude for reactivities above about 2%. In pressurized operation, the amplitude of the irregular fluctuation was quite small, amounting to less than $\pm 5\%$ in all cases, and usually about $\pm 2\%$ to 3%. The transition from the irregular to the oscillatory variation occurred at a somewhat higher reactivity than at atmospheric pressure (at about 2% Δk_S as compared to about 1.6% Δk_S at atmospheric), and the oscillations when they did occur were smaller and more regular in shape than those at atmospheric pressure. Figure 60 is a plot of the ratio of maximum to minimum power resulting from rapid fluctuation, as a function of reactivity, for a number of pressurized runs. Each point represents the maximum rapid fluctuation that was found by examining the total length of the record at the indicated reactivity. The measurements were made on the Brush recorder data. This recorder is fast enough to measure the fluctuations accurately.

Figure 61 is a record of a complete boiling run, on which has been plotted the amplitude (ratio of maximum to minimum power) of the fast fluctuation. Note that the oscillations themselves are not plotted -- only the variation in their amplitude. This plot illustrates the way in which the oscillations build up and die out even when other operating conditions of the reactor are held constant. Figure 62 is a reproduction of the actual power charts from a portion of a run with steam-compensated reactivity less than 2% k_{eff} and illustrates the shape of the small irregular fluctuations. Figure 63 shows sections of the power charts near the end of the run plotted in Figure 61 and includes some of the largest oscillations observed. The shape of the oscillations changes with their amplitude, but the frequency remains relatively constant. Representative shapes of an oscillation of large amplitude and one of small amplitude are reproduced in Figure 64, with a sinusoidal variation drawn for comparison. The oscillations are arbitrarily normalized to the same amplitude, and the zero lines are arbitrarily shifted to make the curves coincide at their maximum and minimum points. It is evident that the larger oscillations have a sharper peak and a broader trough than the smaller ones. This characteristic shape is evidently largely the result of modification of an existing reactivity function of simpler characteristic by the nonlinear response of the reactor kinetic characteristic. O. A. Schulze, using a method suggested by J. W. Butler, has made a harmonic analysis of a typical power oscillation, and by numerical analysis has derived the shape of the reactivity variation causing the power

variation. The resulting reactivity curve can be fit by a cosine variation to within about 10%. For a ratio of maximum power to minimum power of 1.8, the required amplitude of the reactivity variation is about 0.5%.

D. Operation with Fixed Orifice

Two runs were made at a pressure of about 100 psig with the pressure control valve replaced by a fixed orifice. The purpose of these runs were for measurement of steam flow and for calibration of the ion chambers (Appendix C). Behavior of the reactor under this condition was not qualitatively different from that with the pressure control valve. Quantitatively the reactor pressure was, of course, much more strongly dependent upon steam flow, and the resulting effects were accentuated. Operation seemed to be a bit rougher but there was no evidence of instability.

E. Operation in Closed Vessel

In order to bring reactor temperature up to the desired value, the reactor was sometimes operated with all steam outlets closed. The early part of the run of Figure 61 was made under this condition. At 1:56 PM the valve took over control of the pressure, and the run proceeded in the usual way. During operation with the valve closed no unusual effects were observed, but only a small amount of reactivity was required to produce high power. This is, of course, to be expected since all of the heat produced goes into the reactor water, and the steam content of the core is quite small. Figure 65 is a replotted record of a closed vessel run of longer duration, and Figure 66 is a reproduction of the power record from a different run under the same conditions. Again no evidence of instability was observed. The self-regulating mechanism of the reactor during this type of operation is, of course, primarily temperature coefficient of reactivity, and if large reactivity changes are introduced into the reactor by external means, large power changes will result before the reactor finally reaches a new condition of equilibrium power.

F. Discussion of Boiling Operation

As an exploration of the possibilities of boiling reactors, the steady boiling tests were promising. They proved operation to be steady up to steam contents corresponding to at least 2% k_{eff} . At higher reactivities power irregularities occurred, but the resulting oscillatory boiling represents a stable regime which is maintained up to still higher reactivities (to at least 2.8% k_{eff} compensated by steam at 130 psig). At higher reactivities there was a sudden transition to a different region in which peak powers are much higher, but which is still stable in the sense that the peak power of the fluctuation does not increase with time.

It is, of course, hardly to be expected that a boiling reactor of the simple type investigated can be operated up to indefinitely large reactivities without the occurrence of power irregularities, since the removal

of steam by bubbling through long coolant passages involves inherent fluctuations, and only a small change in reactivity is required to cause a large change in power. Obviously, the greater the amount of reactivity compensated by steam in the reactor, the smaller will be the percentage variation in steam content required to produce a given percentage variation in power.

While there is no doubt a limit to the reactivity which can be compensated by steam without causing power fluctuations, there is no reason to believe that the 2 to 2½% limit observed in Borax, which was an exploratory experiment assembled of readily available parts, represents a fundamental limit.

In considering practical applications of boiling reactors, one is naturally interested in the magnitude of the power density that can be achieved. Quite evidently the Borax results do not give direct information on boiling reactors which might employ forced circulation. In drawing conclusions about natural-circulation reactors, the effect of changes in steam coefficient of reactivity must be considered. Low power density is inherent in the Borax design because the reactor is small, has high neutron leakage, and, therefore, a large negative steam coefficient of reactivity. This coefficient will decrease as a natural consequence of increasing the reactor size, as would be done in arriving at most practical designs. The reactor design can, in fact, be adjusted to give as low a value for the coefficient as may be desired, over a limited range of reactivity change. If the amount of reactivity compensated by steam is the only important variable in determining the onset of power fluctuations, the limiting steam fraction in the reactor and, presumably, the maximum power density, should be susceptible to large increases over those observed in Borax. This point has not as yet been determined.

The relatively slow increase in maximum power density attainable as pressure is increased, is in agreement with laboratory tests made at Argonne. These tests show that the ratio of power output to volume content of steam in electrically heated boiling channels increases only slowly as pressure is raised. The power densities observed in Borax are generally in rough agreement with the results of these laboratory tests.

Beyond the results discussed above which are of fundamental importance, the Borax experiment demonstrated certain characteristics of the boiling reactor which might be inferred once its stability has been proven. Most important of these is the fact that the reactor is self-regulating. Aside from some minor effects originating in the temperature coefficient of reactivity, the reactor at any given operating pressure regulates itself to produce a constant amount of steam power for any given constant position of the control rods. If the reactor is provided with power sinks other than vaporization of water, e.g., if cold water is injected into the reactor, the total power of the reactor will increase, while the steam content of the reactor is maintained automatically at a nearly constant value.

VII. SUMMARY OF RESULTS

The following is a brief summary of the Borax results:

1. The formation of steam and consequent ejection of water from the reactor core constitutes an effective, reliable, and fast acting inherent power limiting process which will protect properly designed water-cooled, water-moderated reactors from the effects of large excess reactivities even when the excess reactivity is added effectively instantaneously.

2. In a series of about 70 power excursions covering a wide range of excess reactivities and reactor temperatures the maximum power, total energy, and maximum fuel plate temperature increased smoothly and continuously with increasing excess reactivity and with increasing sub-cooling of the reactor. There was no indication of any sudden change in the general trends, or of any important individual deviations from the average curves.

3. When the externally imposed excess reactivity causing the power excursion was not removed by external means, the Borax reactor, after the initial power surge, would settle down to steady boiling operation or to a "chugging" operation, consisting of a continuing sequence of power surges of relatively constant amplitude lower than that of the initial surge, or to what appeared to be a permanently sub-critical state. The type of behavior exhibited depended on the magnitude of the applied excess reactivity and is expected to depend strongly on reactor design.

4. In power excursions made at saturation temperature, both the total energy released in the excursion, and the maximum fuel plate temperature, increased at a slowly increasing rate with the reciprocal of the exponential period of the excursion. The shortest period used was 0.005 second, corresponding to an excess reactivity of 2.1% k_{eff} . It resulted in a maximum fuel plate temperature of 640F and liberated a total energy of 24 megawatt seconds in the fuel plates.

5. For power excursions of constant period, the total energy release and maximum fuel plate temperature increased at a decreasing rate with the degree of initial subcooling of the reactor water. The most energetic excursion tested had a period of 0.013 sec with 43F subcooling. It released 13 megawatt seconds of energy in the fuel plates and resulted in a maximum plate temperature of 410F.

6. The rapidity of the power limiting process can be described by the observation that, in the excursions made, the power rose from 10% of peak value to peak value and returned to 10% of peak value in a time interval of from 3 to 4.5 exponential periods. The total energy release of the excursion was roughly equal to the product of maximum power times two exponential periods.

7. Roughly half of the total power released in any given excursion was stored in the fuel plates at the time they reached their maximum temperature.

8. The reactor was operated in steady boiling with the steam content of the core as high as that corresponding to 2.6% k_{eff} at atmospheric pressure, and with a steam content up to 2.8% k_{eff} at 130 psig.

9. At 130 psig power fluctuations were small in amplitude (less than $\pm 5\%$ maximum) and irregular in form when the steam content of the reactor corresponded to less than about 2% k_{eff} . At higher steam content power oscillations of characteristic frequency about 1.3 cycles per second appeared. Their amplitude increased with the steam content of the reactor. The maximum ratio of maximum to minimum power observed was 1.9. At atmospheric pressure the power fluctuations had similar characteristics, but were generally larger. When the steam content of the reactor corresponded to 2.6% k_{eff} , there was an abrupt transition from oscillatory boiling to mild "chugging," the peak power increasing from about 1.6 megawatts to about 60 megawatts. The amplitude of the "chugging" pulses did not increase with time.

10. The reactor was self-regulating in steady boiling, tending to produce a characteristic steam power output for any given control rod position at a given pressure. The reactor was operated at pressure with steam flow controlled by a pressure regulating valve, with steam release through a fixed orifice, and with no steam release (closed vessel). No evidence of instability was noted other than the power fluctuations described above.

11. The power output of the reactor increased at a decreasing rate with reactivity. Maximum power was about 850 kw at atmospheric pressure and 1200 kw at 130 psig. The latter value represented a power density of about 10 kw per liter of reactor core. This value is not expected to be characteristic of practical boiling reactors, which would be designed with a much lower steam coefficient of reactivity, and would presumably, therefore, reach higher power densities.

REFERENCES

1. G. Young, Existing Piles, Lectures 14 and 15, "Pile Technology," M-3445.
2. W. M. Breazeale, T. E. Cole, and J. A. Cox, "Preliminary Boiling Experiments in the LITR," Reactor Sci Technol, 2(2): 173-176 (August 1952).
3. W. M. Breazeale, T. E. Cole, and J. A. Cox, "Further Boiling Experiments in the LITR," Reactor Sci Technol, 2(4): 186-191 (December 1952).
4. J. M. West and J. T. Weills, "Supplement to a Report to the Atomic Energy Commission on the Proposed Argonne Research Reactor (CP-5)," ANL-WHZ-299, May 7, 1951.
5. J. R. Dietrich, D. C. Layman, and O. A. Schulze, "The Proposed Boiling Reactor Experiment," ANL-4921, November 12, 1952.
6. "Homogeneous Reactor Project Quarterly Progress Report, for Period Ending July 31, 1953," Part II: Boiling Reactor Research, ORNL-1605, October 20, 1953.
7. H. R. Kroeger, "A 1000 kw Reactor Power Plant," BAC-RL-610, June 15, 1953.
8. W. B. Allred and H. C. Savage, "Critical Bending Load on Fuel Assembly Curved Plates," ORNL-CF-48-7-65.
9. N. M. Dismuke and M. R. Arnette, "Age to Thermal Energy of Fission Neutrons in H₂O-Al Mixtures," MonP-219.
10. J. L. Meem, E. B. Johnson, and H. E. Hungerford, "Energy per Fission and Power of the BSR," ORNL-CF-53-5-21.

APPENDIX A

Detailed Composition and Calculated Nuclear Constants of Borax Reactor

The following compilations of reactor composition and calculations of reactor constants were made prior to the Borax experiments by O. A. Schulze. Initial criticality was predicted correctly, and the effects of fuel additions were foreseen with reasonable accuracy; hence these quantities have not been re-examined since the experiments.

Core Description

The active core is composed of four quadrants separated by channels into which the central control rod and the four blade control rods can move. The subassemblies are located symmetrically about the control rod channels. The number of subassemblies can be varied up to a maximum of 36.

The following table gives pertinent information on the fuel assemblies:

Table I

COMPOSITION AND DIMENSIONS FOR BORAX FUEL ASSEMBLIES

Parts	18 curved plates containing fuel - 2 side plates of 2S Al - spacing between fuel plates 0.117 in.
<u>Fuel Plates</u>	
<u>Core Dimensions</u>	
Length	23.625 in. = 60.00 cm
Width before curving	2.5 = 6.350
Thickness	0.021 = 0.05334
<u>Over-all Dimensions</u>	
Length	24.625 in. = 62.55 cm
Width before curving	2.845 = 7.226
Thickness	0.060 = 0.1524
<u>Composition</u>	
U ²³⁵ content/plate	7.70 gm
Core Al	99.75% pure
<u>Side Plates</u>	
Length (over active core)	23.625 in. = 60.00 cm
Width	3.186 = 8.092
Thickness	0.188 = 0.4775
<u>Slots Between Fuel Plates</u>	
Length	23.625 in. = 60.00 cm
Width	2.62 = 6.655
Thickness	0.117 = 0.2972
<u>Spacing Between Adjacent</u>	
Side Plates	0.039 in. = 0.0991 cm
<u>Unit Cell</u>	
Length	23.625 in. = 60.00 cm
Width	3.035 = 7.7089
Thickness	3.260 = 8.2804

Cell Metal to Water Ratio

The actual metal to water ratio will depend upon the actual fuel subassembly loading because of the presence of the control rod channels which will be filled with water when the rods are out. The first step was to calculate the ratio for the cell (Table 2). Modification for the loading of fuel was then made.

Table 2

CALCULATION OF CELL METAL/WATER RATIO

Part	Name	Length (cm)	Width (cm)	Thickness (cm)	No.	Volume (cm ³)
a	Cell	60.00	7.7089	8.2804	1	3830.0
b	Water between fuel plates	60.00	6.655	0.2972	18	2136.1
c	Water between assemblies	60.00	7.7089	0.094	2	87.0
d	Water between adjacent side plate	60.00	8.092	0.0496	2	48.2
e	Total water (sum b+c+d)					2271.3
f	Total metal (a-e)					1558.7
	Metal/Water = 0.6863					

Control Rod Channels

The actual clearance for the control rods is 0.375 in. for both channels. However, due to the symmetric placement of the fuel assemblies about the centerline, the channel which runs parallel to the fuel plates (herein called the X channel) varies from a minimum between the tips of the side plates of 0.375 in. to a maximum between fuel plates of 0.956 in.

Since in the above calculation the unit cell contains a sheet of water adjacent to the side plates as well as water between the subassemblies, the equivalent widths are 0.625 in. and 0.336 in. for the X and Y channels respectively.

Two-Group Constants

Table 3 lists the macroscopic absorption and transport cross sections which were used in the calculations.

Table 3

NUCLEAR CONSTANTS

Substance	$\bar{\Sigma}_a^*$		Σ_{tr}	
	0.025 ev (68F) cm ⁻¹	0.0316 ev (200F) cm ⁻¹	0.025 ev cm ⁻¹	0.0316 cm ⁻¹
U ²³⁵	27.485	23.722	--	--
H ₂ O**	0.019551	0.016660	2.09876	1.89201
Al	0.011752	0.010453	0.084	0.084

*Averaged over Maxwellian distribution.

**H₂O density assumed: $\rho = 1$ at 68F, $\rho = 0.958$ at 200F.

The age τ was calculated from the following formula:

$$\tau = \frac{\tau^*}{(1 - \alpha)^2}$$

where τ^* was obtained from reference 8 wherein the calculated values of τ for various Al to H₂O ratios were normalized to $\tau = 33$ cm² for pure H₂O.

$\alpha = (1 - \rho_{H_2O}) \times$ fraction of volume occupied by H₂O = fractional void.

Reasonable values for reflector savings based on previous calculations of totally water reflected water-aluminum cores were assumed.

It has been found that MTR fuel assemblies of the type to be used do not give as much reactivity as calculations indicate. It is believed that the difficulty lies in the entrapment of brazing flux containing appreciable amounts of lithium and chlorine. Hence it was reasonable to incorporate a certain amount of distributed poison, calculated as follows: Extrapolation of the data obtained from critical experiments performed on the Bulk Shielding Facility at Oak Ridge indicated that a completely water-reflector core of MTR fuel assemblies would go critical in a 5 by 5 array giving a critical mass of 3.45 kg. Hence, using the above size and critical mass and constants calculated in the above manner, an absorption cross section for the poison was obtained, $\Sigma_a^{\text{distributed poison}}$ (0.025) ev = 0.003, which was 4.1% of the total absorption cross section. A proportionate amount of distributed poison was then incorporated in the calculations.

Self-Shielding of Fuel Plates

Estimates were made of the amount of self-shielding of the fuel by solving for the flux of monoenergetic neutrons in a lattice of alternate slabs of fuel and water. A solution for the flux in the fuel (assuming no scattering) was obtained from the Boltzmann integral transport equation; while in the water region a diffusion theory solution was obtained.

The effect of self-shielding was to reduce the U^{235} cross section by 2%. This value of self-shielding was used throughout the calculations.

Flux Peaking

Experiments in the ZPR have indicated that there was a considerable rise in thermal flux in a water channel. On the basis of those experiments, a 40% increase in thermal flux in control channel Y and a 100% increase in X was assumed, and the absorption of neutrons in the water in those channels was correspondingly increased. This procedure probably overestimates the effect of the water channels on reactivity since the beneficial effect of increased flux in the fuel adjacent to the water channels was neglected.

Reactivity Calculations

The reactivity of various rectangular arrangements of fuel assemblies was calculated at two temperatures, 68F and 200F. Reactivity was calculated from the formula:

$$\frac{\Delta k}{k} = \frac{k_{\infty} - (1 + L^2 B^2)(1 + \tau B^2)}{k_{\infty}}$$

where B^2 is the geometric buckling. Reflector savings were assumed to be the same for all faces of the reactor. The active core height was 60 cm in all cases. The calculated constants are given in Table 4.

Table 4

REACTIVITY CALCULATIONS

Number of Assemblies			Constants												
X dir.	Y dir.	Total	Temp. °F	Ratio Al/H ₂ O	Σ_a Al cm ⁻¹	Σ_a H ₂ O cm ⁻¹	Σ_a poison cm ⁻¹	Σ_a 25 cm ⁻¹	k_{∞}	L^2 cm ²	τ cm ²	$B^2_{geom.}$ cm ⁻²	Reflector Savings cm	$\frac{\Delta k}{k} \%$	
6	4	24	68	0.617	0.004483	0.013123	0.002705	0.048107	1.48064	3.3816	58.7	0.008091	7.88	-1.65	
			200	0.644	0.003988	0.011183	0.002406	0.041520	1.48946	4.3322	63.03	0.007862	8.30	-3.83	
6	5	30	68	0.626	0.004523	0.012882	0.002730	0.048551	1.48853	3.4292	59.1	0.007067	7.90	3.10	
			200	0.653	0.004023	0.010977	0.002428	0.041903	1.49727	4.3926	63.54	0.006880	8.33	1.11	
6	6	36	68	0.632	0.004553	0.012720	0.002746	0.048852	1.50377	3.4621	59.4	0.006398	7.92	6.20	
			200	0.660	0.004049	0.010839	0.002442	0.042163	1.50245	4.4345	63.74	0.006238	8.35	4.41	

APPENDIX B

Transient Instrumentation

Data desired for transient analyses included, besides the total energy measured by foils, reactor power, reactor period, and fuel plate temperature. Attempts to record pressure transients were in most cases unsatisfactory, but a description of these circuits is included. These data were fed to a Heiland oscillograph and recorded. Switches in the control trailer turned the oscillograph off and on and also controlled the chart drive so that selected data could be recorded. The oscillograph accommodated twenty-four galvanometers, more than were ever used simultaneously. Mirrors responding to the individual galvanometer movements displaced light beams, and the signals were recorded as traces on photographic paper. In addition, reactor power was recorded at the control trailer by Brush recorders for operational information. A diagram of the instrumentation is shown in Figure 67.

Boron-coated ionization chambers were used to indicate reactor power, with logarithmic amplification to permit their use over wide ranges on a single record chart. Of three chambers recorded by the Heiland oscillograph, one was of multiparallel plate construction, with gamma compensation. The other chambers were simple uncompensated parallel plate chambers. Both types of chambers, by operation in the CP-2 reactor, were shown to be linear up to output currents of 10^{-5} amp, and to depart little from linearity for currents up to 10^{-4} amp. The logarithmic amplifiers used gave a very nearly linear logarithmic response over an input current range of 10^7 . The small departures from logarithmic output which did occur were calibrated and corrected for. Negative feedback in the amplifier circuit reduced the input time constant and resulted in the frequency response characteristic shown in Figure 68. Since the impedance of the input diode of the amplifier changes with input current to give the desired logarithmic characteristic, the frequency response of the amplifier is a function of the input current. It is evident from Figure 68 that the frequency response is quite adequate for input currents of 10^{-8} amp or higher. It was not difficult to choose locations for the ion chambers such that the important part of the record would be obtained in the current range between 10^{-8} and 10^{-5} amp, where both frequency response and linearity were adequate. The galvanometer used for recording of the ion current had a natural frequency of 450 cycles per second, and was used with 60% to 70% damping (per cent damping equals 100 times ratio of critical damping resistance to damping resistance used). Galvanometer lag resulted in a slight phase shift in the ion chamber records. Corrections were made for this shift where necessary by A. J. Ulrich, using a method suggested by J. W. Butler, which substituted the first and second derivatives of the galvanometer record directly into the differential equation of motion of the galvanometer to determine the true driving function.

The magnitude of the correction is indicated in Figure 69, which shows the galvanometer trace and the corrected curve for one of the fastest transients recorded. The three ion chambers were used on three separate channels; a differentiating circuit was available for one channel to record reactor period when desired.

A fourth nuclear channel used a compensated ion chamber with linear amplification. This signal, together with a logarithmic amplifier signal, was sent to the control trailer where both were reamplified and recorded by Brush recorders. These recorders followed transients sufficiently well to serve as operational guides.

For all results reported here, the fuel plate thermocouples were connected directly to the galvanometers, although Brush amplifiers were available if necessary. The surface thermocouple, which was developed by R. J. Schiltz, consisted of two 3-mil wires, one chromel and the other alumel, percussion welded separately to the surface of the fuel plate at points about 1/4 inch apart. The thermocouple thus consisted actually of a chromel-aluminum and an alumel-aluminum thermocouple in series, with the two aluminum junctions at the same temperature. Since the plate surface itself acted as a junction, the thermocouple followed the surface temperature rapidly and accurately except for any cooling of the surface by conduction along the chromel and alumel wires. Such heat losses obviously were negligible. The installation at the center of the fuel plate, in the uranium-aluminum alloy, is shown diagrammatically in Figure 70. A hole of relatively large diameter was bored to the center of the fuel plate, and the thermocouple wires were welded to the plate alloy. The hole was then filled with a lavite plug, and the surface was covered with plastic cement. Both the center and surface thermocouple wires terminated after about one-half inch, in larger chromel and alumel wires which were covered with glass insulation and threaded through a small diameter aluminum tube leading back to the cold junction box. The lower end of the aluminum tube was sealed with plastic cement. The galvanometers used for thermocouple reading were slower than those used on the ion chambers, in order that more sensitivity might be attained. The natural frequency was 100 cycles per second, and they were used with 60% to 70% damping. Figure 71 shows the correction to the galvanometer record for one of the fastest temperature transients recorded. Corrections were made to all temperature records which were used in such a way as to require it.

The pressure transducers were devices in which movements of a diaphragm (following pressure changes) were detected by strain gauge resistance bridges, and the unbalance signal amplified and recorded. Batteries were used as the power supply, with a switch at the control trailer to turn the power supply off and on as desired. Brush amplifiers were used

to amplify the pressure signals, which were then fed to the Heiland oscillograph. Since the amplifiers had a moderately high drift rate, span and zeroing adjustments were made controllable from both the control trailer and the reactor trailer.

The pressure transducers were mounted on top of the core, and sampled the pressure at mid-core level by thin-walled steel probe tubes which extended down into the core coolant passages.

Photographic records were obtained by mounting both still and motion picture cameras near the reactor and controlling exposure timing from the control trailer. For excursions with periods longer than 15 milliseconds, the cameras were located at the side of the control rod drive superstructure and photographed (through mirrors) the water surface disturbances. With shorter period excursions the expulsion of water from the reactor would have damaged photographic equipment near the reactor. The cameras were, therefore, moved back to give only a general view of the reactor.

APPENDIX C

Power Calibration of Ion Chambers

Conversion of ion chamber readings to reactor power during steady boiling operation was complicated by the circumstances that neutron leakage from the reactor core varied with water temperature and with the steam content of the core, and neutron transmission through the reflector varied with water temperature. The latter variation was quite large because the thickness of the water reflector was several neutron attenuation lengths. The factor for converting ion chamber reading to reactor power thus varied with reactor power and water temperature. A number of calibrations were, therefore, made which employed three different methods and which covered several different operating conditions. The several calibrations are described below.

A. Comparison of Heating Rates

This method compared the heating rate of the reactor when a known amount of electrical heat was added to the system with a comparable heating rate obtained when the reactor was held at constant fission power (chamber reading). Three determinations were made: September 15-17, 1953; October 13, 1953; October 21, 1953.

Since the temperature rise of the reactor represents the net difference between the total heat input and heat losses, it was necessary to determine heat losses through cooling curves. Two sets of data were taken, one on September 17 and one on October 21, 1953:

<u>Date</u>	<u>Mean Temp.</u>	<u>ΔT</u>	<u>Time</u>	<u>$^{\circ}\text{F}/\text{min}$</u>	<u>kw*</u>
September 17	161 $^{\circ}\text{F}$	1.9 $^{\circ}\text{F}$	20 min	0.095	16
October 21	290 $^{\circ}\text{F}$	22.4 $^{\circ}\text{F}$	60 min	0.373	62.3

*Heat capacity of reactor and external system = 9500 Btu/ $^{\circ}\text{F}$.

The heat loss may be assumed to occur between the reactor at a temperature "T" to a constant heat sink (ground at temperature " T_b ") and approximated by the expression

$$kw = a(T - T_b)^{3/2}$$

This reduces to

$$kw = 0.020(T - 73)^{1.5}$$

The relation between the surface areas and thermal insulation of the reactor tank and the pre-heating systems shows that this heat loss is almost equally divided between the two, and the losses are:

$$kw_{\text{reactor}} = 0.01(T-73)^{1.5}$$

$$kw_{\text{cir.system}} = 0.01(T-73)^{1.5}$$

1. Run of September 15, 1953

Input kw from heaters	= 155
Input kw from pump	= <u>11.2</u>
Total heat input	= 166.2 kw

Heating curve start	= 126°F
finish	= 179°F
ΔT	= 53°F
Duration	= 60 min
Rate of temperature rise	= 0.883°F per min

Estimated total heat loss

$$kw_{\text{total}} = 0.02(153-73)^{1.5} = 14.2 \text{ kw}$$

$$\text{Net heat to reactor} = 166.2 - 14.2 = 152 \text{ kw}$$

$$\text{Heat capacity of reactor} = \text{kw} \times 56.9 \frac{\text{Btu}}{\text{kw-min}} \times \frac{1}{\text{°F/min}}$$

$$= 152 \times 56.9 \times \frac{1}{0.883}$$

$$= 9600 \frac{\text{Btu}}{\text{°F}}$$

The heat capacity of the external circulating pre-heat system was 360 Btu/°F, and the net heat capacity of the reactor was 9240 Btu/°F.

On September 17, 1953, the reactor was heated by fission heat. The water level was such that the net heat capacity of the reactor was 91% of that measured on September 15, or 8400 Btu/°F. The temperature rise was 10.6°F in 10 minutes, or 1.06°F/min. The mean temperature was 163°F.

Heat Loss

$$kw_{\text{reactor loss}} = 0.01(163-73)^{1.5} = 8.5 \text{ kw}$$

Heat appearing as sensible heat of reactor

$$\text{kw} = \frac{^{\circ}\text{F}}{\text{min}} \times \frac{\text{Btu}}{^{\circ}\text{F}} \times \frac{\text{min-kw}}{56.9 \text{ Btu}} = 1.06 \left(\frac{8400}{56.9} \right) = 156 \text{ kw}$$

Total fission heat = $156 + 8.5 = 164.5 \text{ kw}$

The mean ion chamber reading was $6.4 \text{ } \mu\text{amp}$.

$$\text{Calibration} = \frac{164.5}{6.4} = 25.7 \frac{\text{kw}}{\mu\text{amp}}$$

2. Runs of October 13, 1953

During these tests, an electrical heat input temperature rise was measured and followed by a fission power heating rate. No cooling curve was taken.

Preliminary measurements indicated that the heaters were delivering 162 kw, and the pump 15 kw, so that the total power input was 177 kw. A temperature rise of 50°F in 54.5 minutes was measured, with the mean temperature being 175°F .

$$\text{kw}_{\text{heat loss}} = 0.02(175-73)^{1.5} = 21 \text{ kw}$$

$$\text{kw input} = 177 \text{ kw}$$

Net kw to reactor sensible heat = 156 kw

$$\text{Rate of temperature rise} = \frac{50}{54.5} = 0.917^{\circ}\text{F}/\text{min}$$

$$\text{Heat capacity of system} = (156 \times 56.9 / 0.917) = 9700 \text{ Btu}/^{\circ}\text{F}$$

$$\text{Heat capacity of reactor} = 9340 \text{ Btu}/^{\circ}\text{F}$$

Heating the reactor by fission heat yielded a temperature rise of 12°F in 15 minutes, or $0.77^{\circ}\text{F}/\text{min}$. The mean temperature was 172°F .

$$\text{kw}_{\text{heat loss}} = 0.01(172-73)^{1.5} = 10 \text{ kw}$$

$$\text{kw sensible heat} = \frac{9340(0.77)}{56.9} = 125 \text{ kw}$$

Total fission heat = 135 kw

The scale reading was $5.46 \text{ } \mu\text{amp}$.

$$\text{Calibration} = \frac{135}{5.46} = 24.7 \frac{\text{kw}}{\mu\text{amp}}$$

3. Runs of October 21, 1953

During these tests an electrical heating rate, a fission heating rate, and a cooling curve were taken. The cooling data were previously used to determine the formula for heat losses.

The fission heating curve was derived during closed tank, pressurized operation, and shows a discontinuity shortly after the start of the run. This was due to the pressure control valve cracking open and bleeding steam.

The electrical heating run showed the rate of temperature rise as 48.4°F/hour, the mean temperature being 245°F. The electrical system was not calibrated, and the 177 kw value obtained on October 13 was used.

$$\text{kw}_{\text{system loss}} = 0.02(245-73)^{1.5} = 45 \text{ kw}$$

$$\text{kw input} = 177 \text{ kw}$$

$$\text{Net kw to reactor as sensible heat} = 132 \text{ kw}$$

$$\begin{aligned} \text{Rate of temperature rise} &= 48.4^\circ\text{F/hr} \\ &= 0.81^\circ\text{F/min} \end{aligned}$$

$$\text{Heat capacity of system} = 132 \times 56.9 \times \frac{1}{0.81} \text{ Btu}/^\circ\text{F} = 9300 \text{ Btu}/^\circ\text{F}$$

$$\text{Heat capacity of reactor} = 9300 - 340 \text{ Btu}/^\circ\text{F} = 8960 \text{ Btu}/^\circ\text{F}$$

Only the initial period of the reactor fission heating run is valid for calibrating data. Plotting the saturation temperatures derived from the pressure record, and the temperature record itself, leads to an indicated 3.1°F/min temperature rise; mean temperature was 297°F. An unknown amount of steam was present in the core.

$$\text{kw appearing as sensible heat} = \frac{3.1^\circ\text{F}}{\text{min}} \times \frac{8960}{56.9} = 490 \text{ kw}$$

$$\text{kw heat loss} = 0.01(297-73)^{1.5} = 31 \text{ kw}$$

$$\text{Total fission heat} = 521 \text{ kw}$$

The chamber reading was 31 μamp , so

$$\text{Calibration} = \frac{521}{31} = 16.8 \frac{\text{kw}}{\mu\text{amp}}$$

B. Heat Balances Based on Steam Flow Measurements

1. Runs of October 21, 1953

Run #6 of October 21: This and run #1, October 22, were runs in which the steam generated was metered and discharged to the atmosphere, and a reactor heat balance established. Several approximations must be made:

- a. The reactor water level was increased by injection twice throughout the run. The data analyzed started when reactor level was low, just before a period of injection, and finished with an unrecorded level. Assume reactor sensible heat to be 9000 Btu/°F.
- b. Various notations of injection rates indicate that the rate of injection was approximately 2.5 pounds per second. This was never accurately metered.
- c. Temperature of the injected water was assumed to be 50°F.
- d. Injected water was well mixed, and temperature distribution was uniform.

	<u>Time</u>	<u>Reactor Pressure</u>	<u>Temperature</u>
Start	12:42	94 psia	323.4°F
Finish	1:01	90 psia	320.3°F
	19 min		-3.1°F

Mean orifice pressure = 90.1 psia

Orifice diameter = 1.004 in.

Injection period = 8.5 min

Latent Heat of System

From the orifice calibration, Appendix D:

$$\text{Flow area} = \frac{\pi D^2}{4} + 0.025 = \frac{\pi}{4}(1.004^2) + 0.025 = 0.815 \text{ sq in.}$$

$$\text{Flow} = 0.0198 AP^{0.91} = 0.0198 (0.815)(90.1)^{0.91} = 0.969 \text{ lb/sec}$$

At 94 psia mean, $h_{fg} = 892.3 \text{ Btu/pound}$

$$\begin{aligned}\text{Heat to form steam} &= \frac{\text{pounds}}{\text{sec}} \times \frac{60 \text{ sec}}{\text{min}} \times h_{fg} \times \text{min.} \\ &= 0.969(19)(892.3)(60) = 98.6 \times 10^4 \text{ Btu}\end{aligned}$$

Sensible Heat to Reactor

$$\text{Sensible heat} = c_p \Delta T = 9000 (-3.1) \text{ Btu} = -2.8 \times 10^4 \text{ Btu}$$

Sensible Heat to Injection Water

$$\text{Injection time} = 8.5 \text{ min} = 510 \text{ sec}$$

$$\text{Total injection} = 510 \times 2.5 = 1.28 \times 10^3 \text{ pounds}$$

$$\text{Sensible heat} = 1.28 \times 10^3 (322-50)(1) = 34.8 \times 10^4 \text{ Btu}$$

Reactor Heat Loss

$$\text{Heat loss} = 0.01(322-73)^{1.5} = 40 \text{ kw} = 40(19)(56.9) = 4.33 \times 10^4 \text{ Btu}$$

$$\begin{aligned}\text{Total fission heat} &= 98.6 \times 10^4 \text{ Btu (steam)} \\ &\quad 34.8 \times 10^4 \text{ Btu (injection)} \\ &\quad \underline{4.3 \times 10^4 \text{ Btu (heat loss)}} \\ &137.7 \times 10^4 \\ &\quad \underline{-2.8 \times 10^4 \text{ Btu (reactor sensible heat)}} \\ &134.9 \times 10^4 \text{ Btu}\end{aligned}$$

Also,

$$\text{Mean power} = \frac{134.9 \times 10^4}{19 \times 56.9} = 1270 \text{ kw}$$

Calibration

The average scale reading was 79.8 μ amp, and

$$\text{Calibration} = \frac{1270}{79.8} = 15.9 \frac{\text{kw}}{\mu\text{amp}}$$

2. Runs of October 22, 1953

Run #1, October 22, 1953. An 0.868 inch orifice was used to increase reactor pressure over Run #6, October 21, 1953. Since no extensive period of stability was established, two parts of this run are analyzed.

The first period, 11:47 to 11:56, was a period of increasing pressure with no injection. As in 1:

	<u>Time</u>	<u>Reactor Pressure</u>	<u>Temperature</u>
Start	11:47	104.6 psia	331°F
Finish	11:56	118.2 psia	341°F
	9 min		10°F

Mean orifice pressure = 109.1 psia

Orifice diameter = 0.868 in.

No injection period

Latent Heat of Steam

$$\text{Orifice area} = \frac{\pi}{4}(0.868)^2 + 0.025 = 0.617 \text{ in.}$$

$$\text{Flow} = 0.0198 (0.617)(109)^{0.91} = 0.864 \text{ lb/sec}$$

$$\text{At } h_{fg} = 882.5 \text{ Btu/lb}$$

$$\text{Heat to form steam} = 0.864 (9)(60)(882.5) = 41.2 \times 10^4 \text{ Btu}$$

Sensible Heat to Reactor

$$\text{Sensible heat} = (10)(9200) = 9.2 \times 10^4 \text{ Btu}$$

Reactor Heat Loss

$$kw = 0.01(336-73)^{1.5} = 50 \text{ kw}$$

$$\text{Heat loss} = 50 (56.9)(9) = 2.6 \times 10^4 \text{ Btu}$$

Total Fission Heat

$$\text{Total fission heat} = 41.2 \times 10^4 \text{ Btu}$$

$$9.2 \times 10^4 \text{ Btu}$$

$$2.6 \times 10^4 \text{ Btu}$$

$$\hline 53.0 \times 10^4 \text{ Btu}$$

$$\text{Mean power} = \frac{53.0 \times 10^4}{9 \times 56.9} = 1035 \text{ kw}$$

Calibration

The average scale reading was 82.5 μamp , and

$$\text{Calibration} = \frac{1035}{82.5} = 12.6 \frac{\text{kw}}{\mu\text{amp}}$$

✓

The second period, from 11:58 to 12:18, was a period of decreasing pressure, with 7.7 minutes of injection.

	<u>Time</u>	<u>Reactor Pressure</u>	<u>Temperature</u>
Start	11:58	117.2 psia	339.5°F
Finish	12:18	90.0 psia	320.3°F
	20 min		-19.2°F

Mean orifice pressure = 101.1 psia

Injection period = 7.7 min

Latent Heat of Steam

$$\text{Flow} = 0.0198 (0.617)(101)^{0.91} = 0.813 \text{ lb/sec}$$

At $h_{fg} = 888 \text{ Btu/pound}$

$$\text{Heat to form steam} = (0.813)(60)(20)(888) = 86.6 \times 10^4 \text{ Btu}$$

Sensible Heat to Reactor

$$\text{Sensible heat to reactor} = 9200(-19.2) = -17.7 \times 10^4 \text{ Btu}$$

Reactor Heat Loss

$$\text{kw} = 0.01(330-73)^{1.5} = 43 \text{ kw}$$

$$\text{Heat loss} = 43 (56.9)(20) = 4.9 \times 10^4 \text{ Btu}$$

Sensible Heat to Injection Water

$$\text{Injection time} = 7.7 \text{ min} = 462 \text{ sec}$$

$$\text{Total injection} = 462 \times 2.5 = 1.15 \times 10^3 \text{ pounds}$$

$$\text{Sensible heat} = 1.15 \times 10^3 (330-50) = 32.2 \times 10^4 \text{ Btu}$$

$$\begin{aligned} \text{Total fission heat} = & 86.6 \times 10^4 \\ & 4.9 \times 10^4 \\ & 32.2 \times 10^4 \\ \hline & 123.7 \times 10^4 \\ & -17.7 \times 10^4 \\ \hline & = 106.0 \times 10^4 \text{ Btu} \end{aligned}$$

Also,

$$\text{Mean power} = \frac{106 \times 10^4}{20 \times 56.9} = 931 \text{ kw}$$

Calibration

Mean scale reading was 63.4 μamp ,

$$\text{Calibration} = \frac{931}{63.4} = 14.7 \frac{\text{kw}}{\mu\text{amp}}$$

C. Foil Activation

On September 21 a number of cobalt foils were distributed through the reactor core to measure the power distribution and were activated by reactor operation under boiling conditions at atmospheric pressure. Three identical foils were exposed by R. G. Cochran, in the Bulk Shielding Reactor at Oak Ridge National Laboratory, to a calibrated integrated thermal flux. By comparison of the foil counting rates, the integrated thermal flux in the Borax reactor was determined. The total energy liberated during the Borax operation was determined from the integrated flux by the relations of reference 10 on the assumption that the activation cross section of cobalt and the fission cross section of U^{235} have the same variation with neutron energy.

The total energy of the run, as determined from the foils, was 77 megawatt seconds. The integrated ion chamber reading during the run was 4070 microampere seconds. The resulting ion chamber calibration is 18.9 kilowatts per microampere. The Borax running time during the calibration was about 2.5 minutes. The average power during the run was, therefore, about 500 kilowatts.

D. Calibration Curves

The results of the various calibrating runs have been plotted in Figure 72 as a function of the reactor temperature at which they were made. Calculations were made of the fractional leakage of neutrons from the reactor to the outer edge of the reflector at various water temperatures, assuming an effective reflector thickness of 10 in. Such calculations were made with no steam void in the reactor core, and with 10% void. The absolute magnitudes of these leakage curves were consistently but arbitrarily normalized to make the two curves fall among the experimental calibration points, as shown in Figure 72. The no-void curve thus falls near the points of September 17 and October 13, which resulted from runs with no boiling, and the 10% void curve falls near the remainder of the points, which were made with at least some boiling in the reactor. These two curves were taken to define the ion chamber calibration. Curves for other void contents were added, using the same calculation and normalization as for the curves of Figure 72. The ion chamber calibration for any given operating conditions was then read from the set of curves at the appropriate water temperature and void content. The void content for any given operating condition was determined from the reactivity compensated by steam, assuming a steam coefficient of reactivity of 0.25% k_{eff} per per cent steam void.

APPENDIX D

Measurement of Steam Flow Through an Orifice at Critical Pressure

The theoretical flow of a perfect gas through an orifice when the downstream pressure is less than critical pressure (approximately 50% of the upstream pressure) is given by:

$$w = CA_2P_1 \left[\frac{g}{RT_1} k \left(\frac{2}{k+1} \right)^{\frac{k+1}{k-1}} \right]^{\frac{1}{2}}$$

where, in consistent units,

w = wt flow rate

A_2 = throat area of orifice

P_1 = upstream pressure

g = gravitational constant

R = gas constant

k = ratio of specific heats

C = flow coefficient

T_1 = upstream temperature (absolute)

The value of the flow coefficient "C" is dependent upon the orifice design and is not well established for critical flow conditions. For non-critical flow, the value of "C" through a square edged orifice is approximately 0.60; this is due to the fact that the true flow area associated with the orifice is much smaller than the actual area of the orifice throat, i.e., the jet continues to contract beyond the orifice. For a well rounded convergent orifice "C" approaches 1.0 (as for a nozzle) and may be closely approximated at 1.0 for critical flow. This is the basis for the Grashof formula for critical steam flow through a well rounded orifice:

$$w = 0.0165 A P^{0.97}$$

where w = wt flow, pounds per sec

A = throat area, square inches

P = absolute upstream pressure, pounds per square inch.

The introduction of "P" as a power function approximates the departure from perfect gas laws.

The use of a square or sharp edged orifice for critical pressure flow measurements yields a poorly predictable flow coefficient due to jet formation, but gives the most reproducible geometry when subsequent calibration is to be made. For this reason, a square edged orifice, machined according to ASME Test Code Specifications was used to meter steam flow during the pressurized runs of the boiling reactor experiment, and a subsequent calibration of the system was made at Argonne National Laboratory.

The piping arrangement shown in Figure 73 very closely approximates the metering arrangement of Borax. It permits the metering of steam flow through the critical orifice by a non-critical (low pressure drop) orifice installed according to Test Code Specifications, and introduced the same arrangement of condensate bleed holes and thermocouple placement. Two critical orifice plates were calibrated: one with a throat diameter of 0.800 in., and one with a throat diameter of 1.000 in. The calibration curve so obtained is represented by Curve 74 and reduces to

$$w = 0.0198 A P^{0.91}$$

where w = pounds steam per second

A = throat area in square inches plus 0.025 square inch
(area of bleed holes)

P = absolute upstream pressure

The formula so obtained is probably accurate within 2 - 3% .

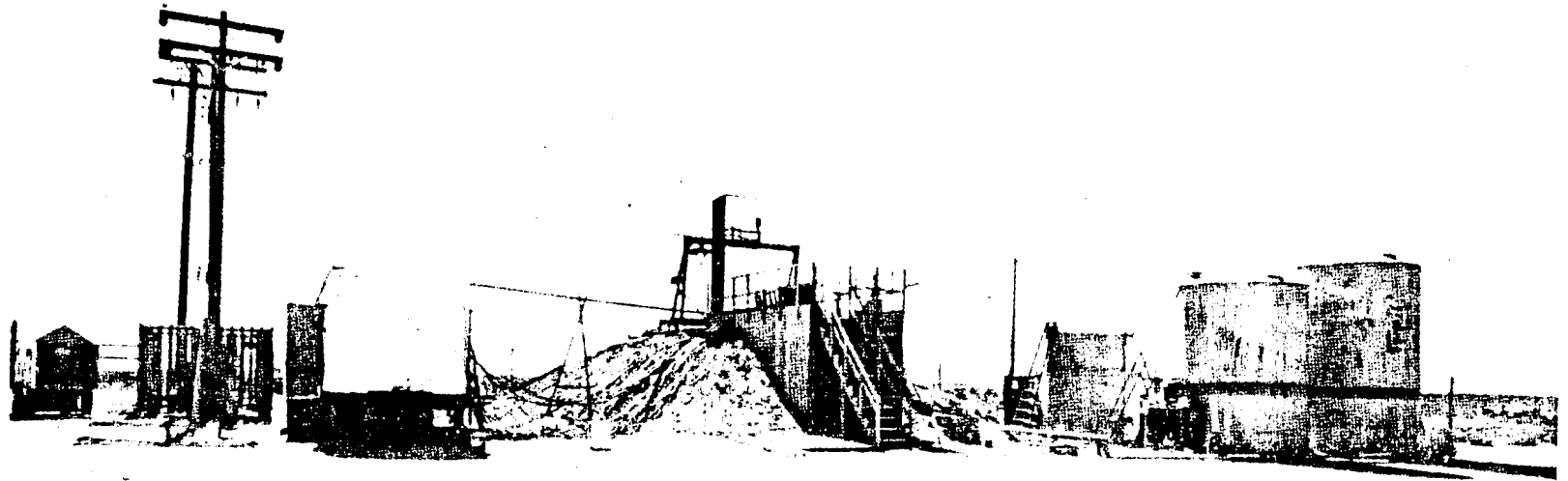


FIG. 1
REACTOR SITE

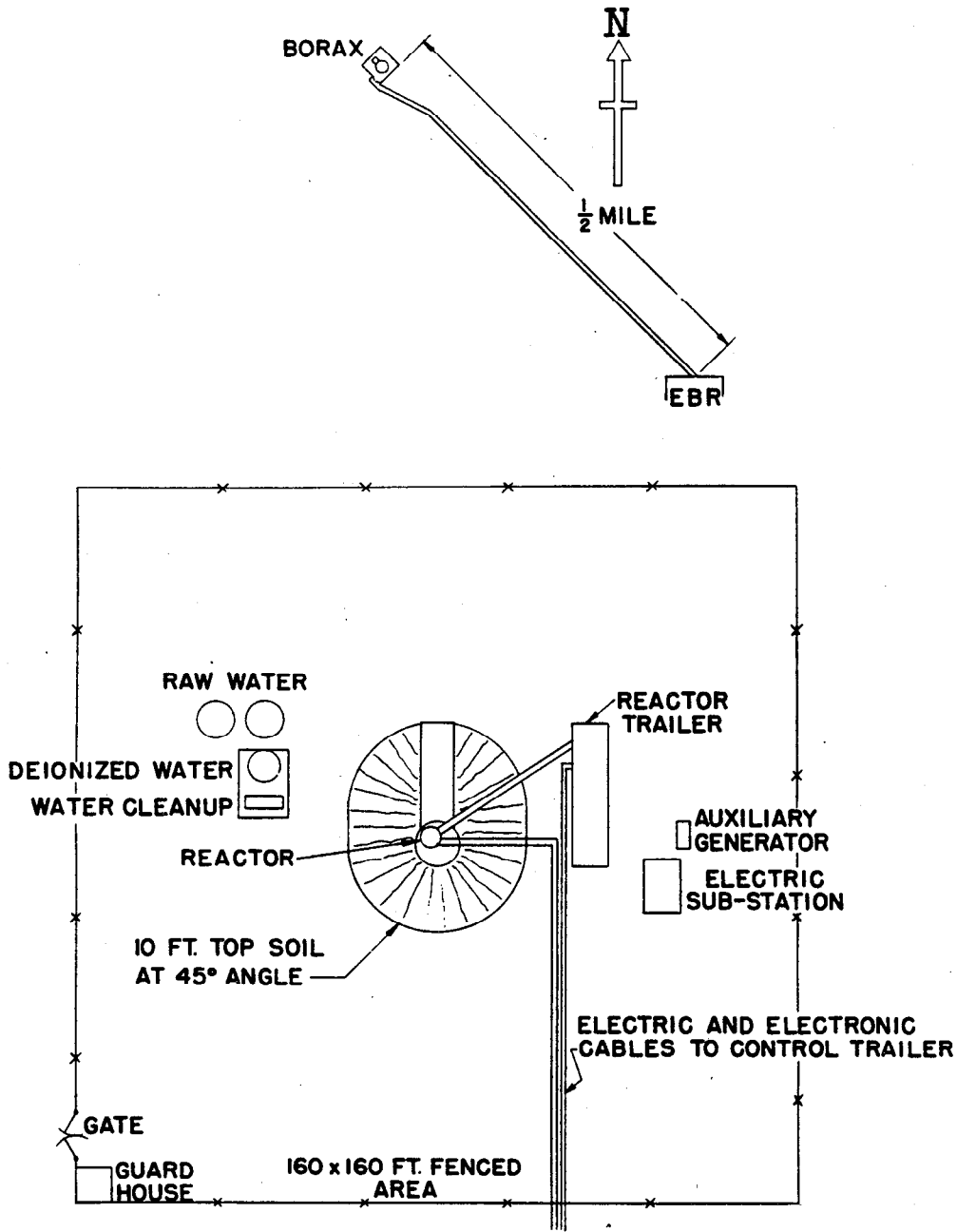


FIG. 2
SITE PLAN FOR BORAX

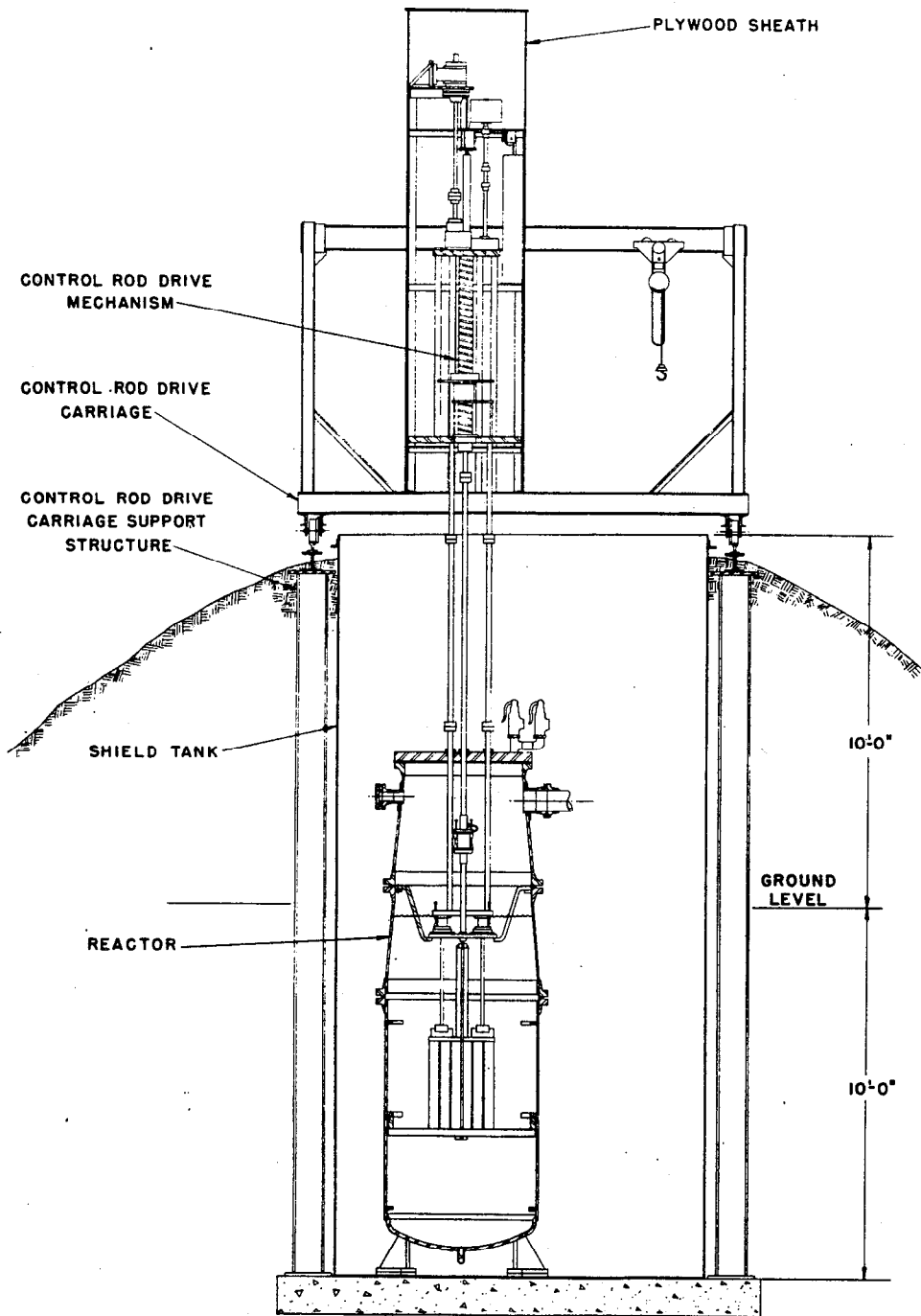


FIG. 3
BORAX VERTICAL SECTION

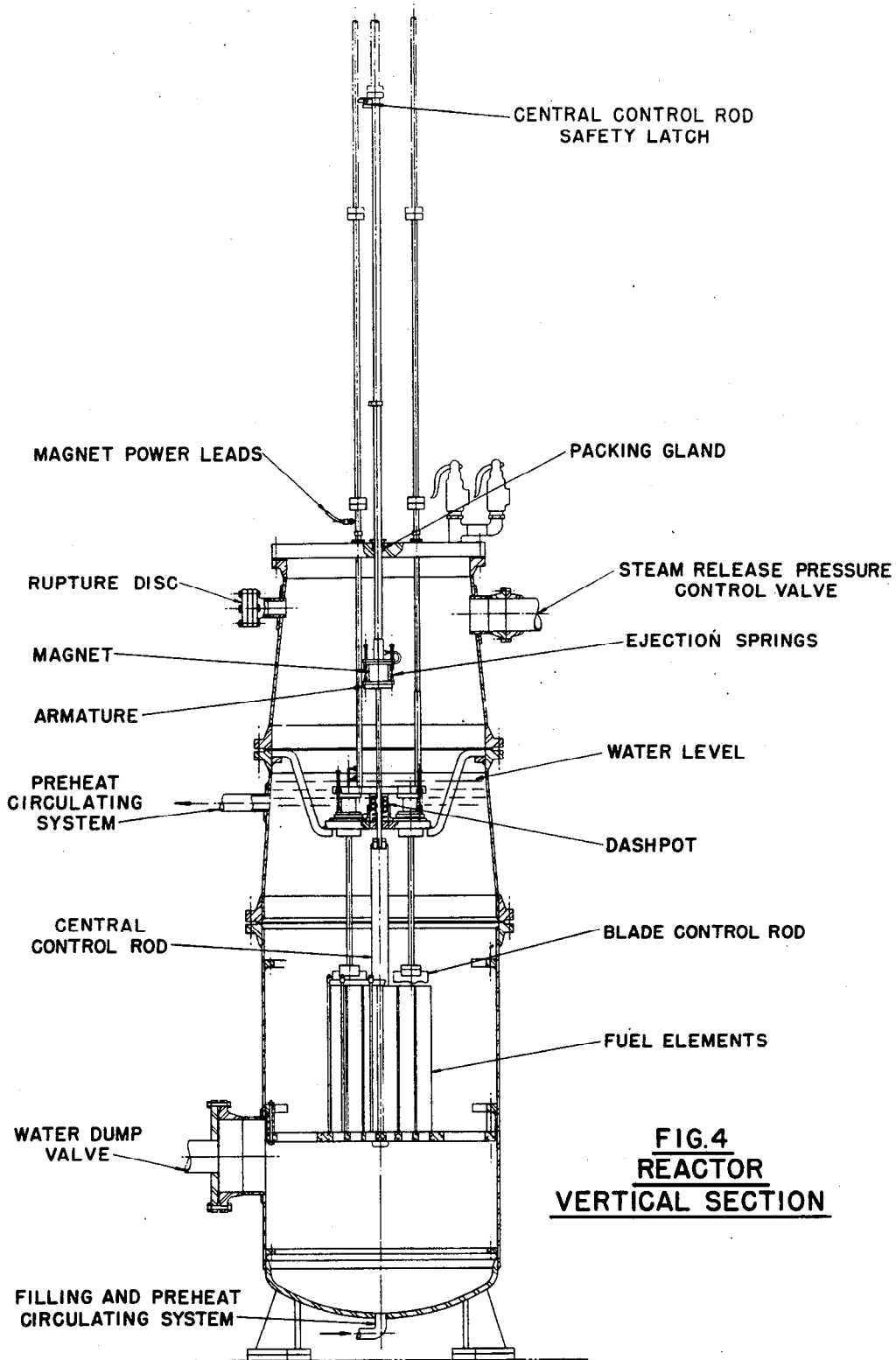


FIG.4
REACTOR
VERTICAL SECTION

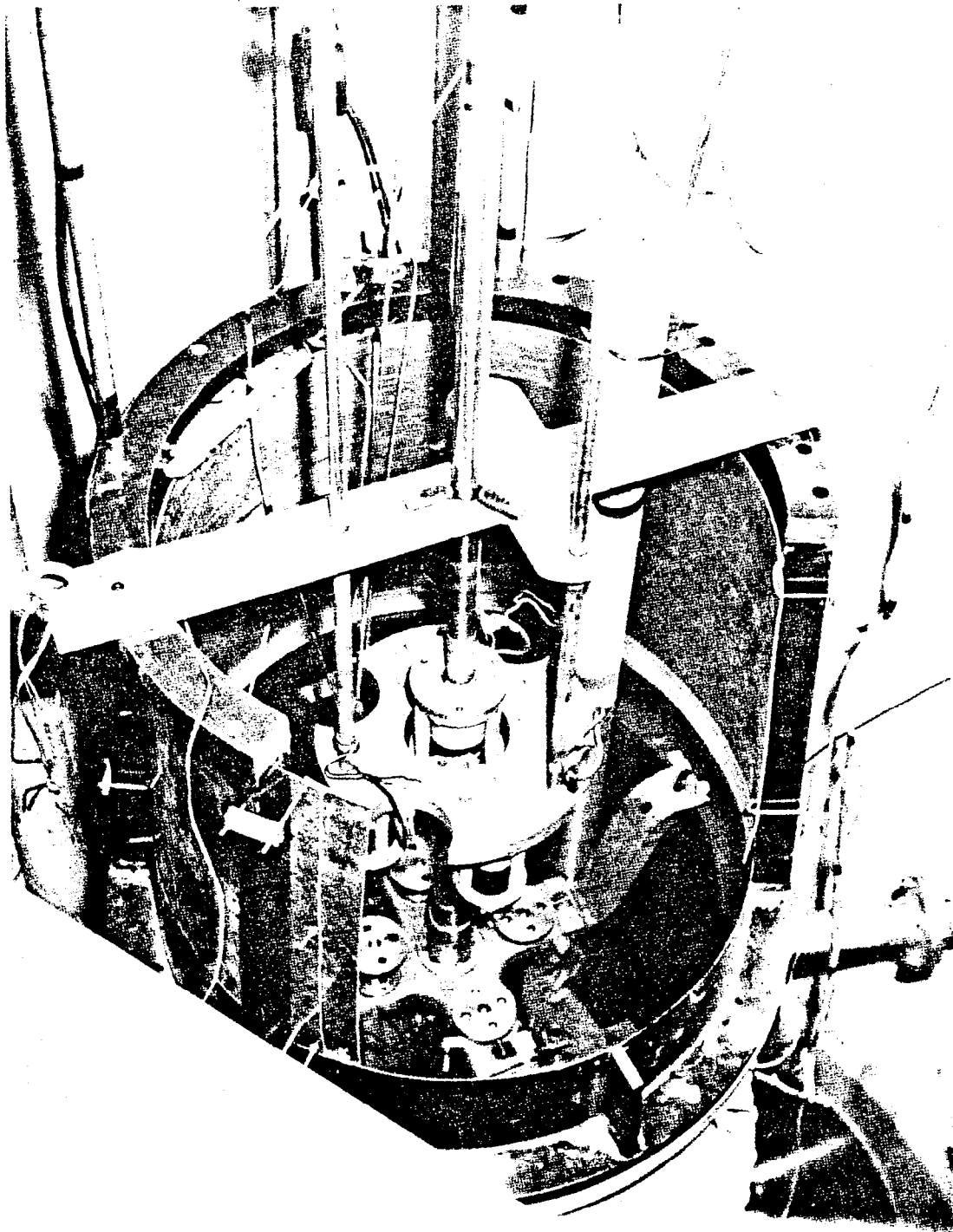


FIG. 5
MAGNET ASSEMBLY DETAILS

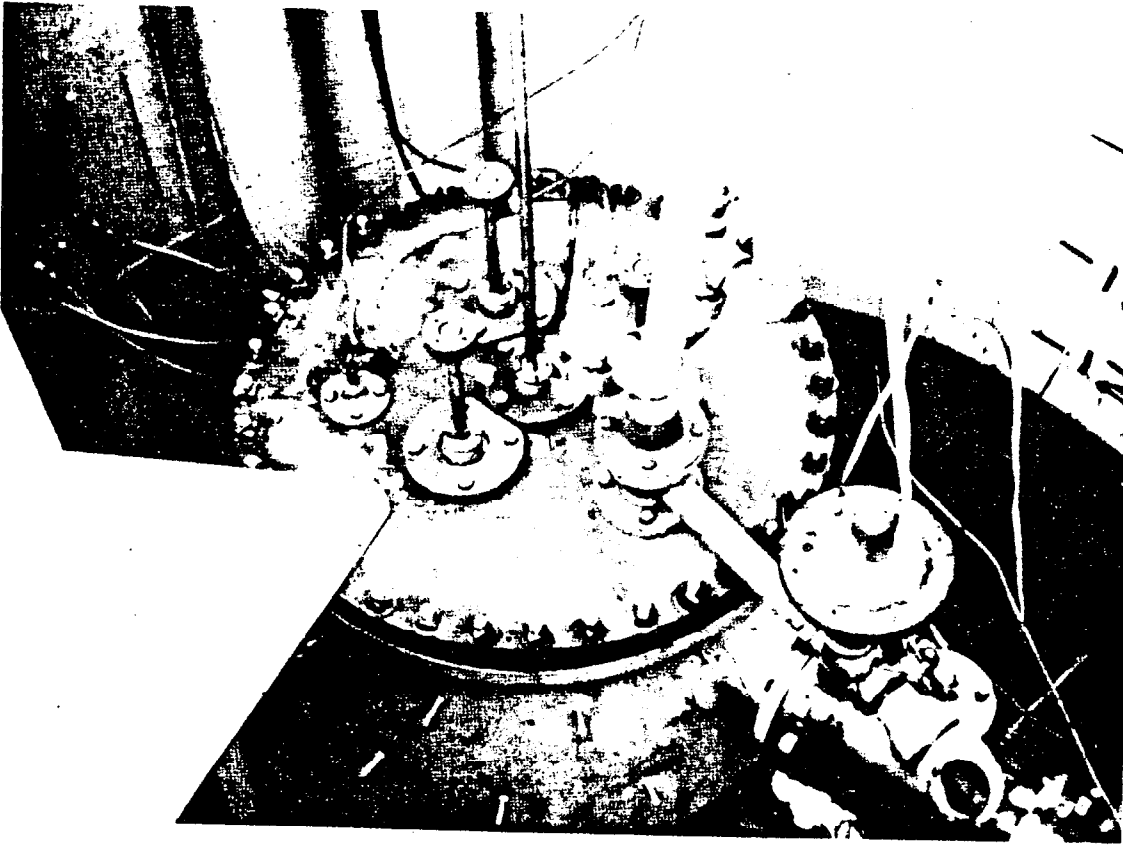


FIG. 6
PRESSURIZED REACTOR TOP VIEW

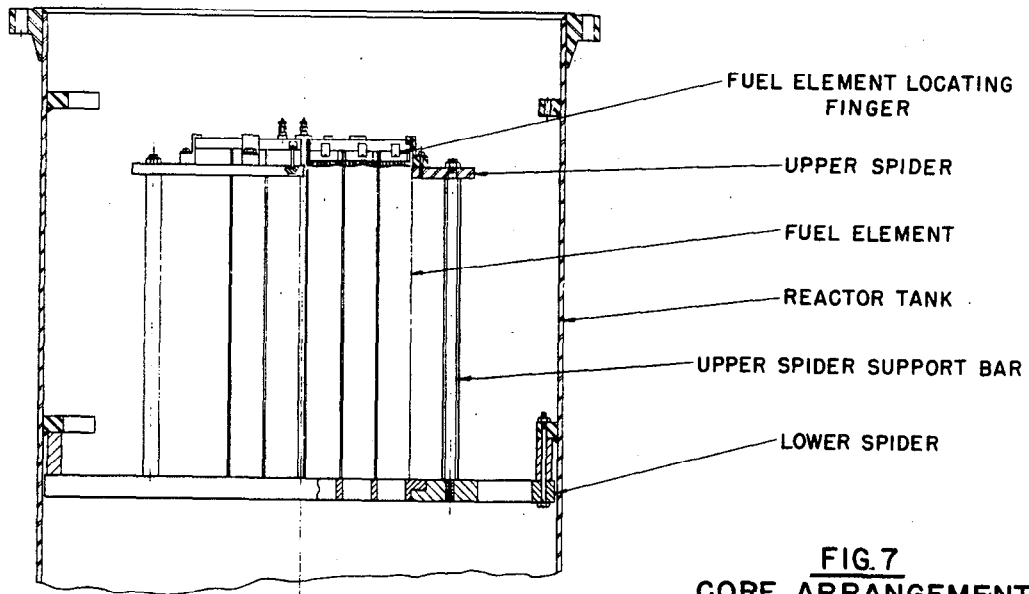
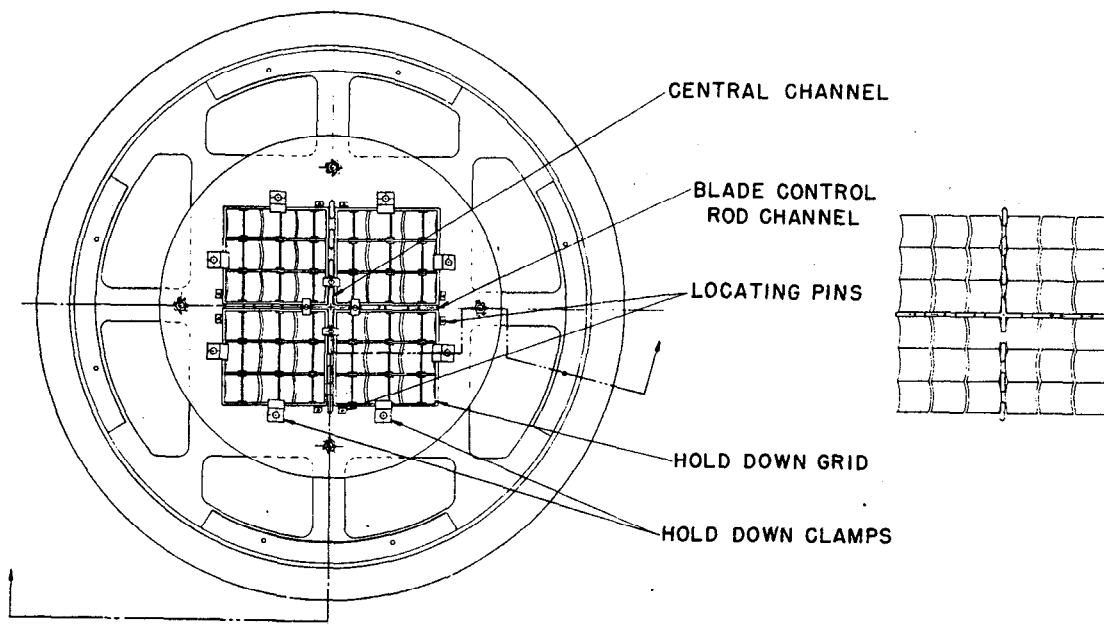


FIG. 7
CORE ARRANGEMENT

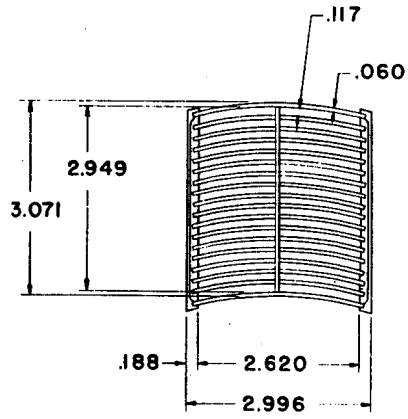
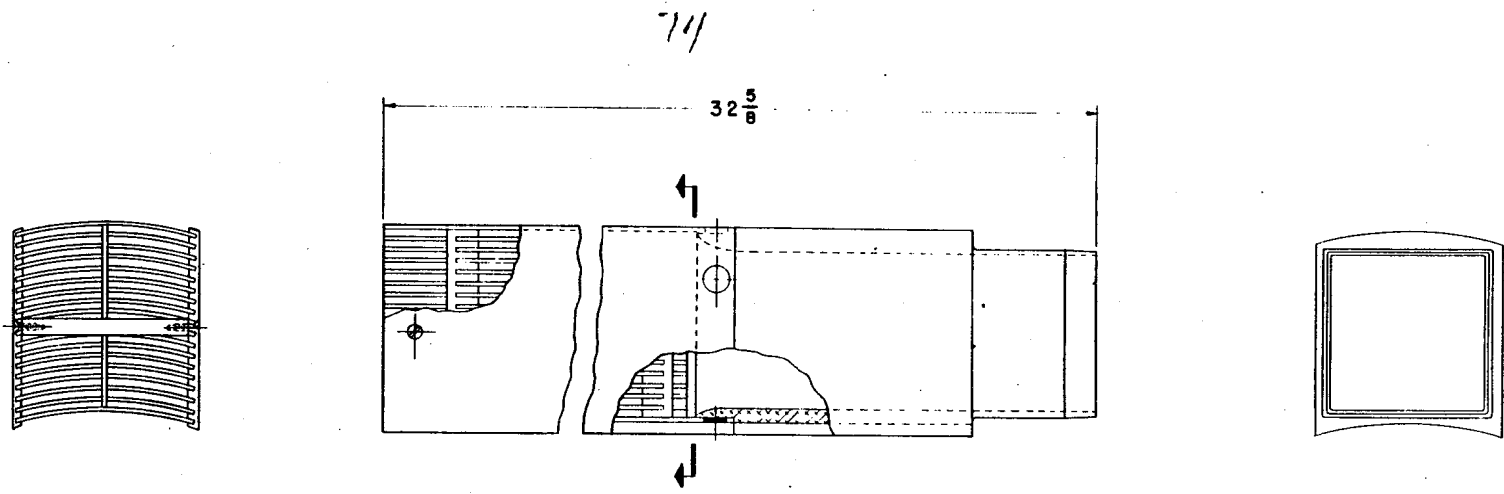


FIG. 8
STANDARD FUEL ASSEMBLY

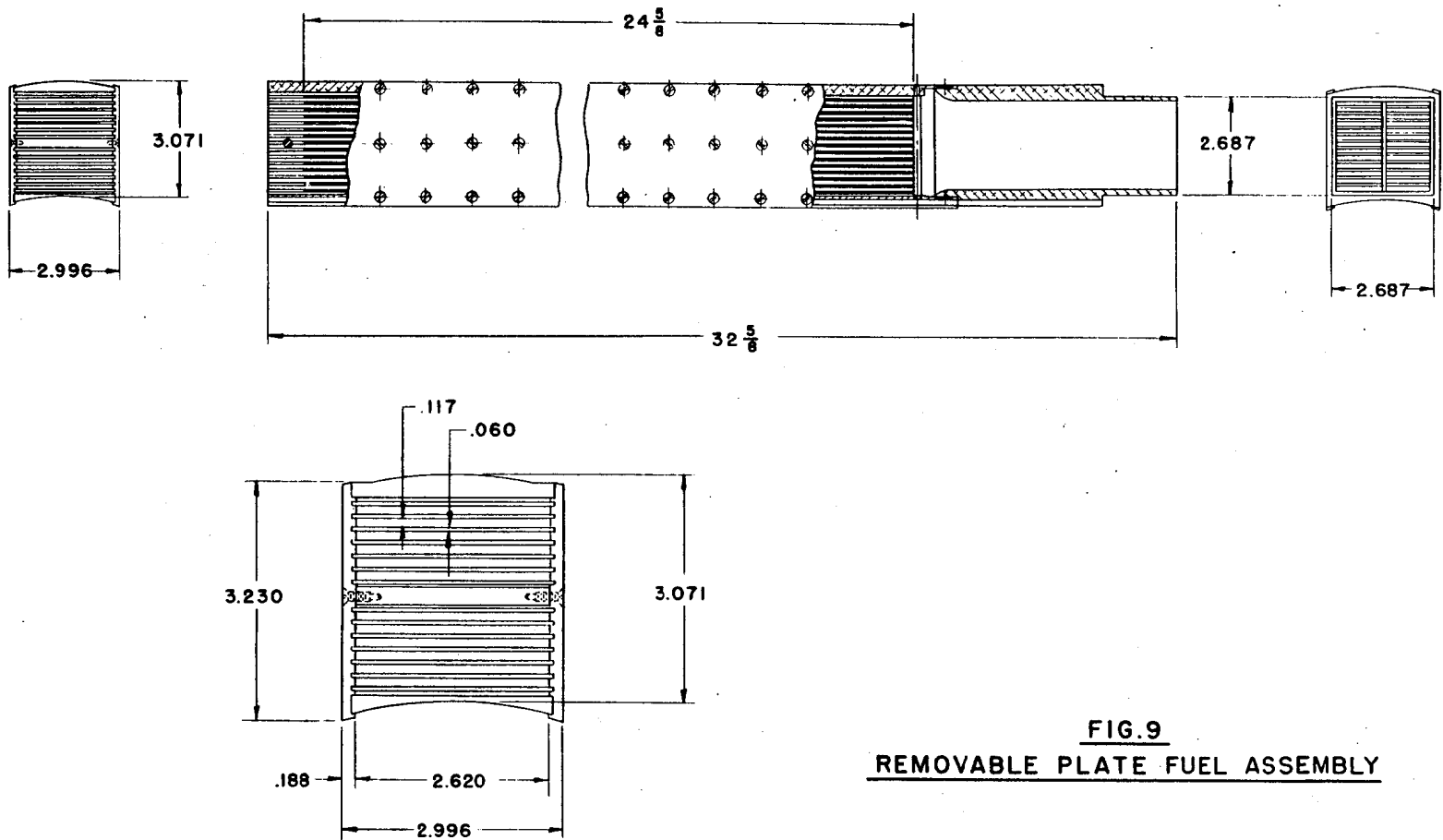
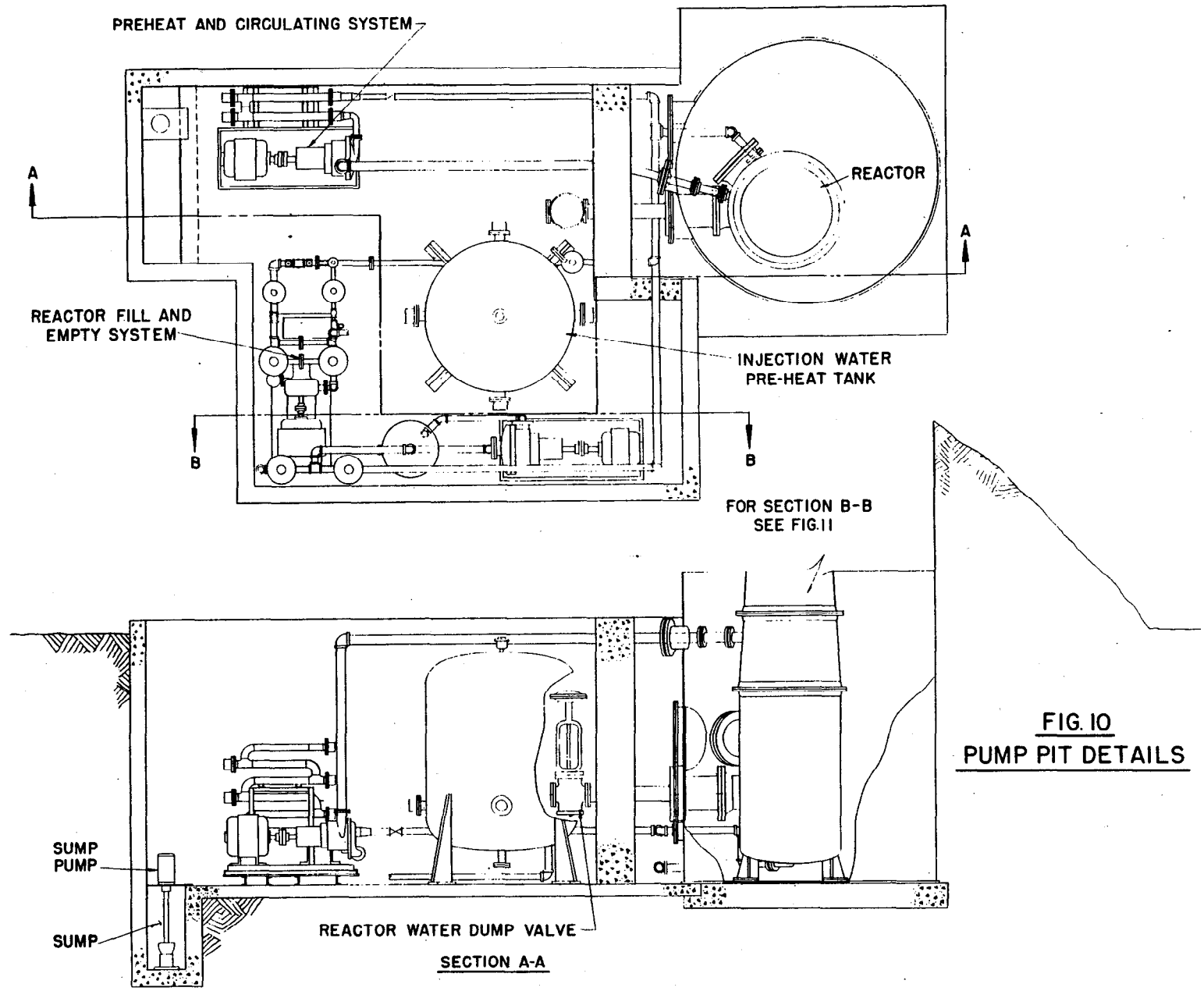


FIG. 9
REMOVABLE PLATE FUEL ASSEMBLY



11

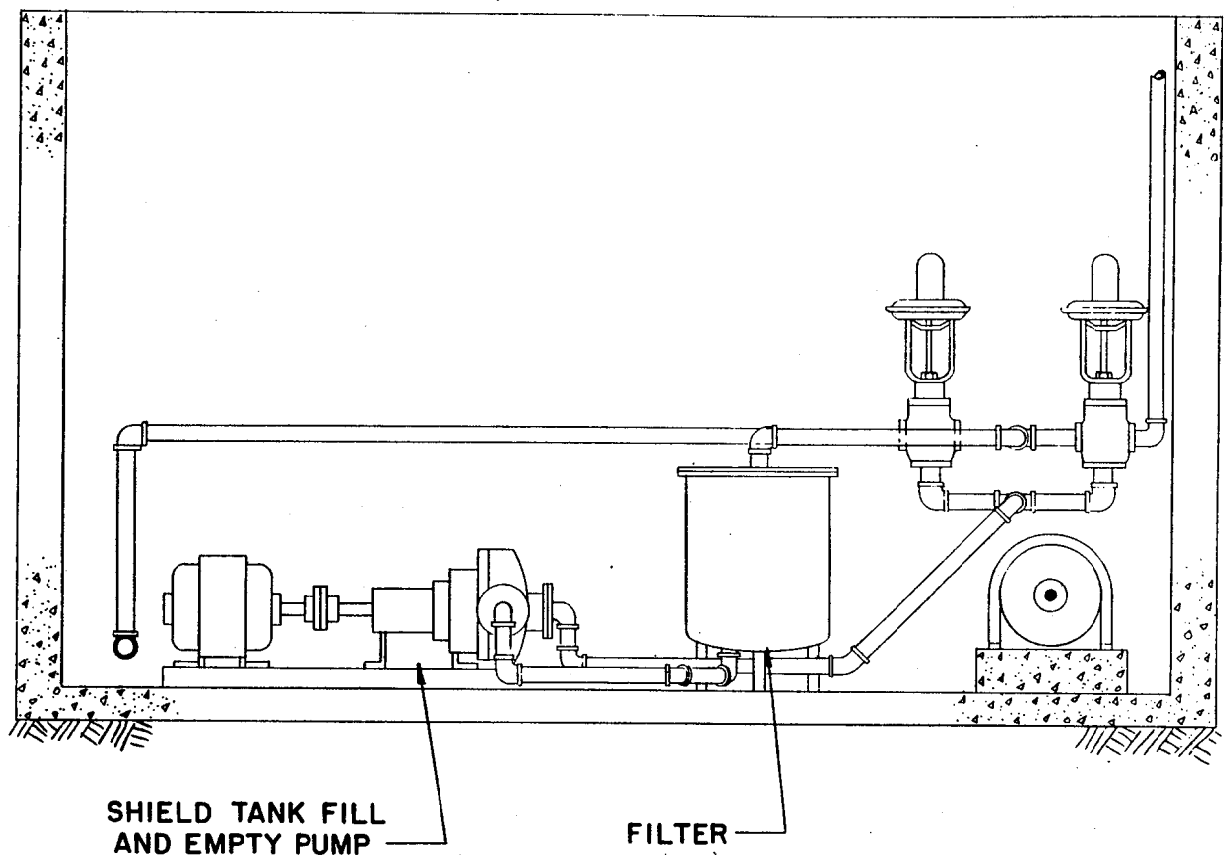


FIG. II
PUMP PIT DETAILS
SECTION B-B

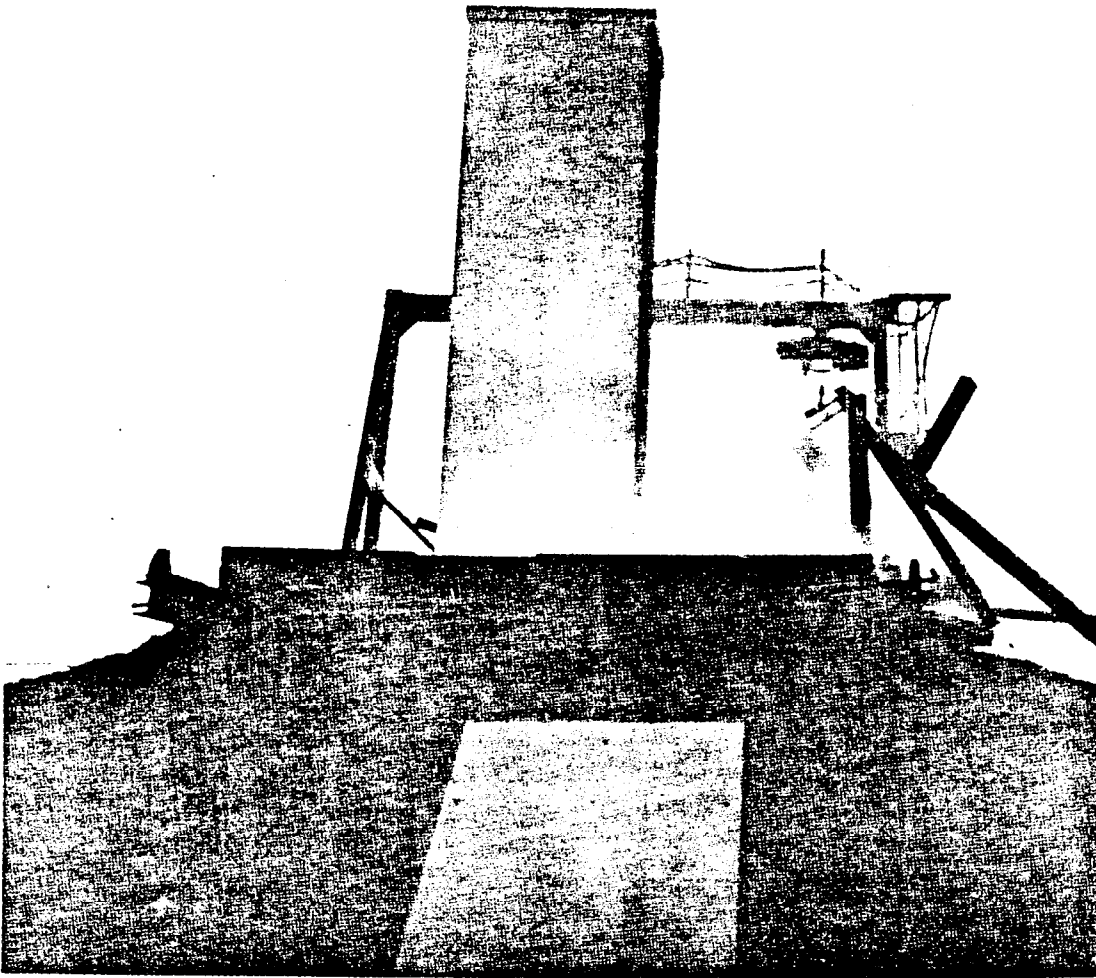


FIG. 12

CONTROL ROD DRIVE STRUCTURE

NOTE MIRRORS MOUNTED FOR PHOTOGRAPHIC RECORDS OF TRANSIENTS

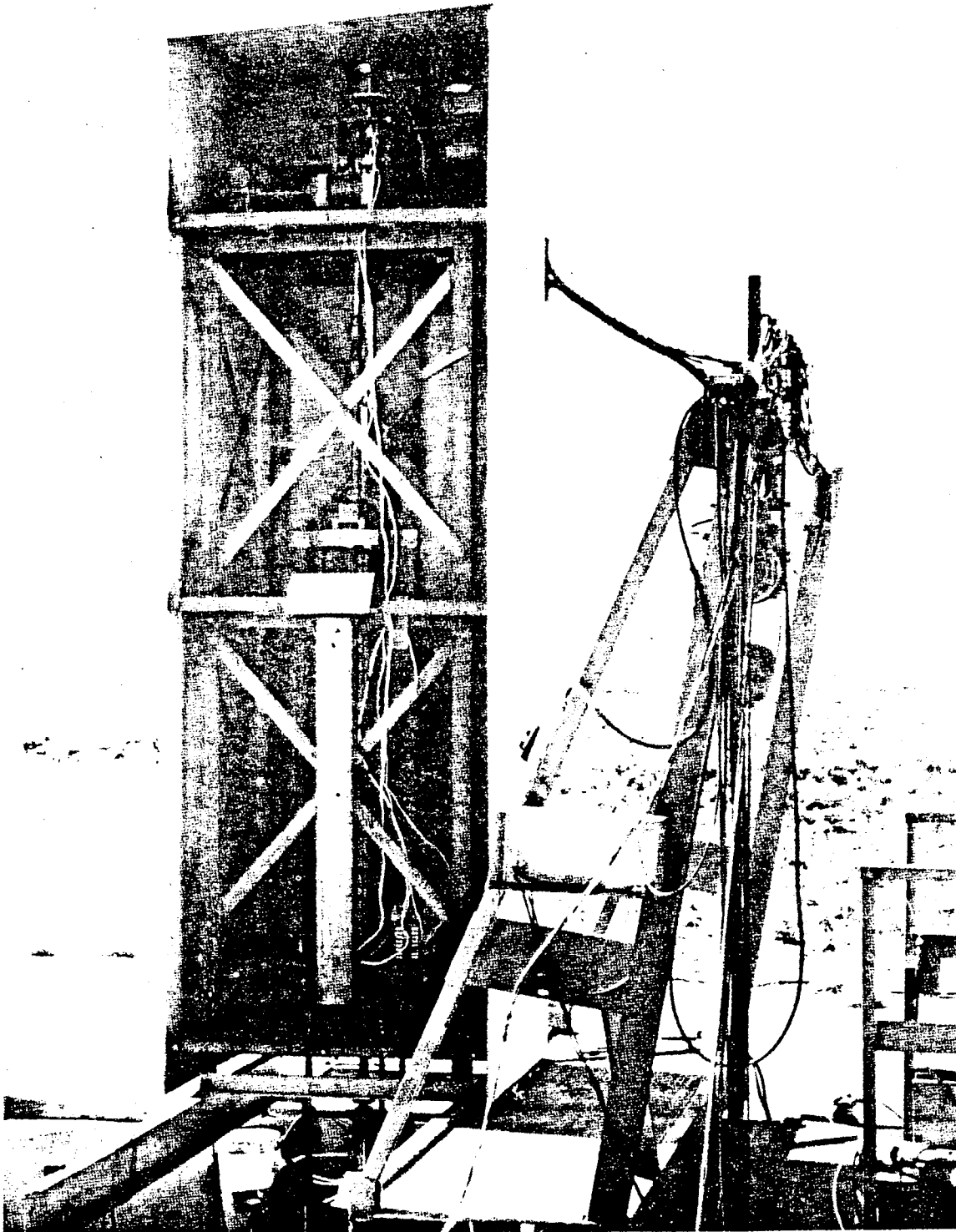


FIG. 13
CONTROL ROD DRIVE ASSEMBLY

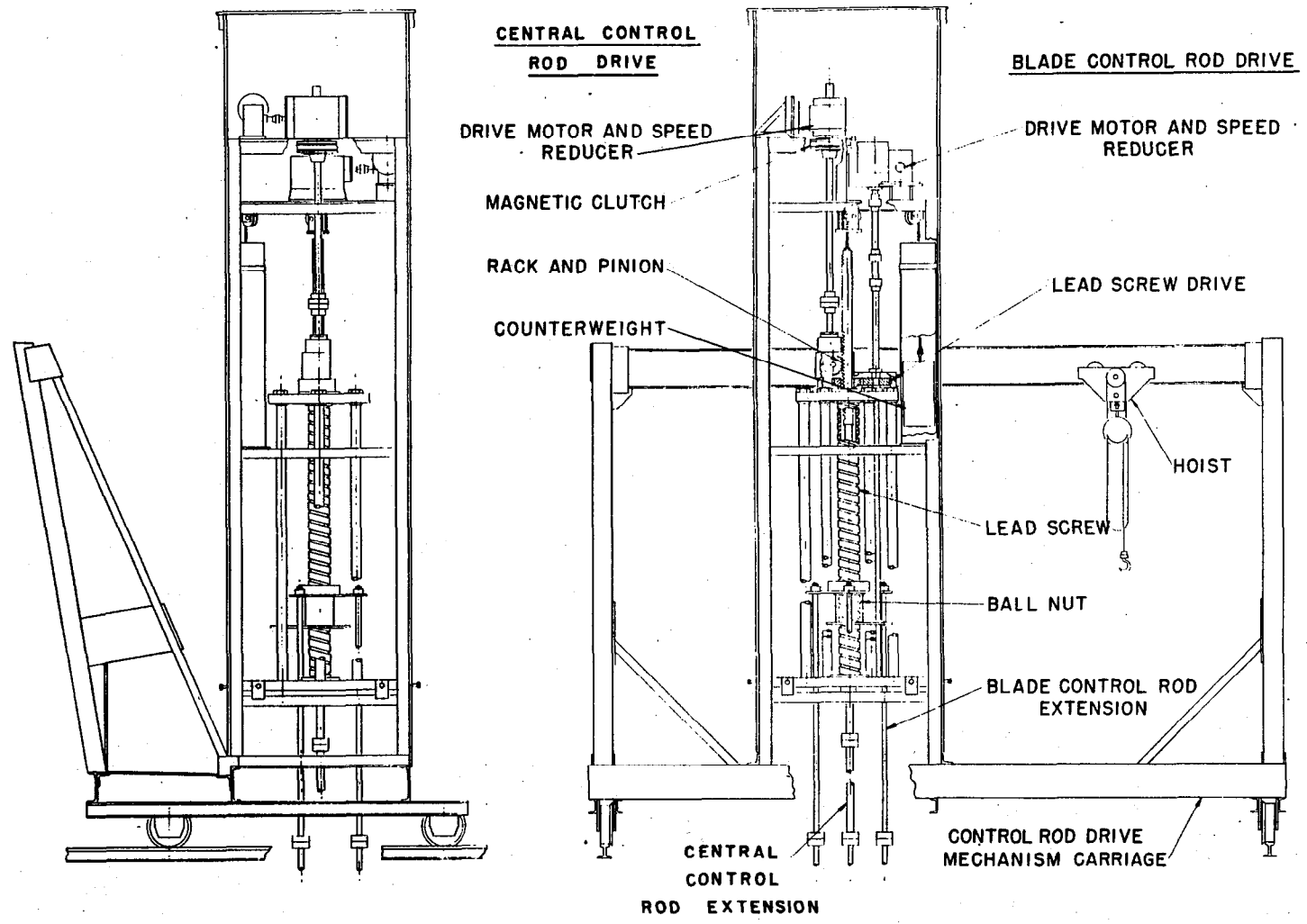


FIG.14
CONTROL ROD DRIVE ASSEMBLY

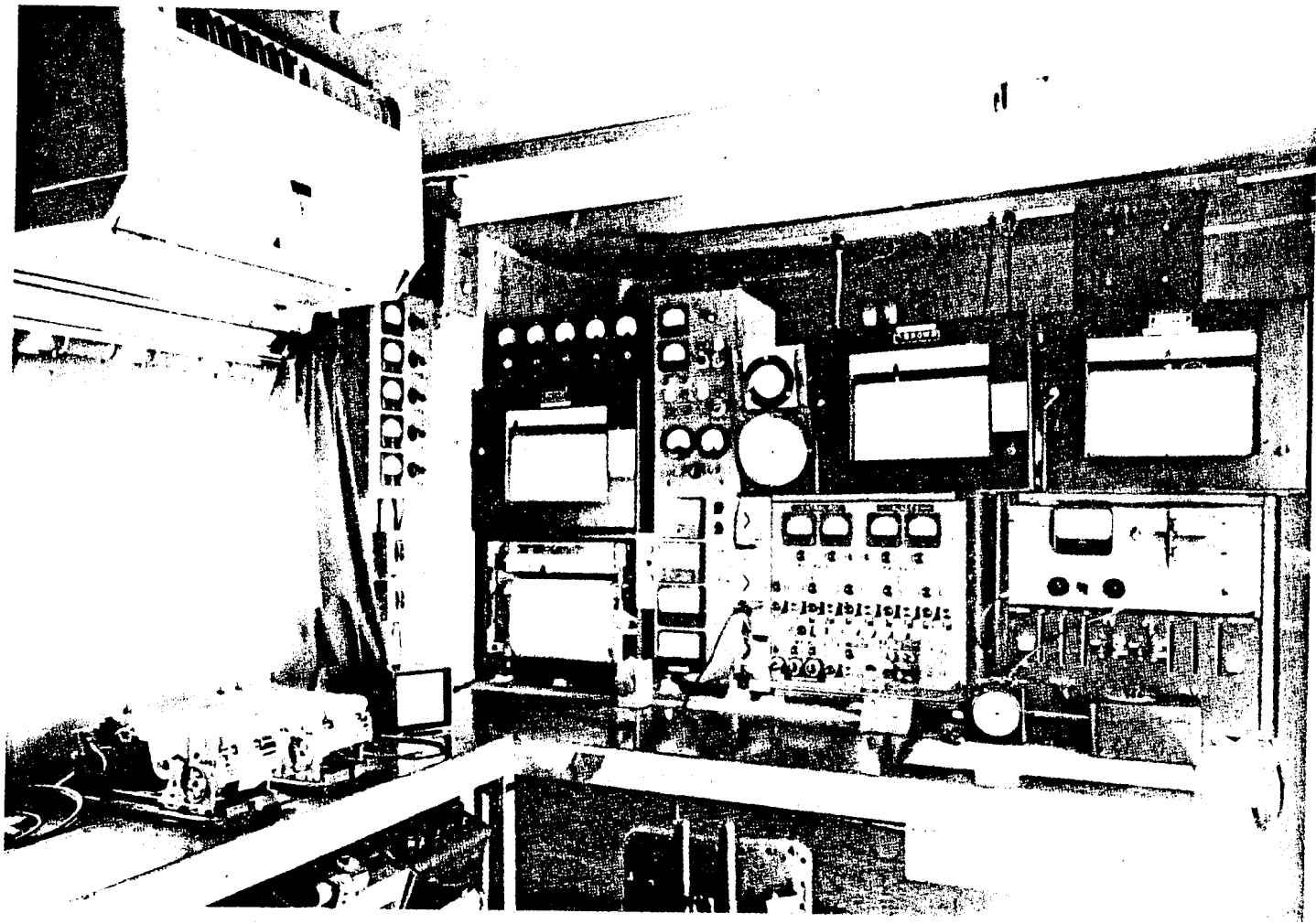
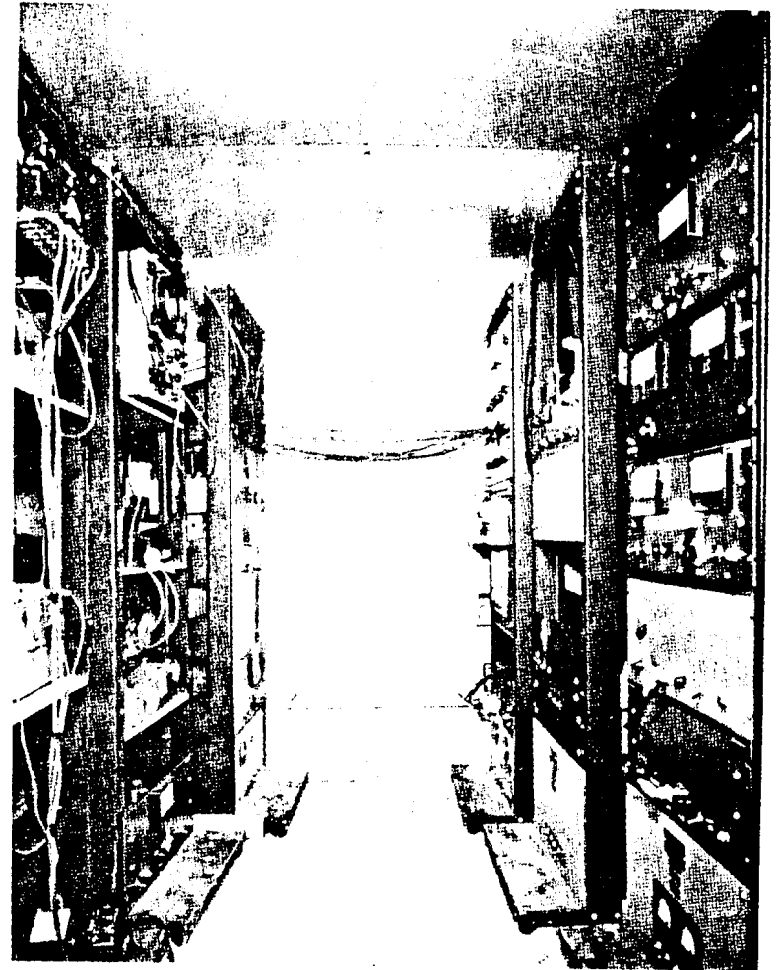


FIG. 15
NUCLEAR CONTROL BOARD



REAR VIEW



FRONT VIEW

FIG. 16
REACTOR TRAILER

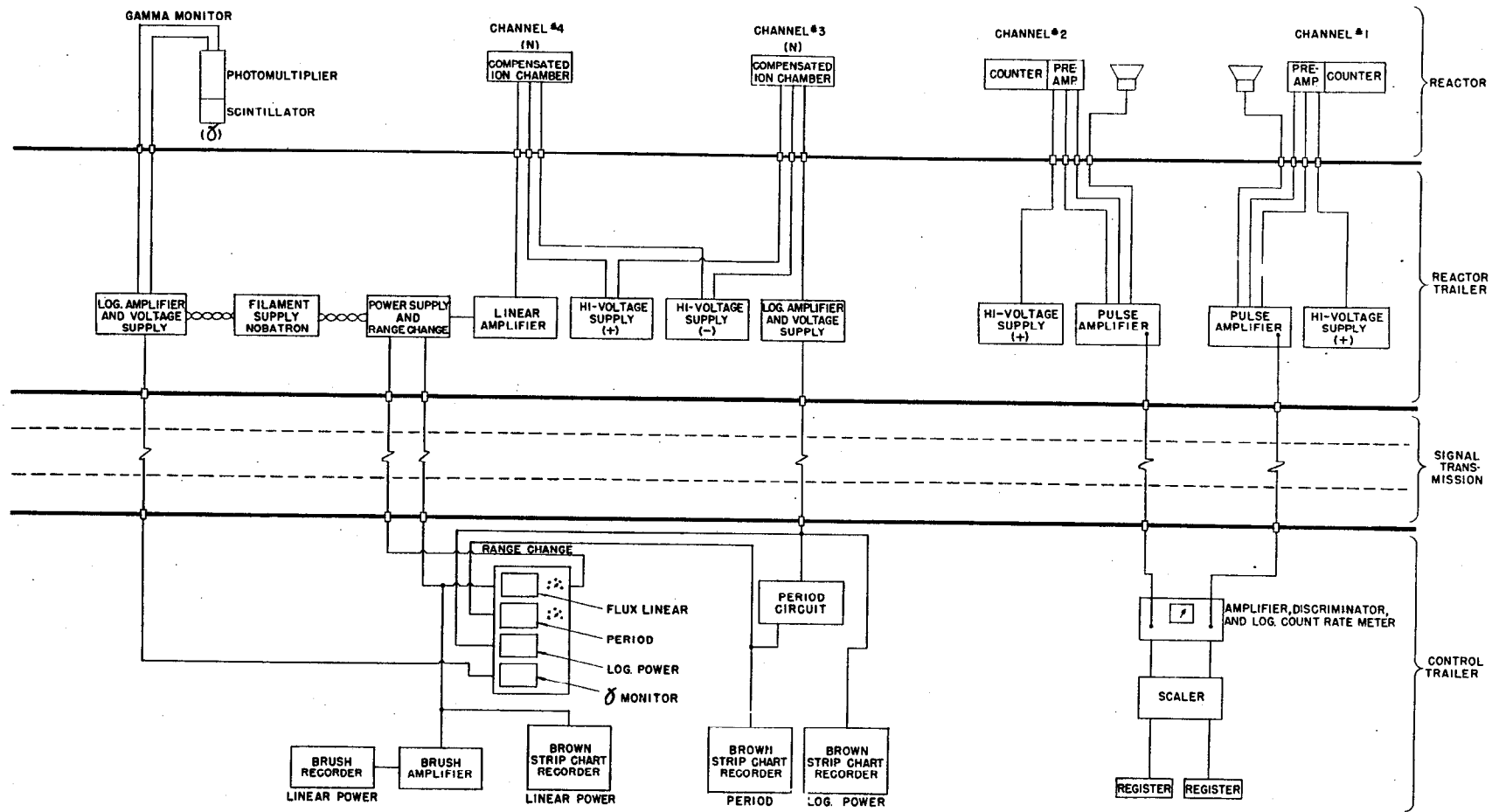


FIG.17
NUCLEAR CONTROL INSTRUMENTATION

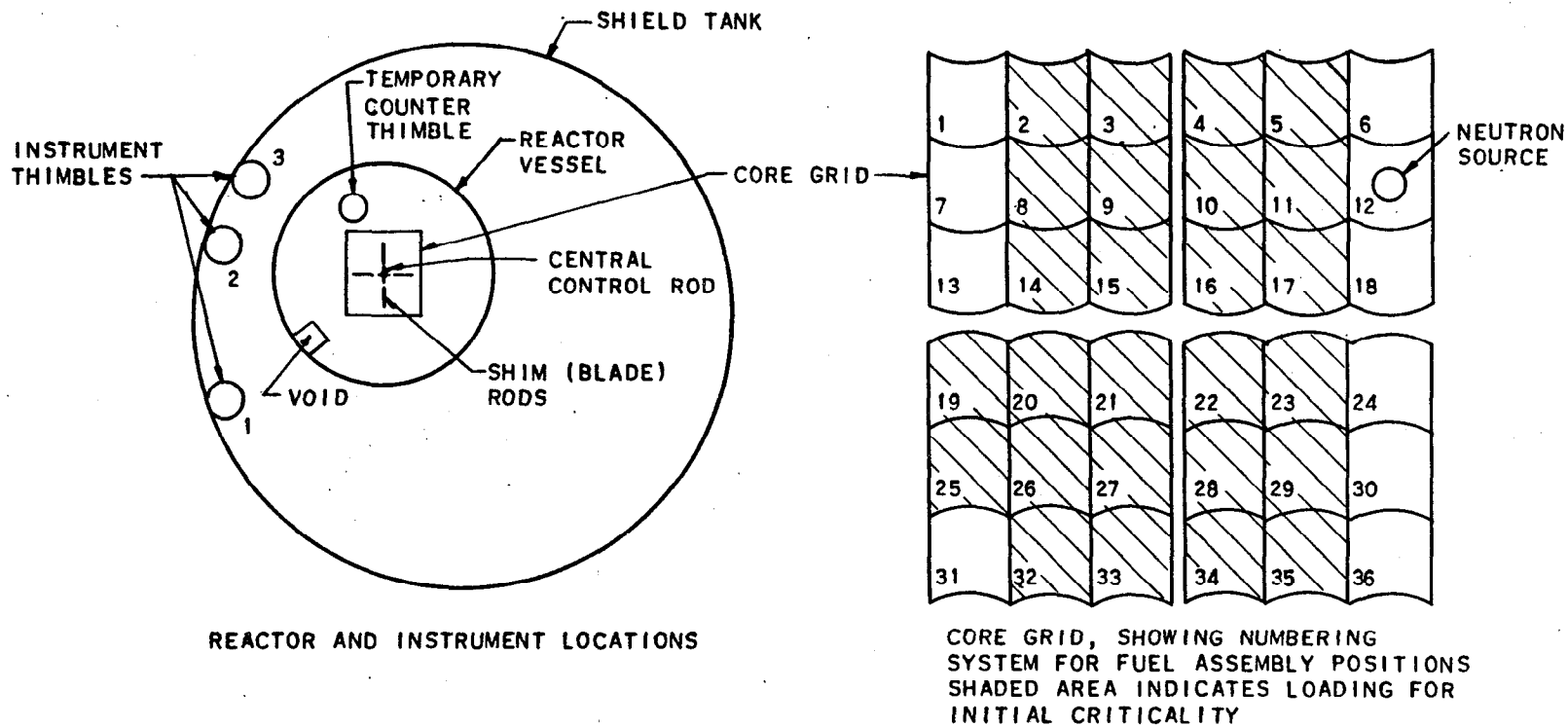


FIG. 18
 DIAGRAM OF INSTRUMENT LOCATIONS
 IN RELATION TO REACTOR CORE

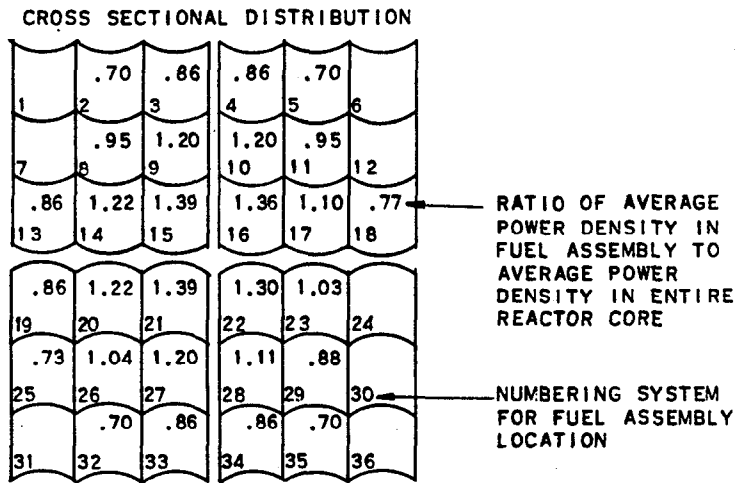
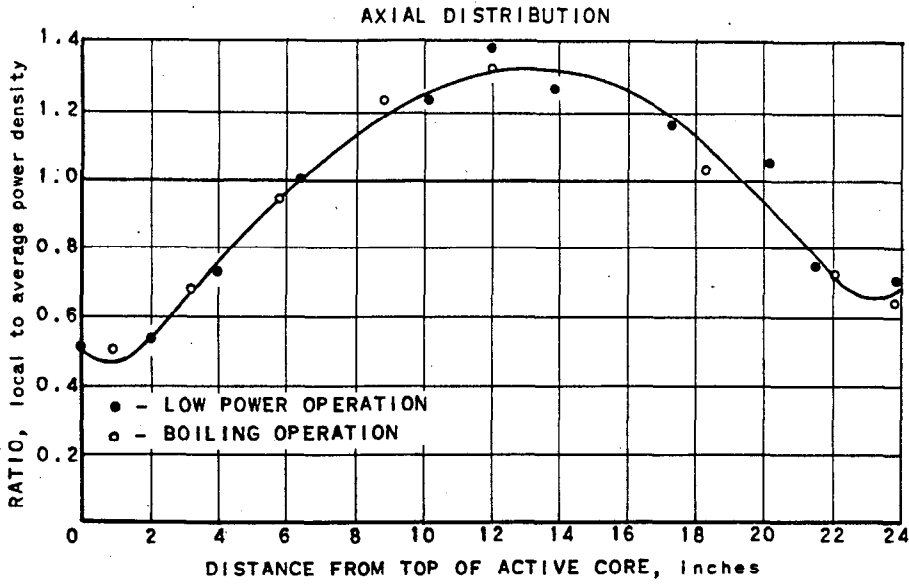


FIG. 19
DISTRIBUTION OF POWER DENSITY
IN REACTOR CORE

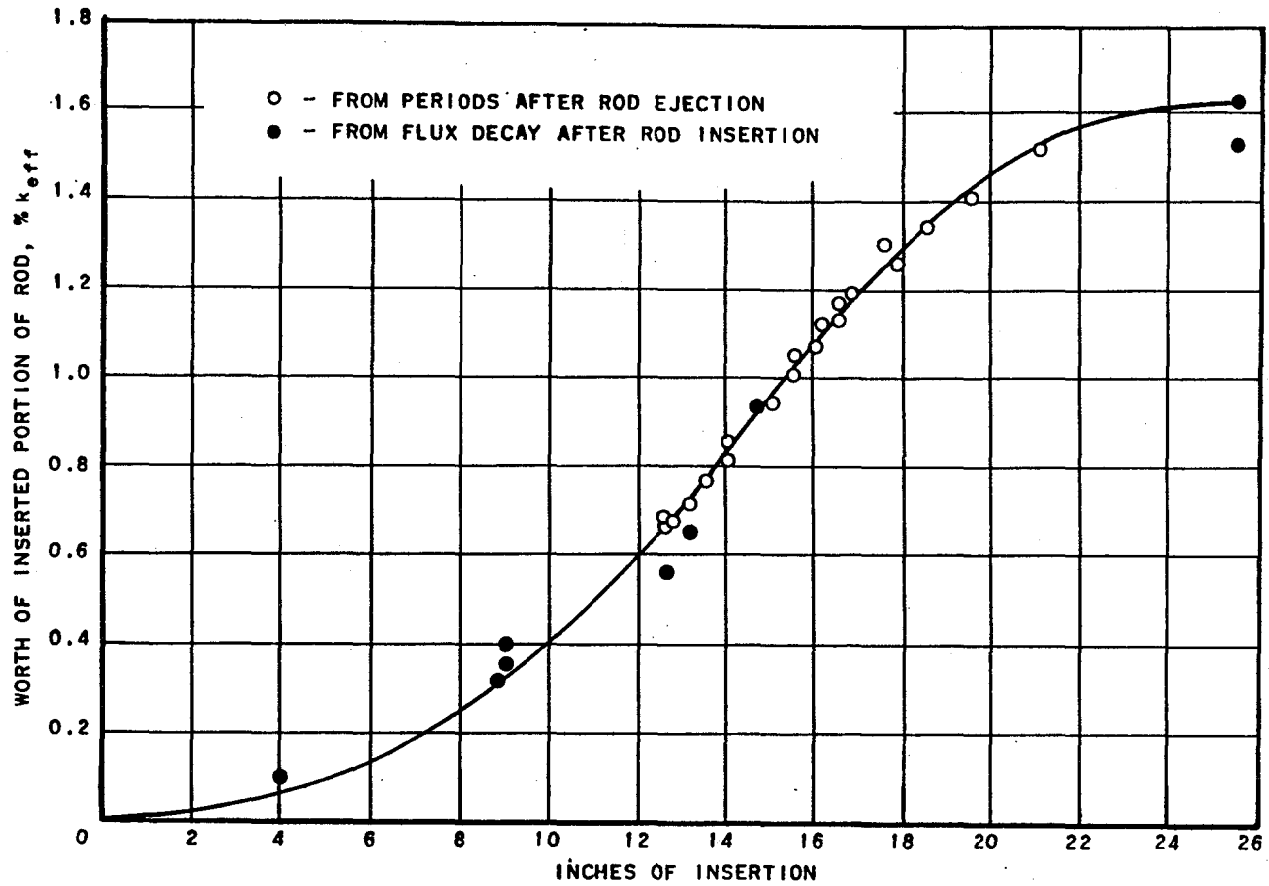


FIG. 20
WORTH OF CENTER ROD CONTAINING
1.17-INCH CADMIUM STRIP

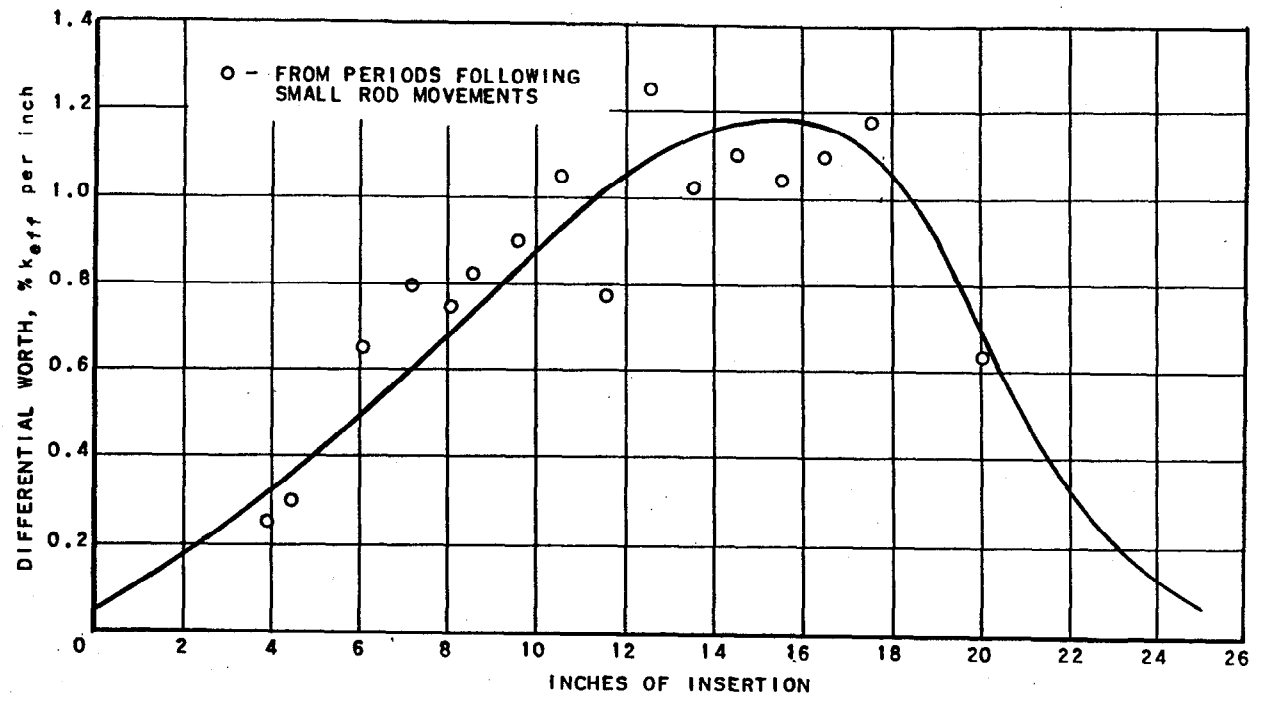


FIG. 21
DIFFERENTIAL WORTH OF CENTER ROD
CONTAINING 1.17 - INCH CADMIUM STRIP

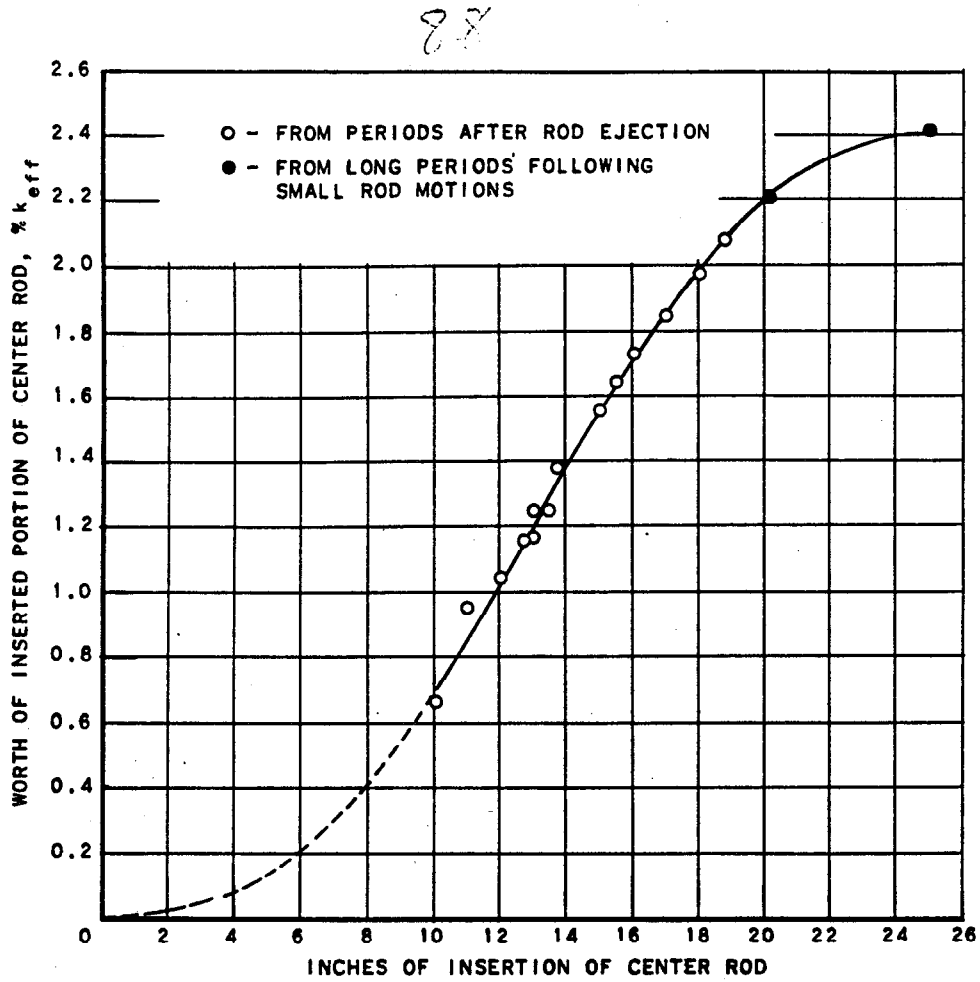


FIG. 22
WORTH OF CENTER ROD CONTAINING
2.34 - INCH CADMIUM STRIP, WITH
SHIM RODS PARTLY INSERTED

89

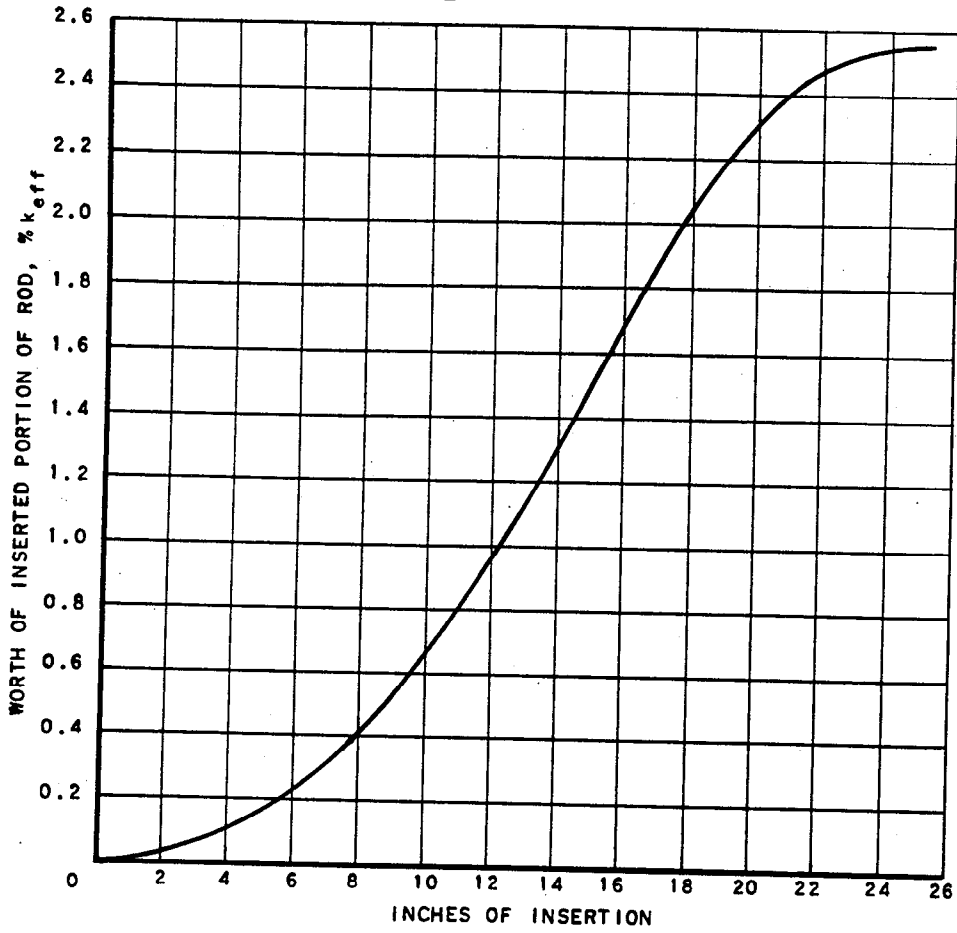


FIG. 23
WORTH OF CENTER ROD CONTAINING
2.34 - INCH CADMIUM STRIP, WITH
SHIM RODS OUT

70

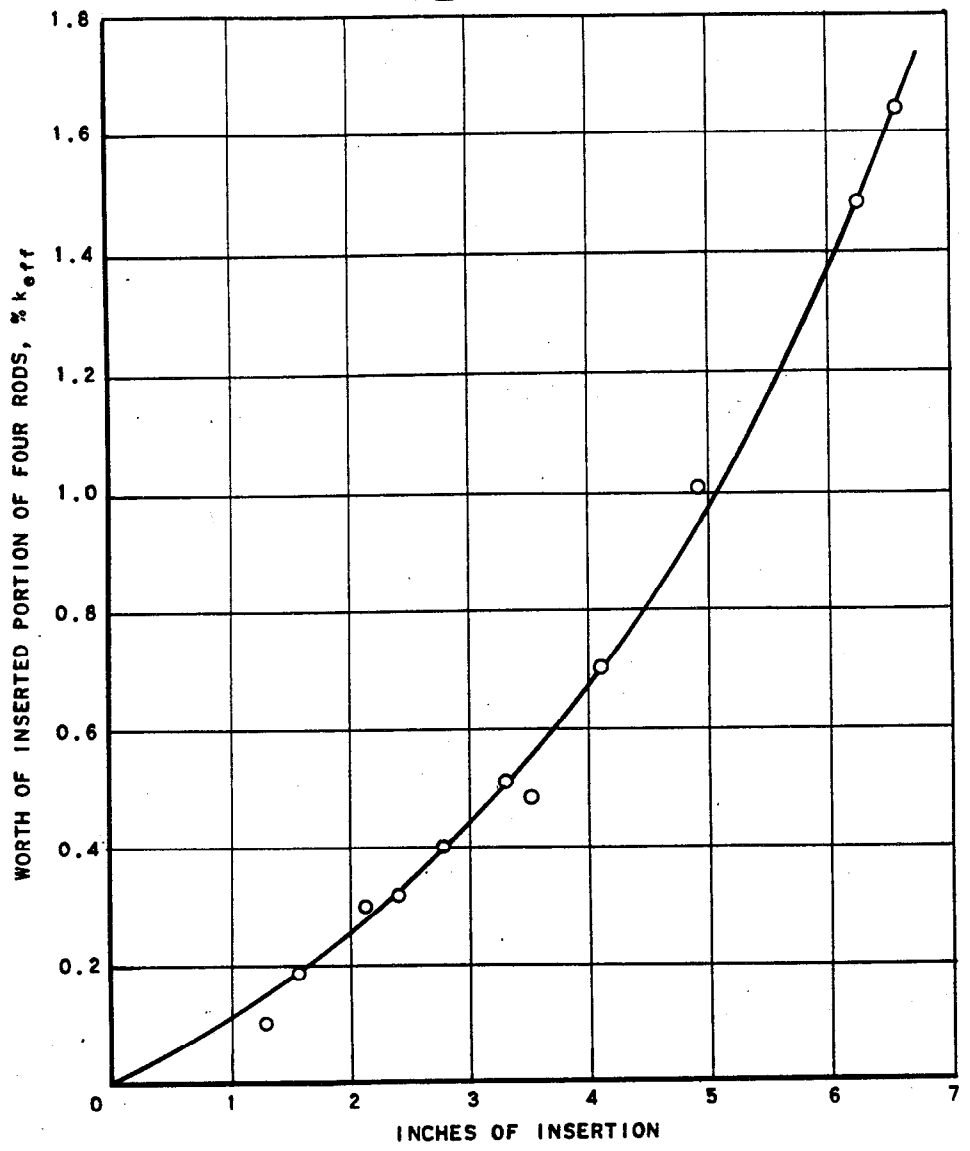


FIG. 24
WORTH OF FOUR PARTIALLY
INSERTED SHIM RODS

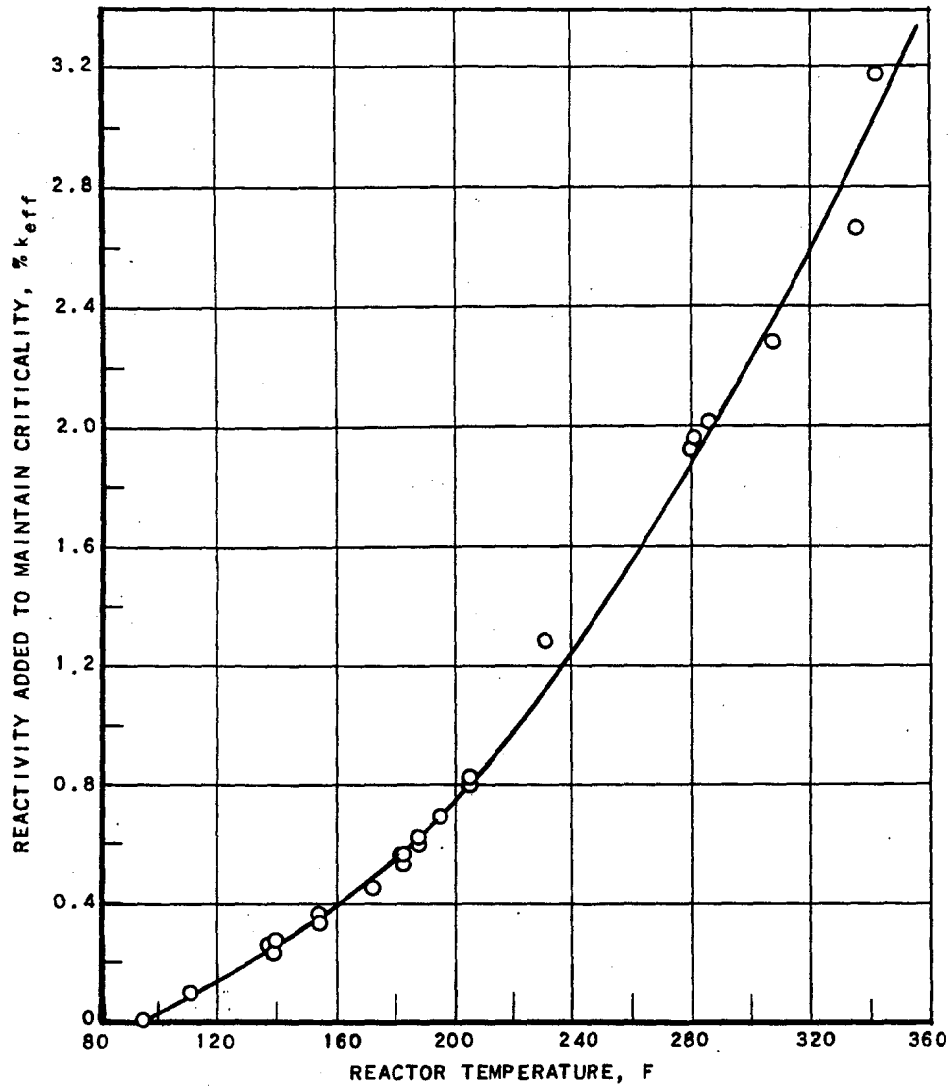


FIG. 25
REACTIVITY CHANGE WITH TEMPERATURE

92

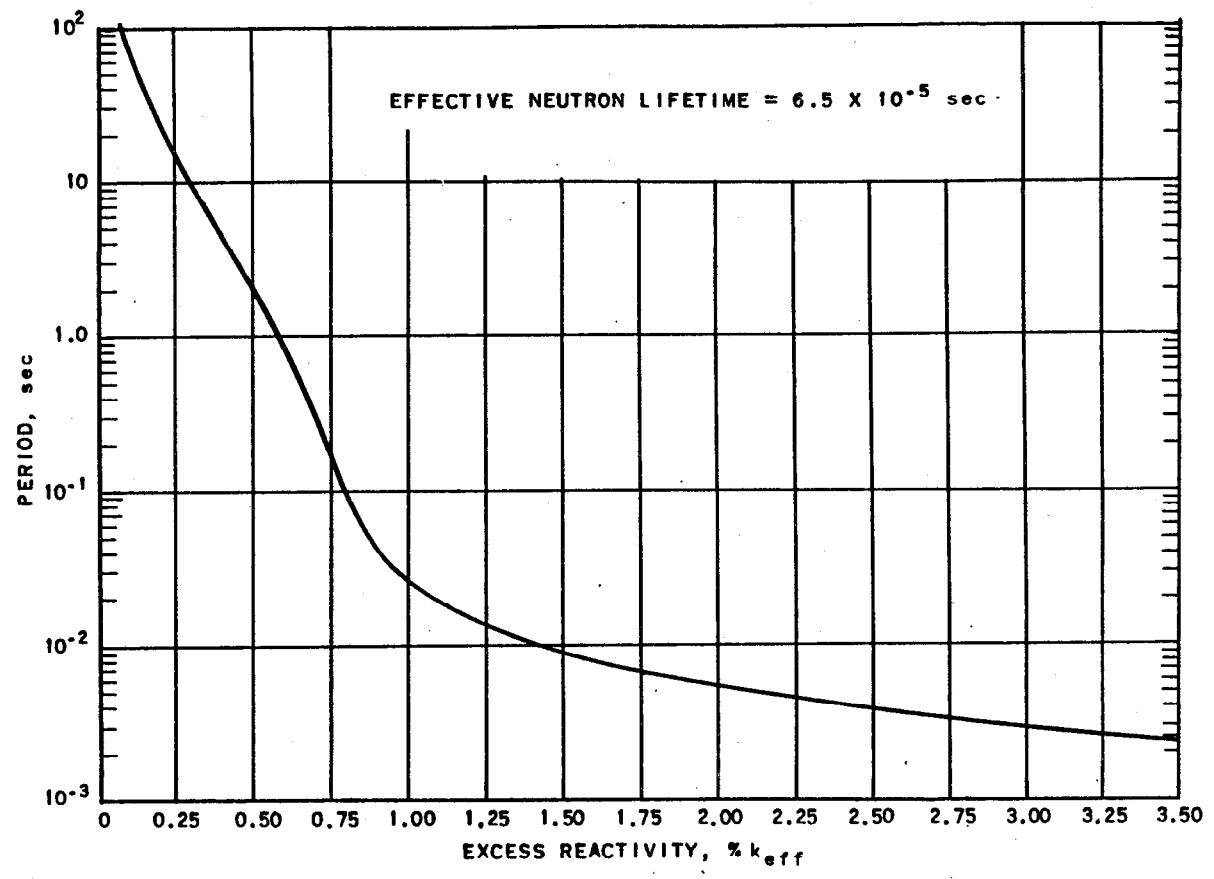


FIG. 26
CALCULATED ASYMPTOTIC PERIOD AS
FUNCTION OF EXCESS REACTIVITY

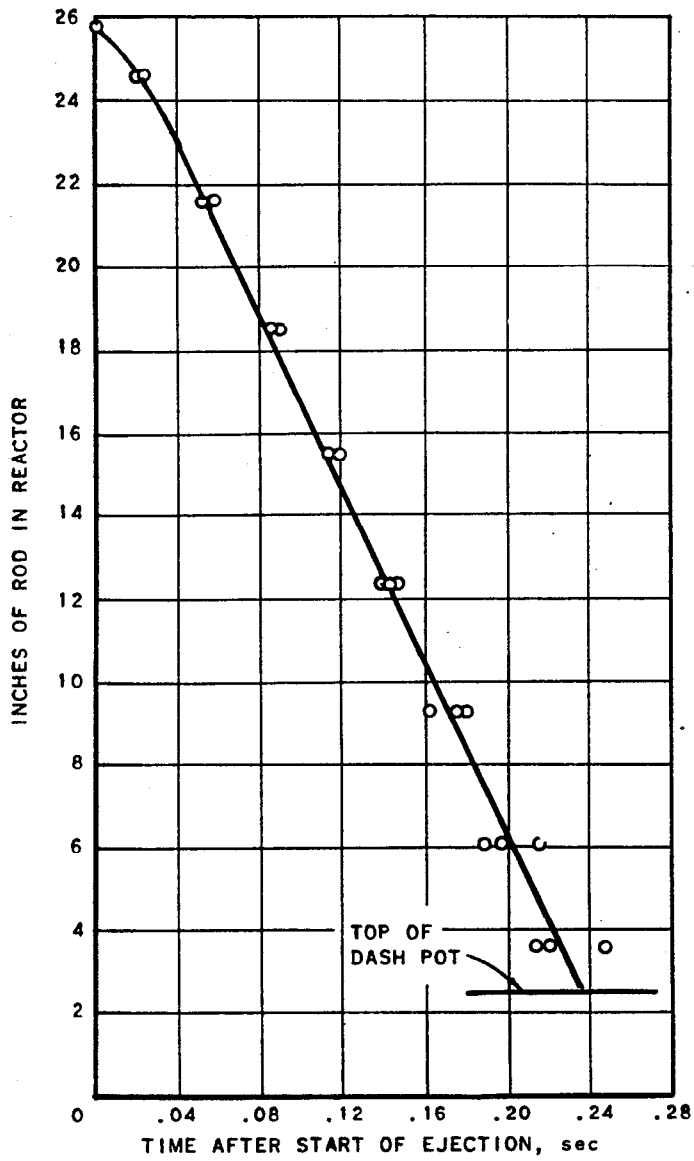


FIG. 27
RATE OF EJECTION OF CENTER ROD

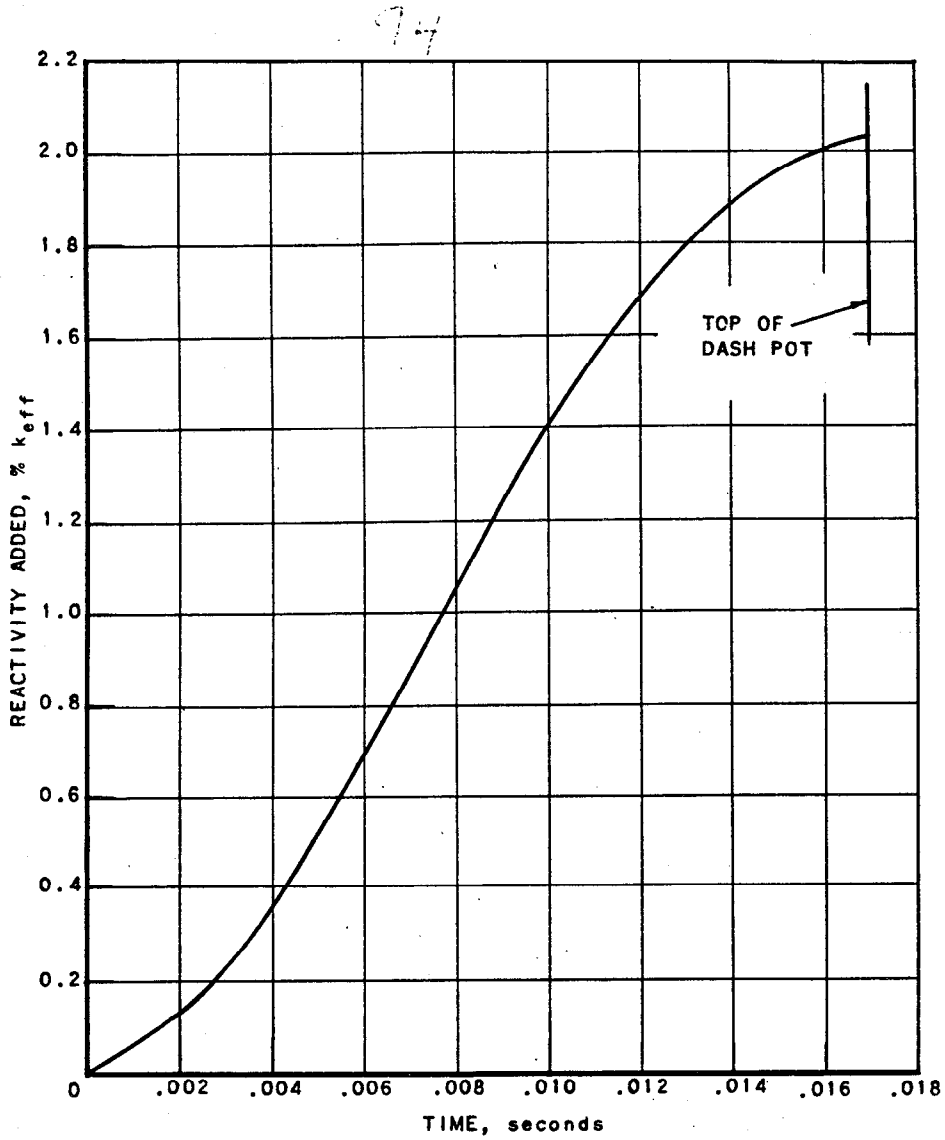


FIG. 28
RATE OF ADDITION OF REACTIVITY
DURING FASTEST TRANSIENT

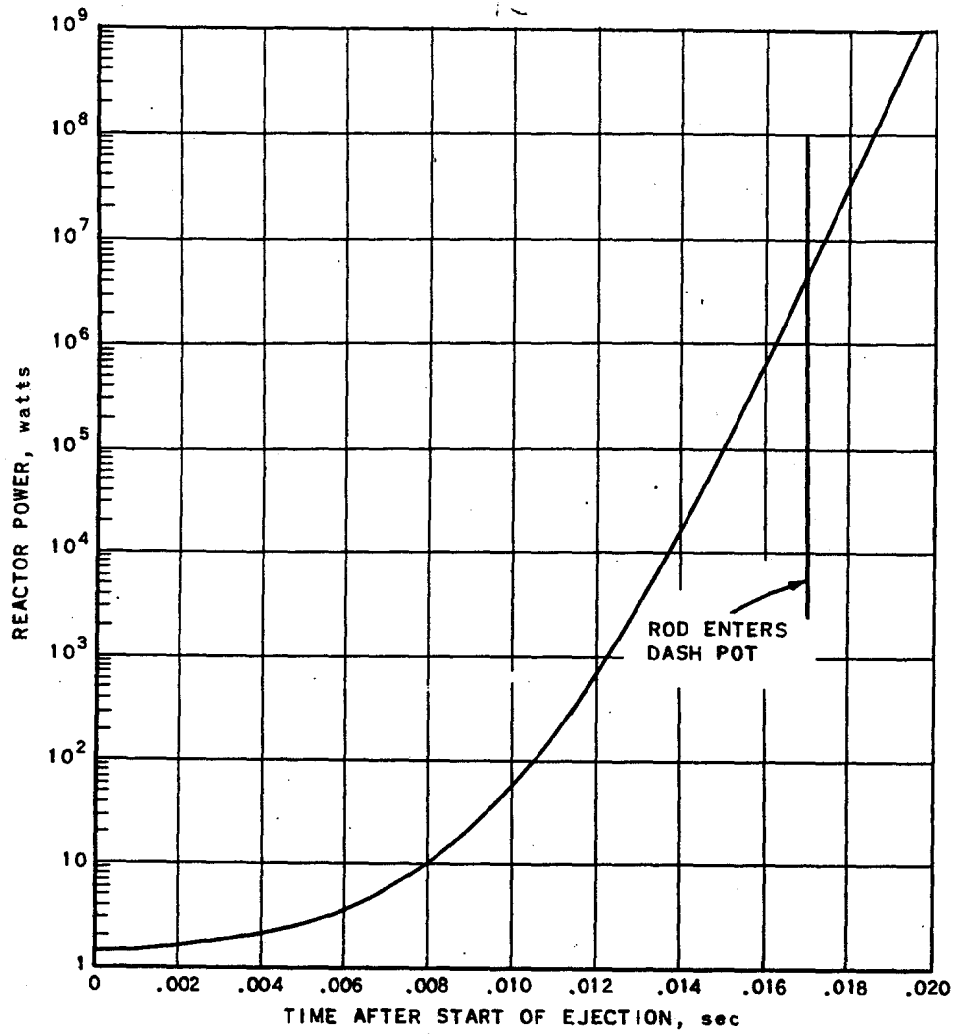


FIG. 29
CALCULATED POWER INCREASE DURING
ROD EJECTION FOR FASTEST TRANSIENT

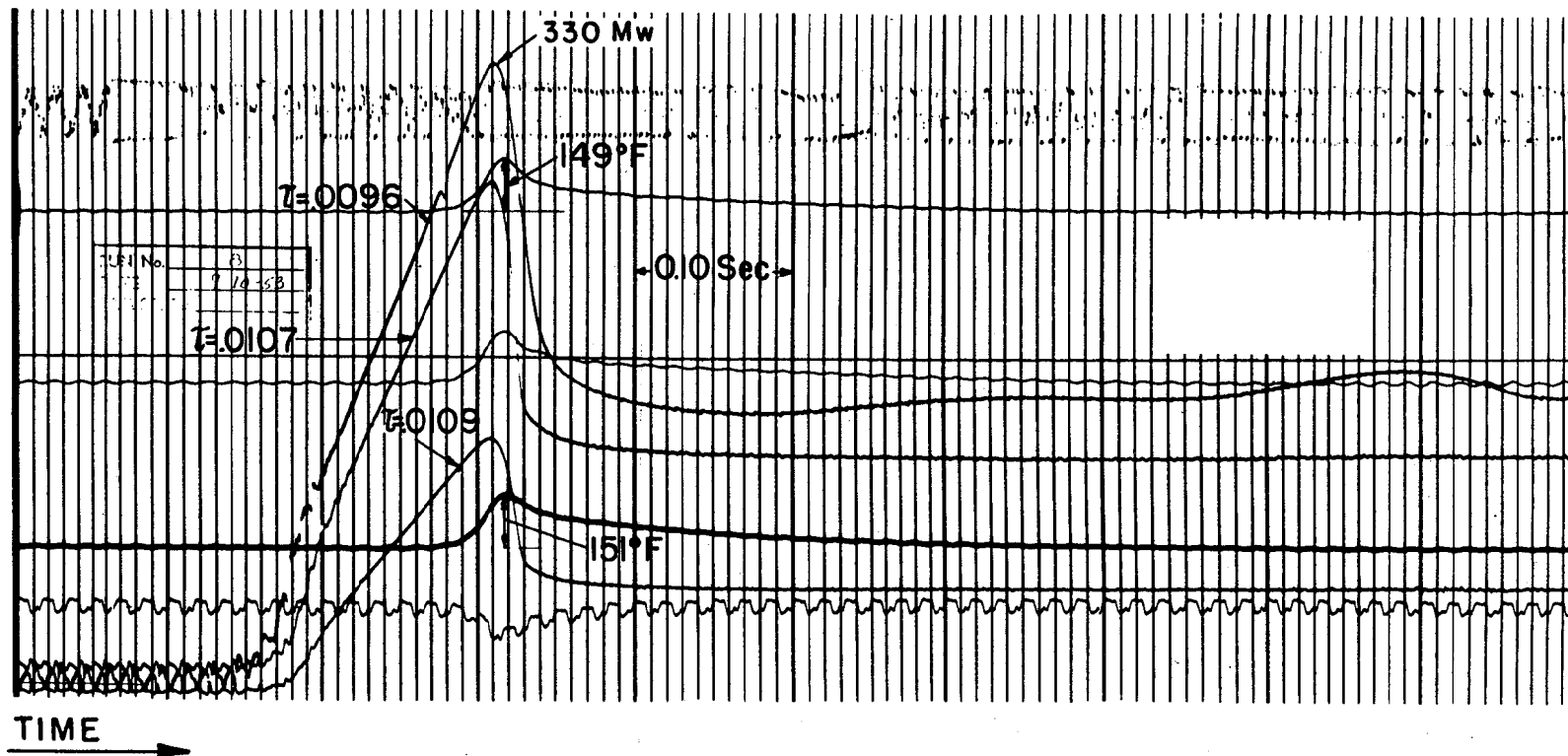


FIG. 30

TYPICAL RECORD OF BORAX EXCURSION

REACTOR WATER WAS INITIALLY AT SATURATION TEMPERATURE.

THE MEASURE PERIODS (τ) ARE MARKED ON THE THREE (LOGARITHMIC) ION CHAMBER RECORDS.

THE TEMPERATURE RISE OF 149F IS AT THE SURFACE OF FUEL PLATE 11; THE RISE OF 151F IS AT THE CENTER OF THE SAME FUEL PLATE. (SEE FIGURE 37.)

THE NOISY TRACE NEAR THE TOP OF THE RECORD IS FROM A MICROPHONE AT THE REACTOR.

THE BOTTOM-MOST TRACE IS FROM A PRESSURE TRANSDUCER IN THE REACTOR CORE.

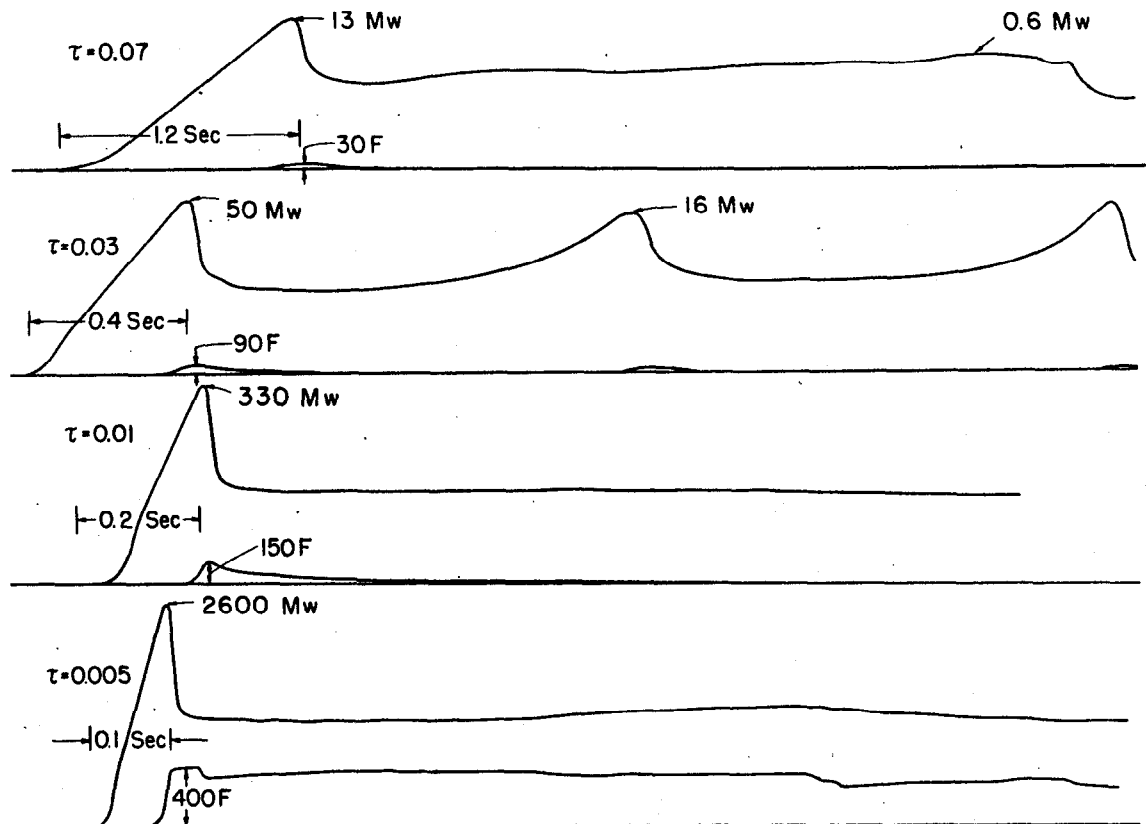


FIG. 31

REPRESENTATIVE RECORDS OF EXCURSIONS AT SATURATION TEMPERATURE
WITH VARIOUS EXCESS REACTIVITIES

THESE WERE TRACED DIRECTLY FROM THE GALVANDMETER RECORDS.

NOTE THAT THE TIME SCALE CHANGES FROM RUN TO RUN.

THE PERIOD (τ) OF THE EXCURSION IS MARKED ON EACH RUN IN SECONDS. THE TEMPERATURE RECORD IS FROM THE CENTER OF FUEL PLATE 11 (SEE FIGURE 37).

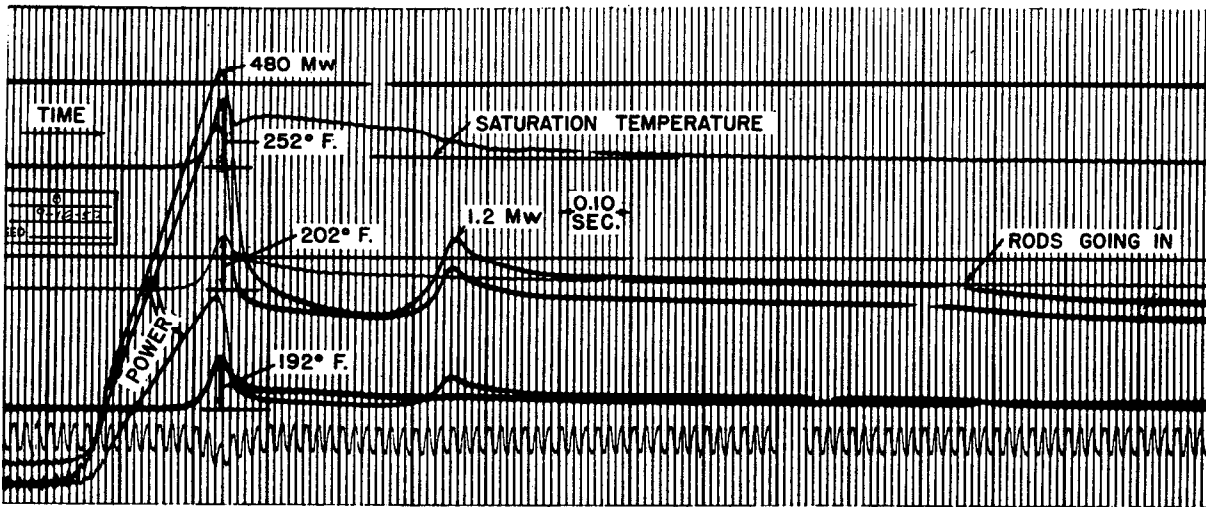
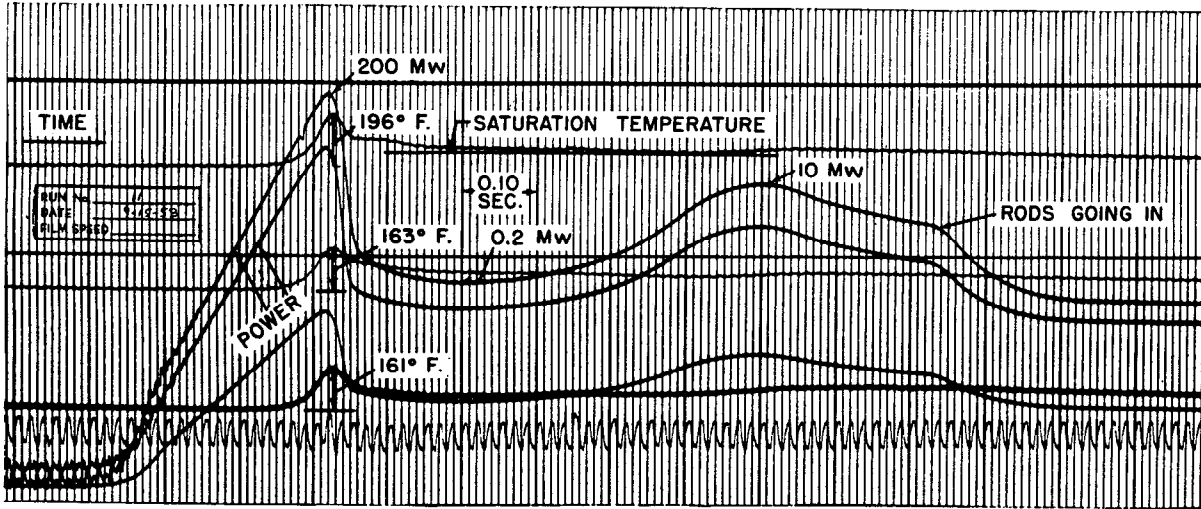
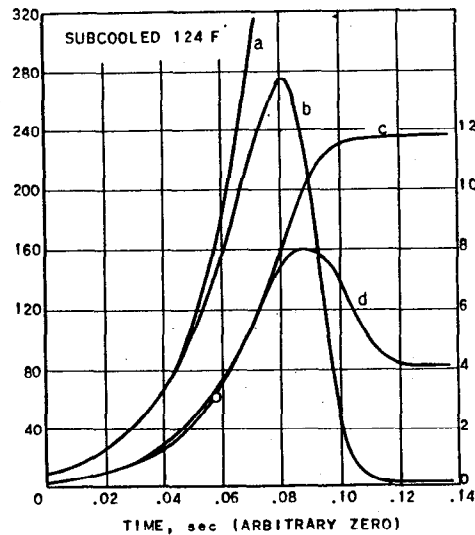
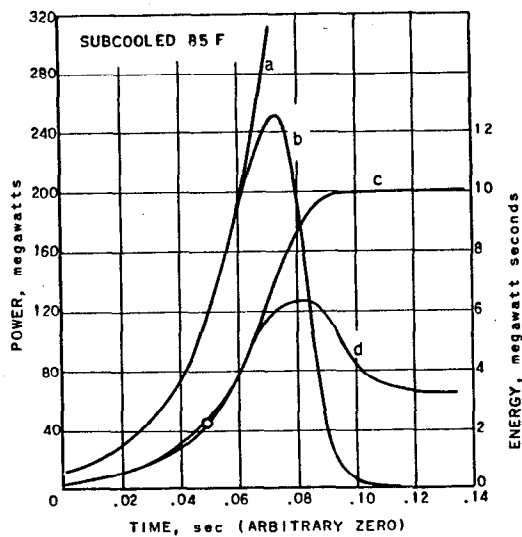
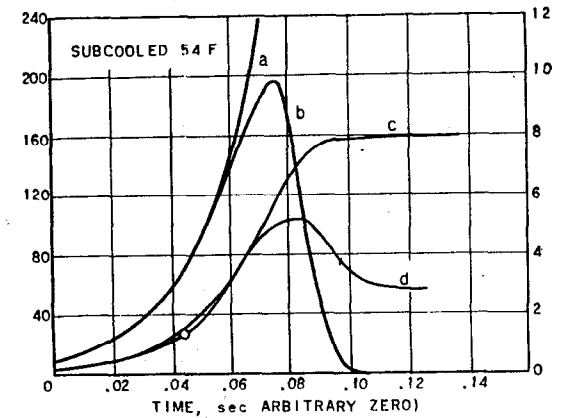
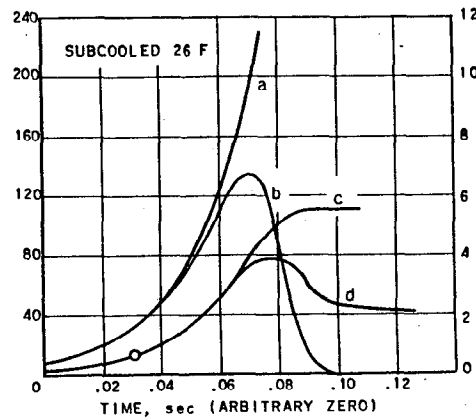
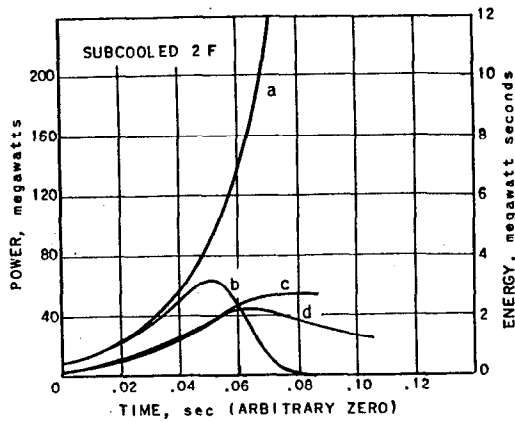


FIG. 32

RECORDS OF POWER EXCURSIONS FROM THE SUBCOOLED CONDITION
(CF FIG. 30)

THE UPPER RECORD IS FROM AN EXCURSION OF 0.022 SECOND PERIOD, WITH 54°F SUBCOOLING; THE LOWER RECORD IS FROM AN EXCURSION OF 0.013 SECOND PERIOD, WITH 43°F SUBCOOLING.

THE TOP TEMPERATURE TRACE ON EACH RECORD IS FROM THE CENTER OF FUEL PLATE 4 (SEE FIG. 37); THE MIDDLE TRACE IS FROM THE CENTER OF PLATE 1, AND THE BOTTOM TRACE FROM THE SURFACE OF PLATE 1. THE THREE POWER TRACES ON EACH RECORD ARE FROM ION CHAMBERS OF THREE DIFFERENT SENSITIVITIES, ON LOGARITHMIC SCALES.



- CURVE a - CONTINUATION OF EXPONENTIAL OF INITIAL POWER RISE
- CURVE b - REACTOR POWER
- CURVE c - TOTAL HEAT ENERGY GENERATED IN FUEL PLATES (INTEGRAL OF CURVE b)
- CURVE d - HEAT CONTENT OF FUEL PLATES (FROM PLATE TEMPERATURE)
- FUEL PLATE REACHES SATURATION TEMPERATURE

FIG. 33
POWER, ENERGY, AND TEMPERATURE VARIATIONS
DURING EXCURSIONS OF 0.022 sec PERIOD
WITH VARIOUS DEGREES OF SUBCOOLING

(ONLY ENERGY APPEARING AS HEAT
IN FUEL PLATES CONSIDERED)

100

- CURVE a - CONTINUATION OF EXPONENTIAL OF INITIAL POWER RISE
- CURVE b - REACTOR POWER
- CURVE c - TOTAL HEAT ENERGY GENERATED IN FUEL PLATES (INTEGRAL OF CURVE b)
- CURVE d - HEAT CONTENT OF FUEL PLATES (FROM PLATE TEMPERATURE)
- O - FUEL PLATE REACHES SATURATION TEMPERATURE

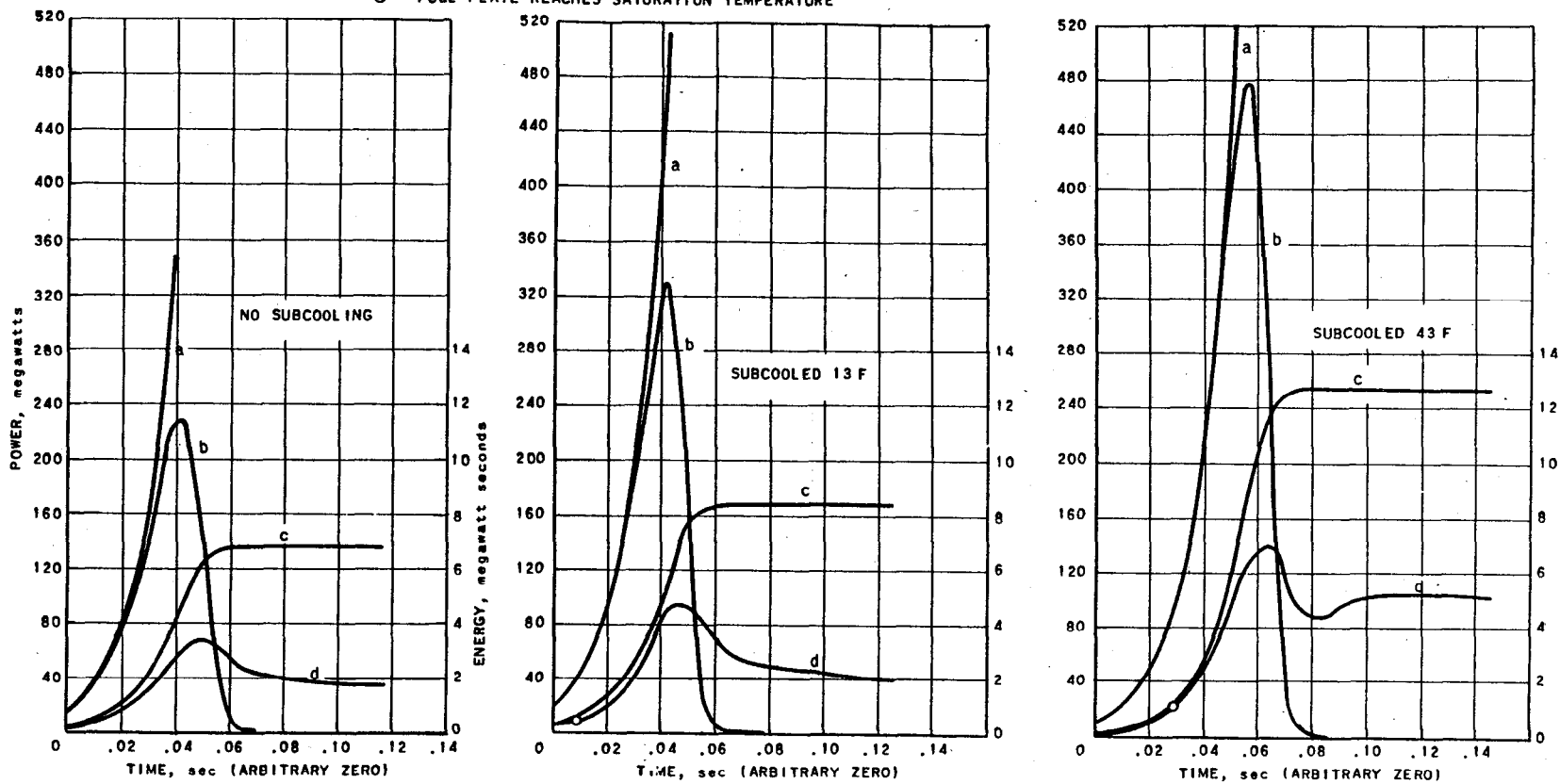


FIG. 34
 POWER, ENERGY, AND TEMPERATURE VARIATIONS DURING EXCURSIONS
 OF 0.013 sec PERIOD WITH VARIOUS DEGREES OF SUBCOOLING
 (ONLY ENERGY APPEARING AS HEAT IN FUEL PLATES CONSIDERED)

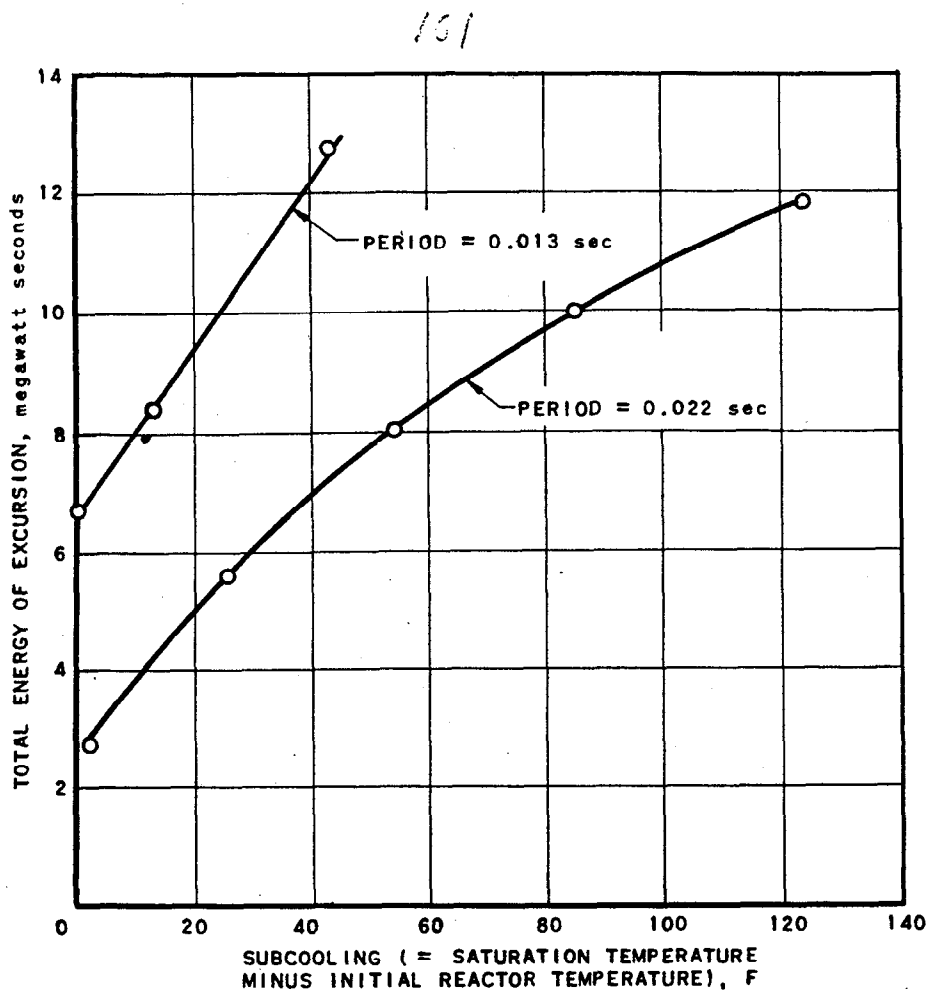


FIG. 35
EFFECT OF SUBCOOLING ON TOTAL
ENERGY OF POWER EXCURSION
(ONLY ENERGY APPEARING AS HEAT
IN FUEL PLATES CONSIDERED)

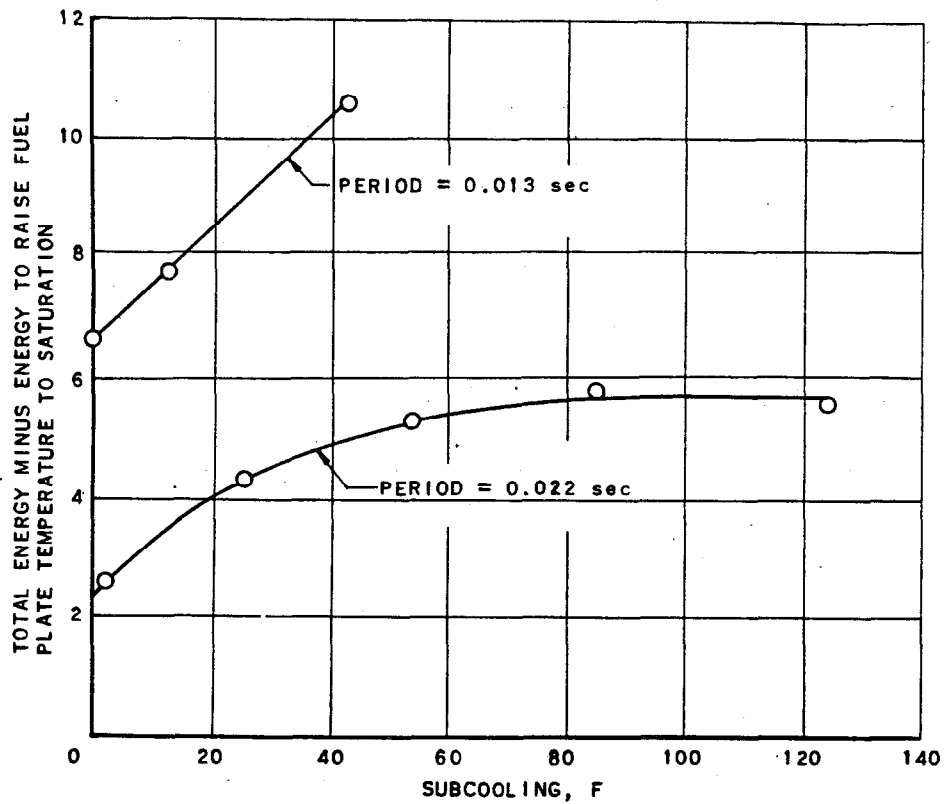
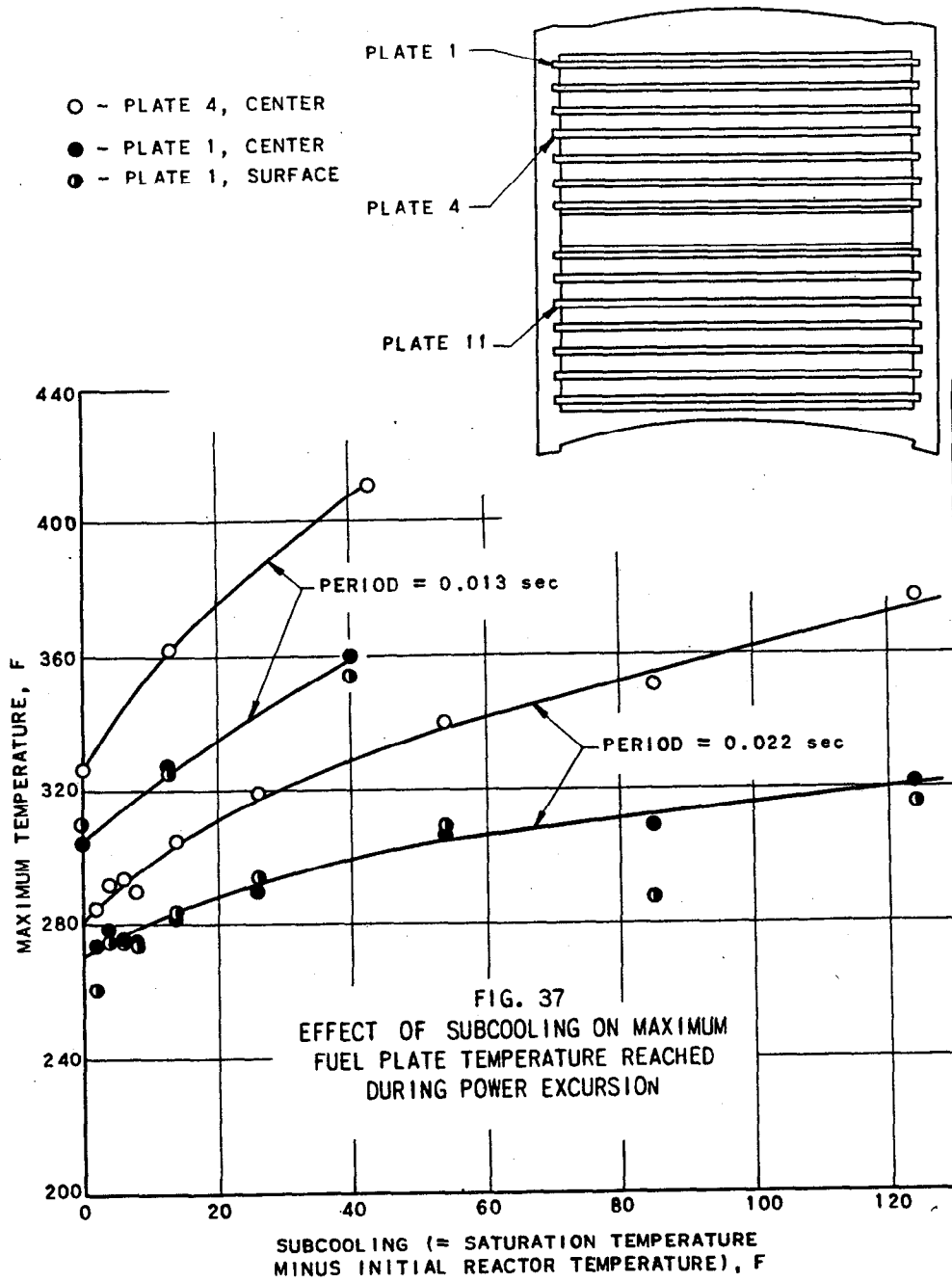


FIG. 36
ENERGY OF POWER EXCURSION IN EXCESS
OF THAT REQUIRED TO RAISE FUEL
PLATE TEMPERATURE TO SATURATION
(ONLY ENERGY APPEARING AS HEAT
IN FUEL PLATES CONSIDERED)



104

104

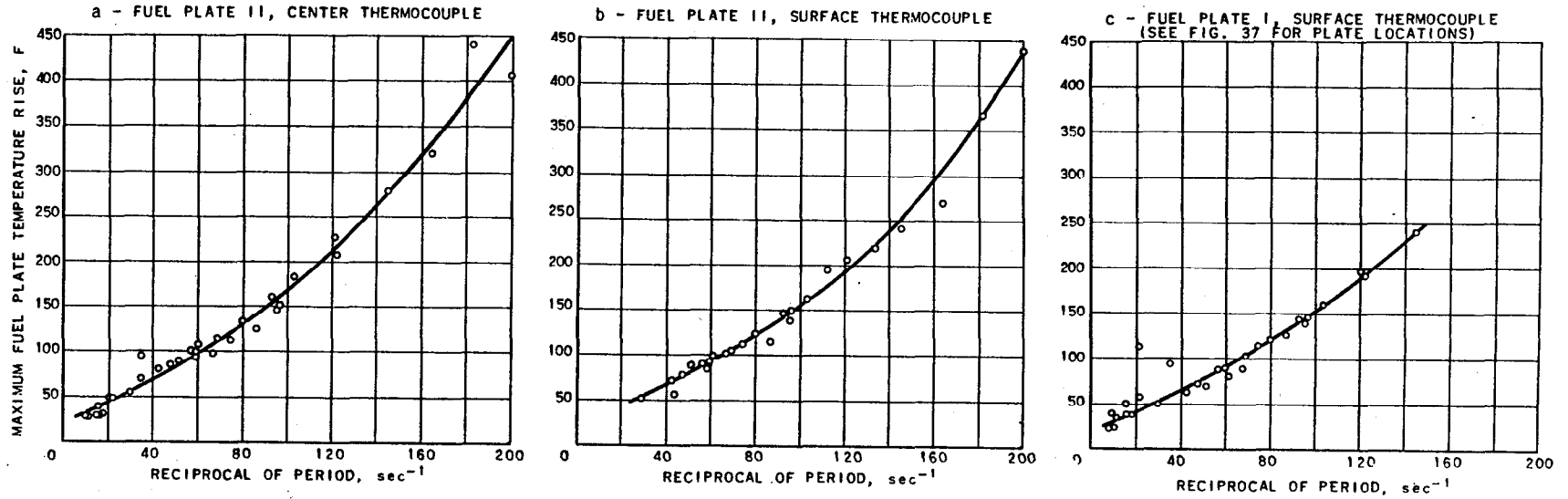


FIG. 38
MAXIMUM FUEL PLATE TEMPERATURE RISE FOR POWER
EXCURSIONS OF VARIOUS PERIODS, WITH REACTOR
INITIALLY AT SATURATION TEMPERATURE

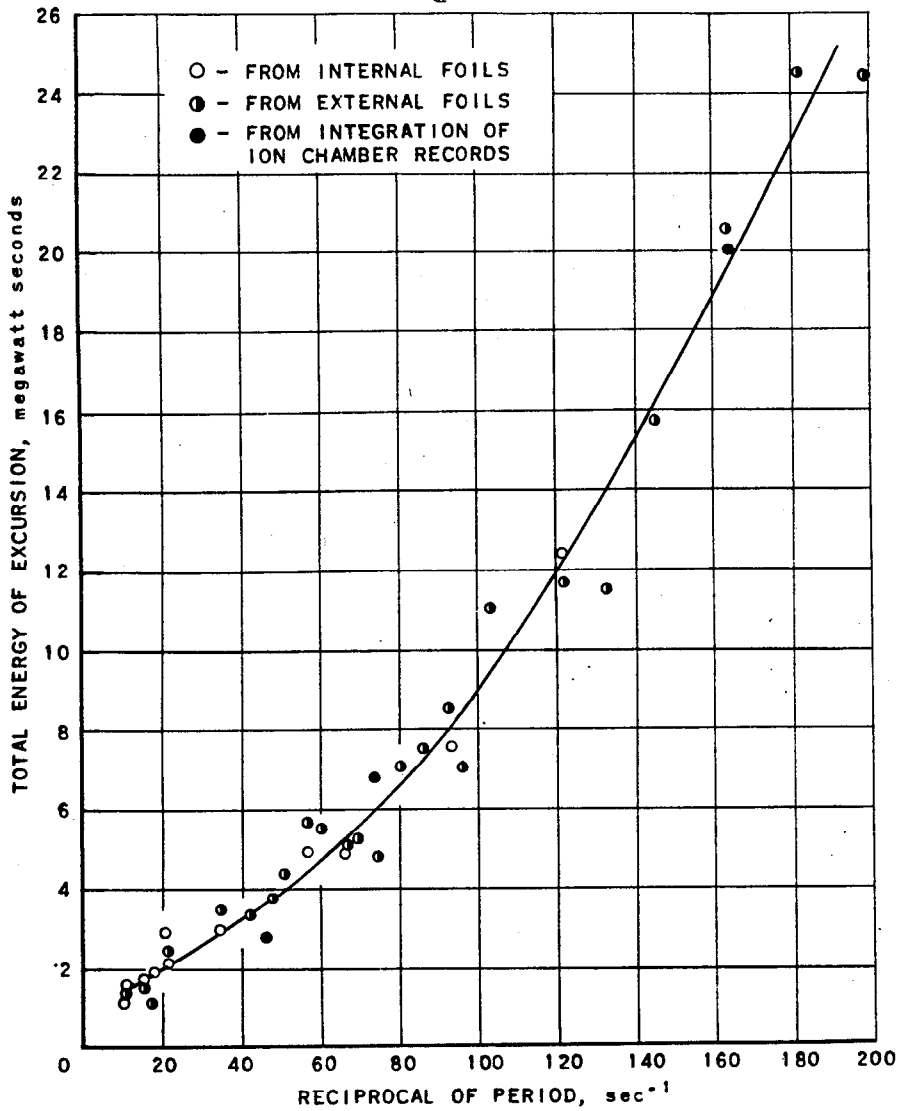


FIG. 39
TOTAL ENERGY OF POWER EXCURSION FOR
EXCURSIONS OF VARIOUS PERIODS,
WITH REACTOR INITIALLY AT SATURATION TEMPERATURE

(ONLY ENERGY APPEARING AS HEAT
IN FUEL PLATES CONSIDERED)

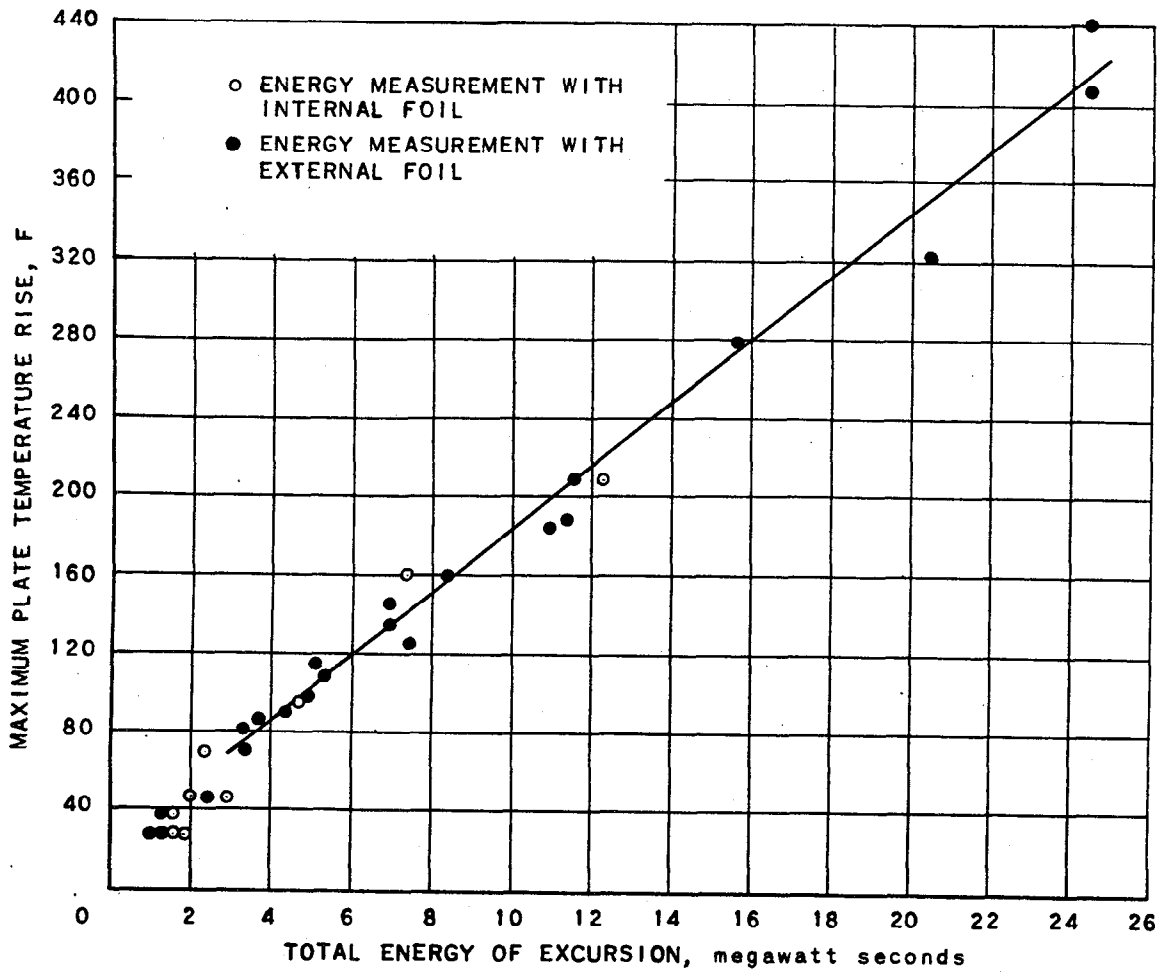


FIG. 40
RELATION BETWEEN TOTAL ENERGY OF POWER EXCURSION
AND MAXIMUM FUEL PLATE TEMPERATURE RISE
FOR EXCURSIONS OF VARIOUS PERIODS
AT SATURATION TEMPERATURE

(CENTER TEMPERATURE OF PLATE 11)

108

108

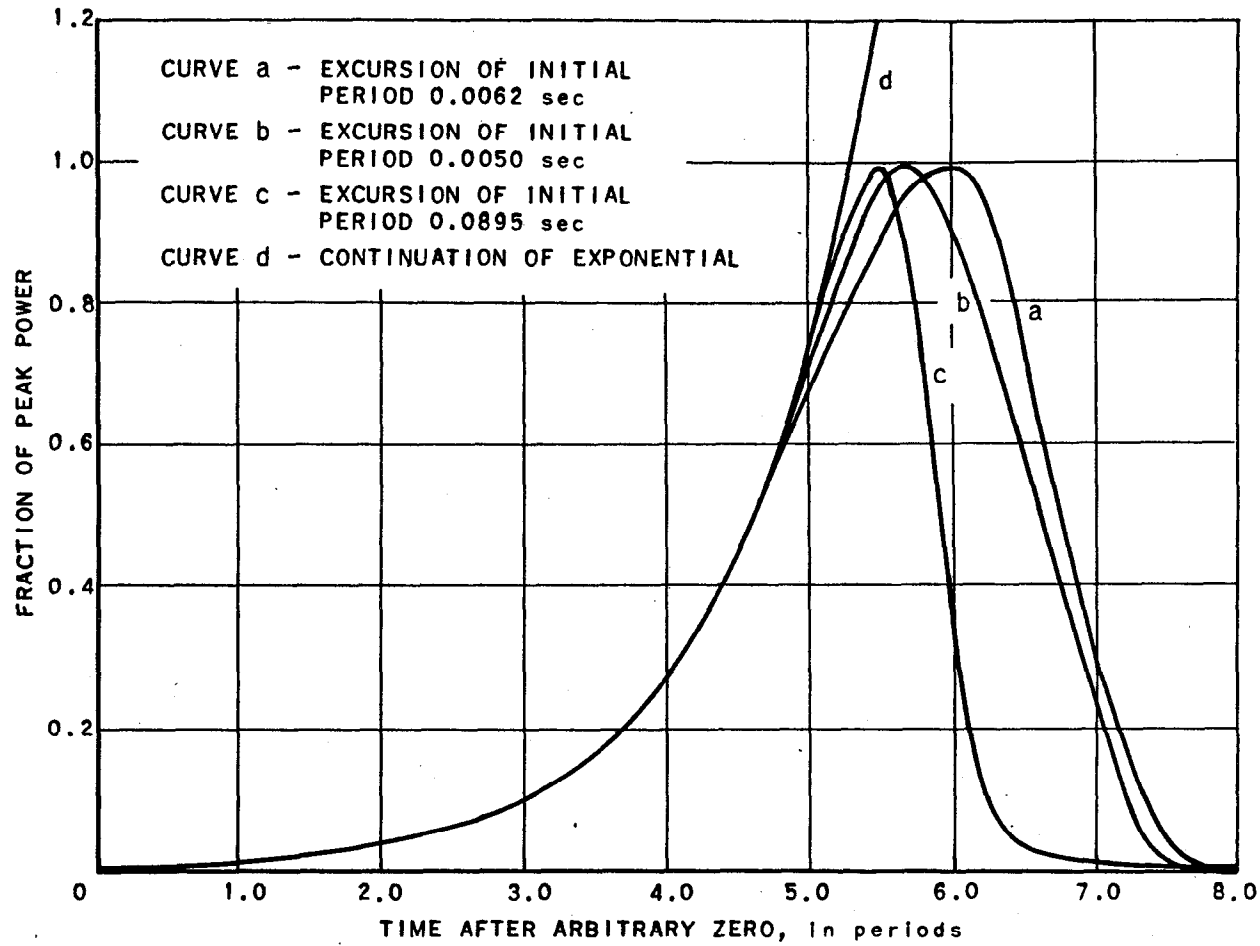


FIG. 42
COMPARISON OF THREE POWER EXCURSIONS
OF DIFFERENT INITIAL PERIODS

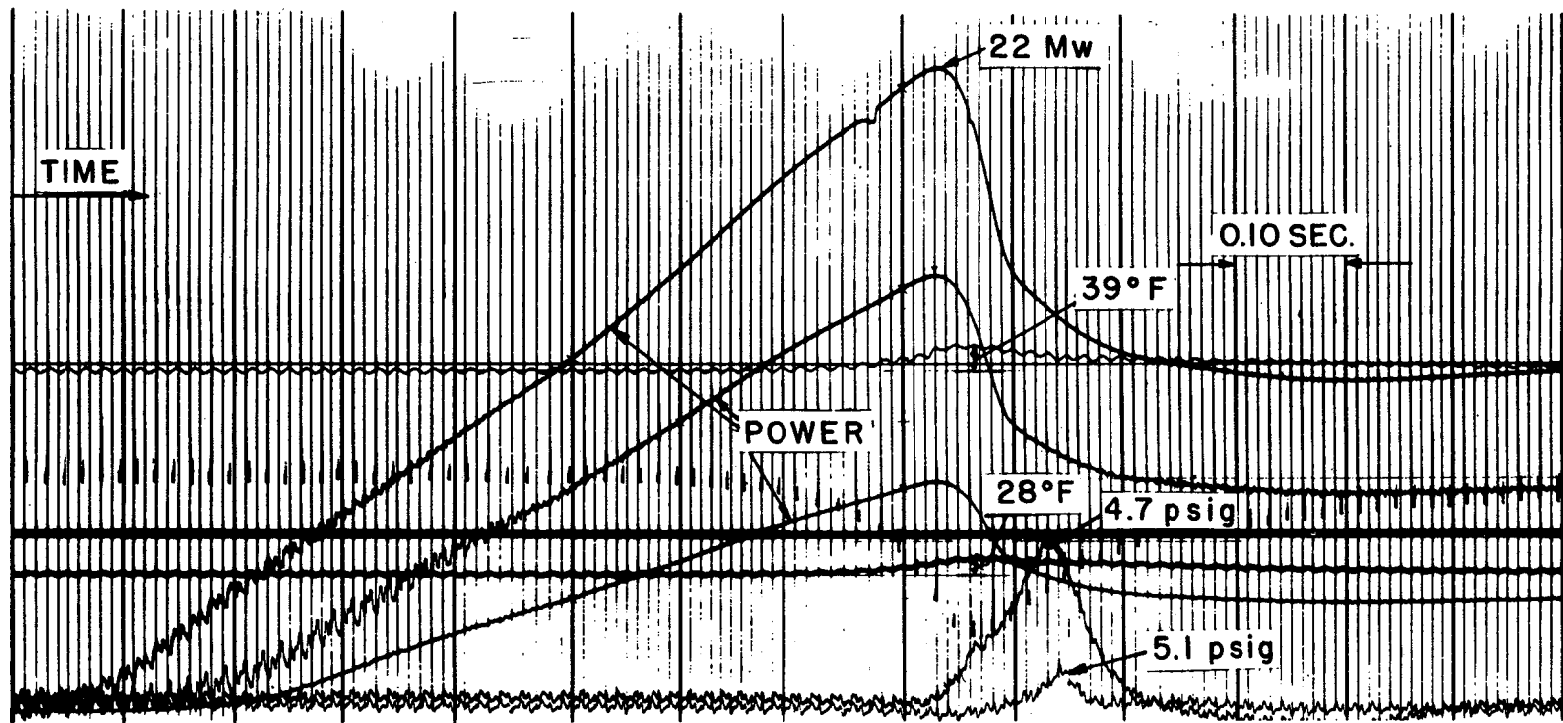


FIG. 43

RECORD OF POWER EXCURSION SHOWING PRESSURE VARIATION

THE EXCURSION WAS MADE WITH REACTOR TEMPERATURE INITIALLY AT SATURATION, WITH 0.058 SECOND PERIOD.

THE TWO PRESSURE TRACES ARE FROM TRANSDUCERS HAVING DIFFERENT SENSITIVITIES. THE UPPER TEMPERATURE TRACE IS FROM THE SURFACE OF FUEL PLATE 1; THE LOWER TRACE FROM THE CENTER OF PLATE 11.

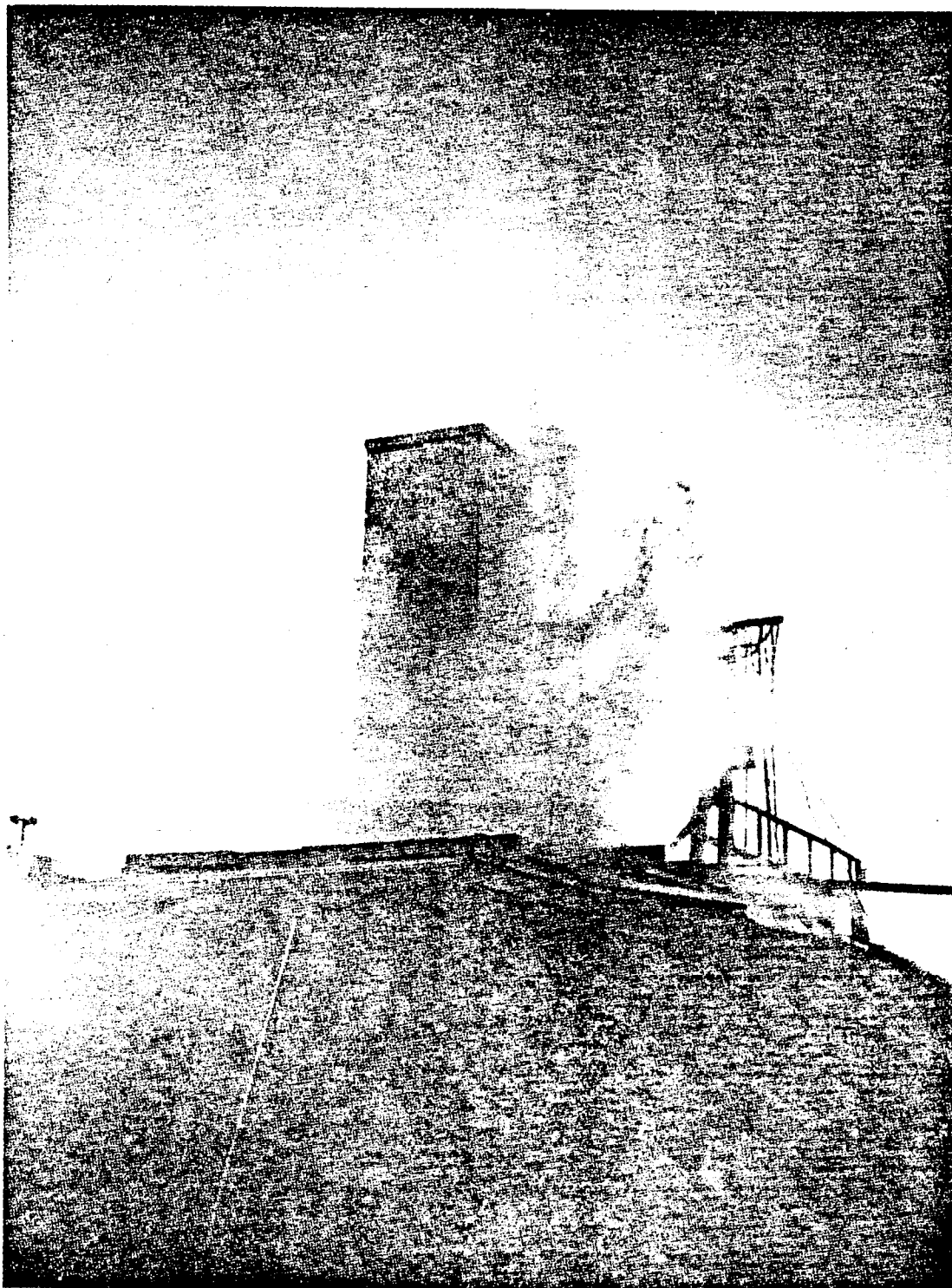
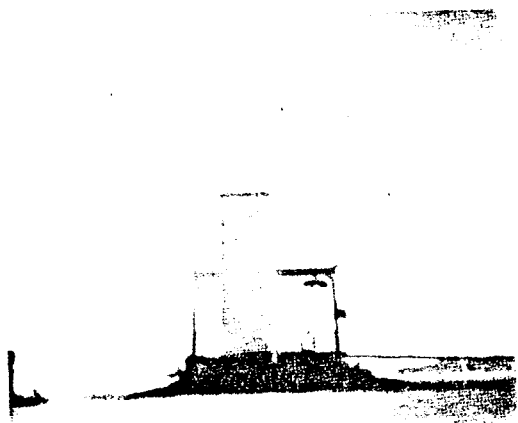
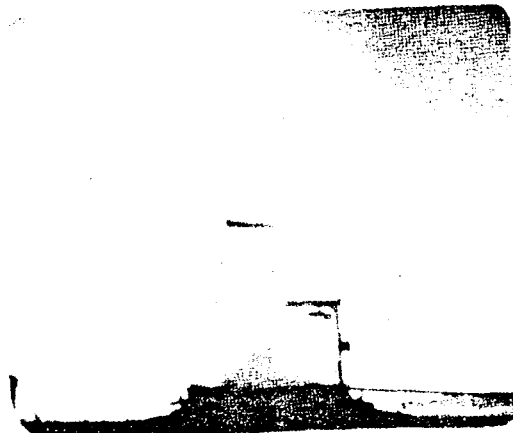


FIG. 44

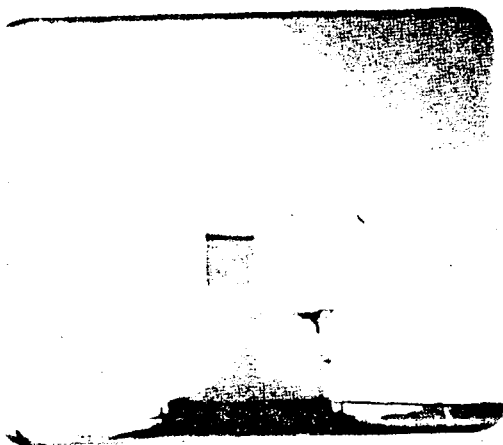
WATER EXPULSION DURING FIVE MILLISECOND EXCURSION



approx. 600 msec.



840 msec.



1180 msec.



1600 msec.



1950 msec.

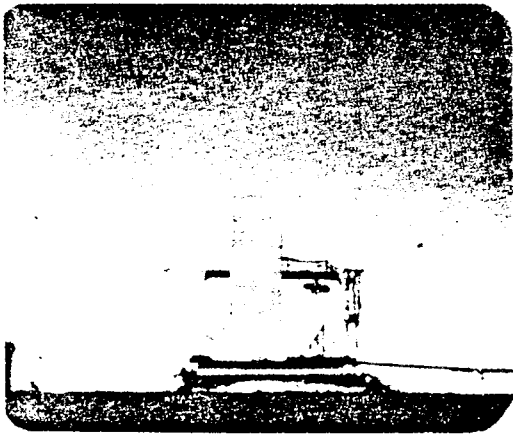


2200 msec.

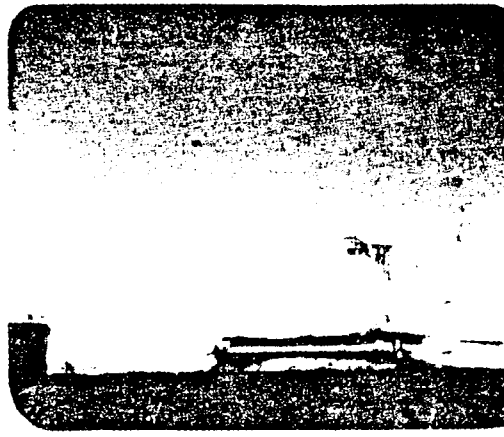
Figure 45
9/11 - #7

Boiling

Period 6.1 milliseconds



approx. 500 msec



600 msec.



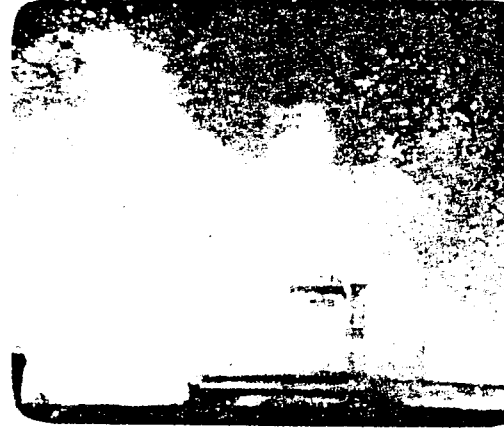
700 msec.



1070 msec.



1730 msec.



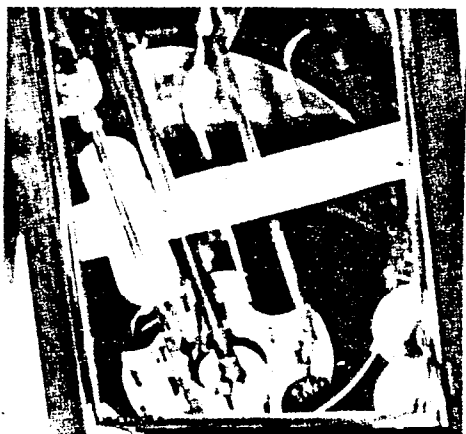
2600 msec.

Figure 46

9/11 - #9

Boiling

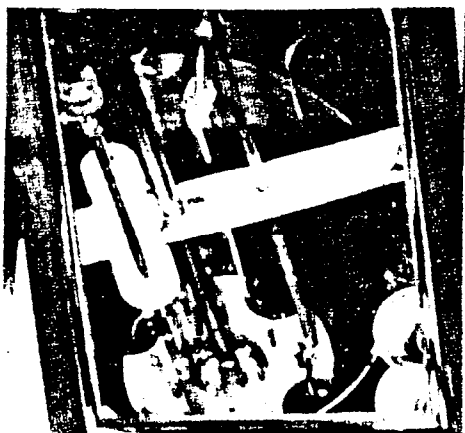
Period 5 milliseconds



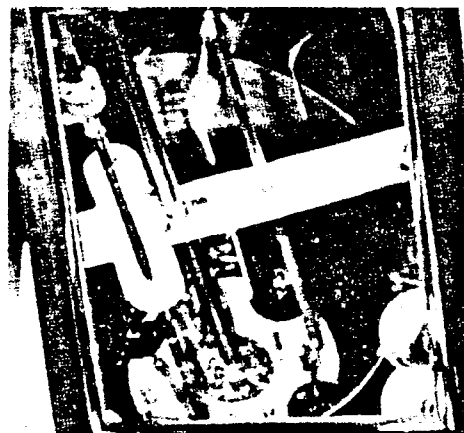
Start



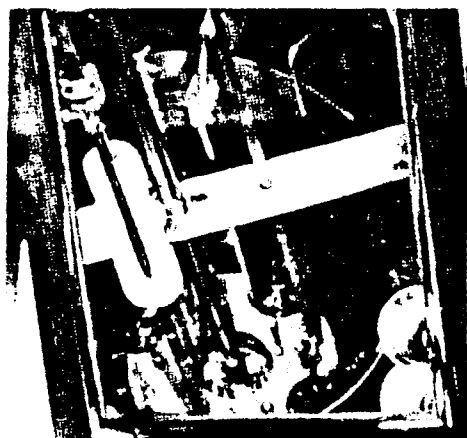
500 msec.



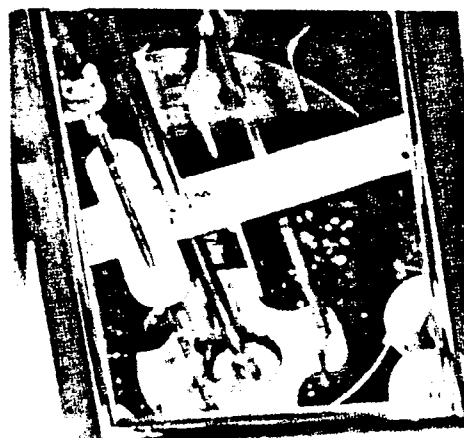
740 msec.



860 msec.



1200 msec.



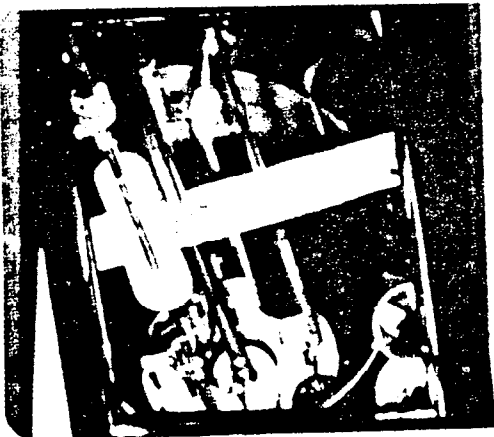
1420 msec.

Figure 47

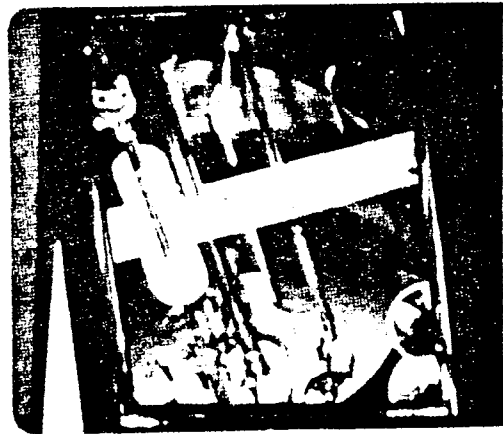
9/15 - #8

Subcooled 8.4°F.

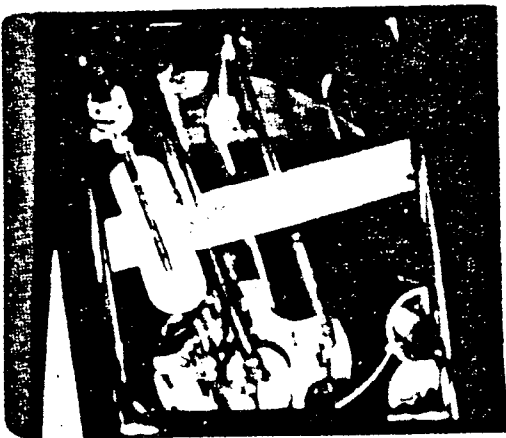
Period 22.2 milliseconds



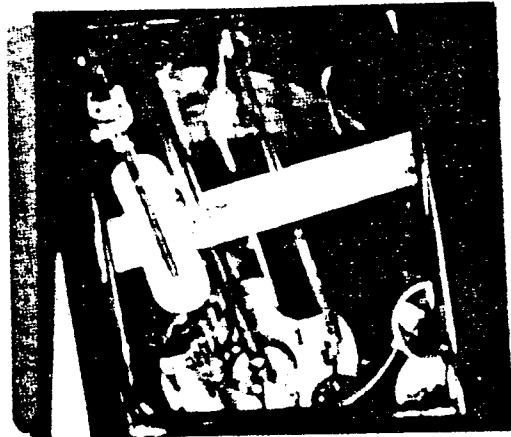
Start



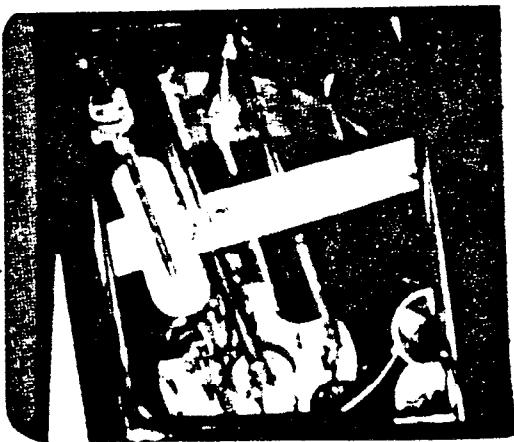
400 msec.



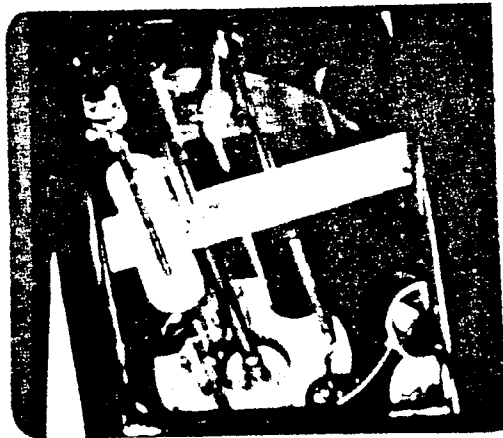
620 msec.



920 msec.



1200 msec.



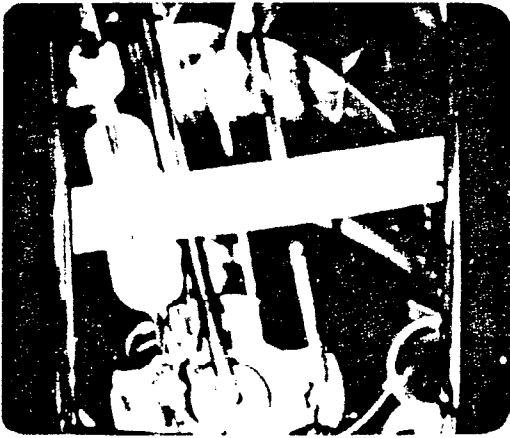
1350 msec.

Figure 48

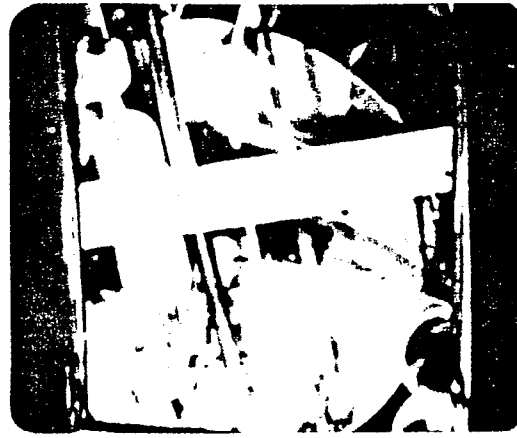
9/15 - #10

Subcooled 25.6 °F.

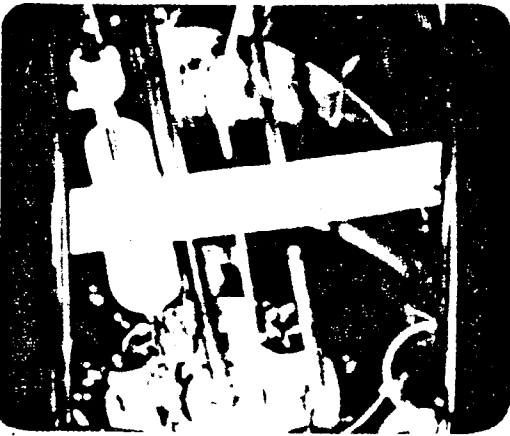
Period. 21.8 milliseconds



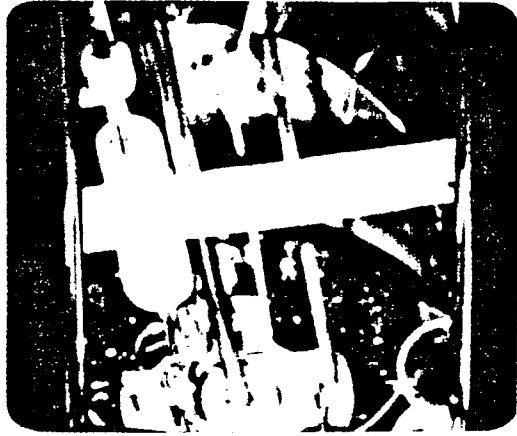
Start



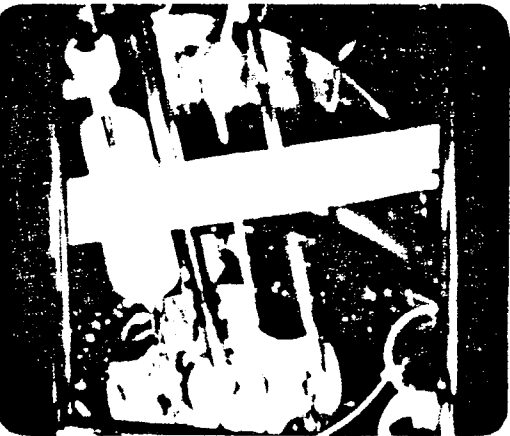
360 msec.



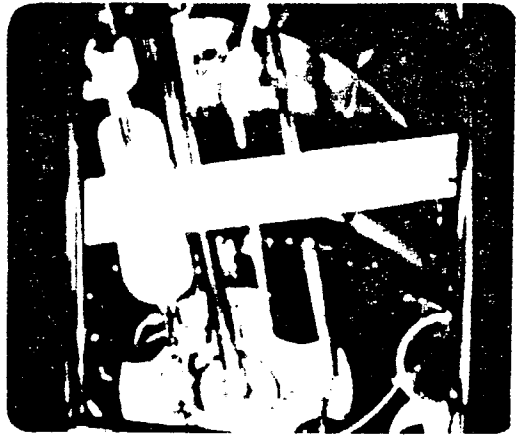
440 msec.



600 msec.



880 msec.



1300 msec.

Figure 49
9/15 - #13

Subcooled 124°F

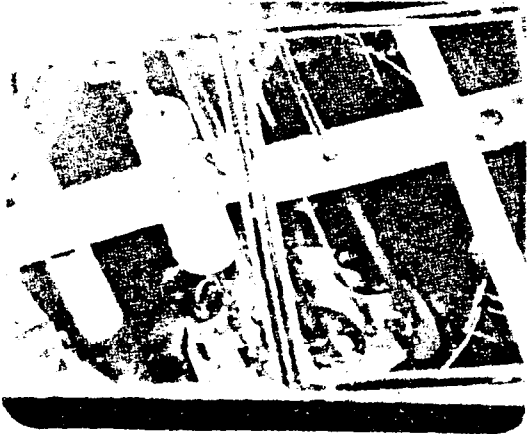
Period 20.2 milliseconds



Start



560 msec.



860 msec.



1220 msec.



1680 msec.



1860 msec.

Figure 50
9/16 - *2

Boiling

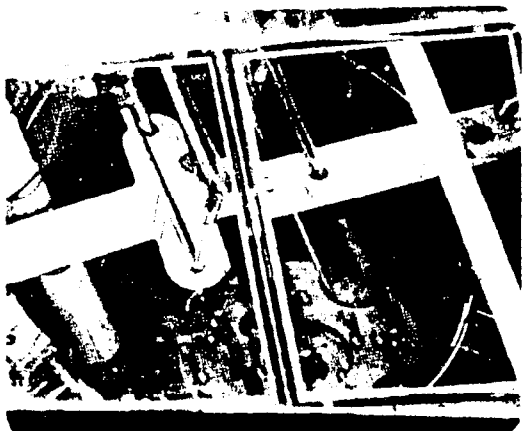
Period 23 milliseconds



Start



380 msec.



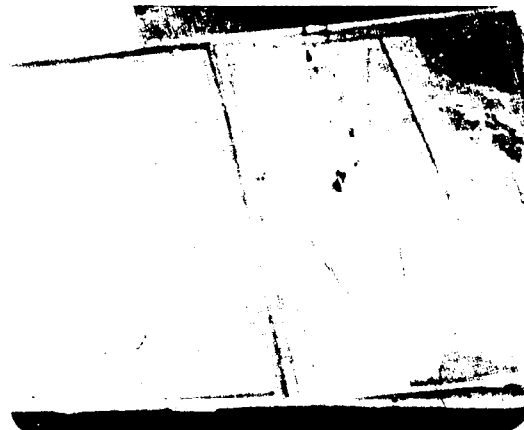
540 msec.



720 msec.



960 msec.



1220 msec.

Figure 51
9/16 -#4

Boiling

Period 13.6 milliseconds

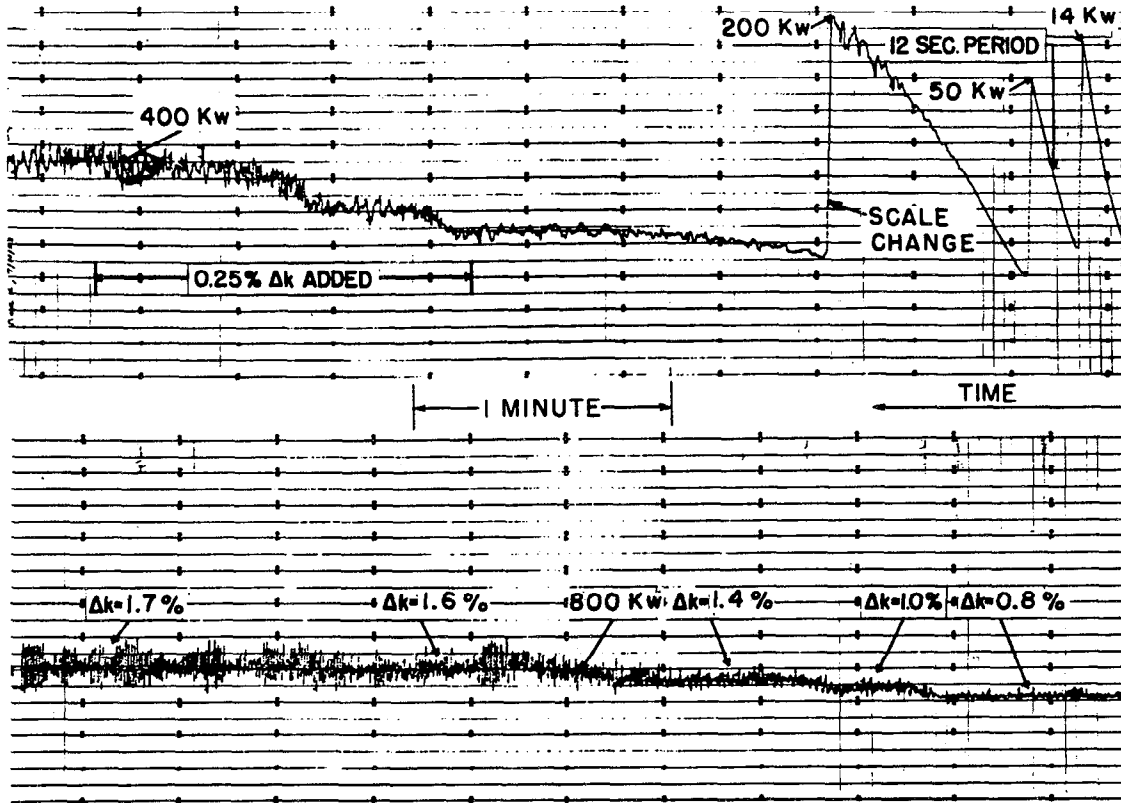


FIG. 52

POWER CHART SHOWING APPROACH TO POWER AND BOILING OPERATION
AT ATMOSPHERIC PRESSURE (RUN 2, 9/18/53)

THE REACTOR TEMPERATURE WAS INITIALLY AT SATURATION. THE REACTOR WAS BROUGHT UP TO POWER ON A 12-SECOND PERIOD WHICH LEVELED OFF INTO STEADY OPERATION AS BOILING BEGAN. FURTHER REACTIVITY ADDITIONS WERE MADE TO INCREASE POWER. THE Δk NOTATIONS INDICATE REACTIVITY COMPENSATED BY STEAM.

THE CHARTS ARE FROM A BROWN ELECTRONIK RECORDER SHOWING OUTPUT OF COMPENSATED ION CHAMBER. ZERO IS AT BOTTOM OF CHART. PEN SPEED IS HIGH ENOUGH TO SHOW AMPLITUDE OF VARIATIONS WITH REASONABLE ACCURACY. THERE IS A TIME GAP OF ABOUT A MINUTE BETWEEN UPPER AND LOWER CHARTS, DURING WHICH A SCALE CHANGE WAS MADE.

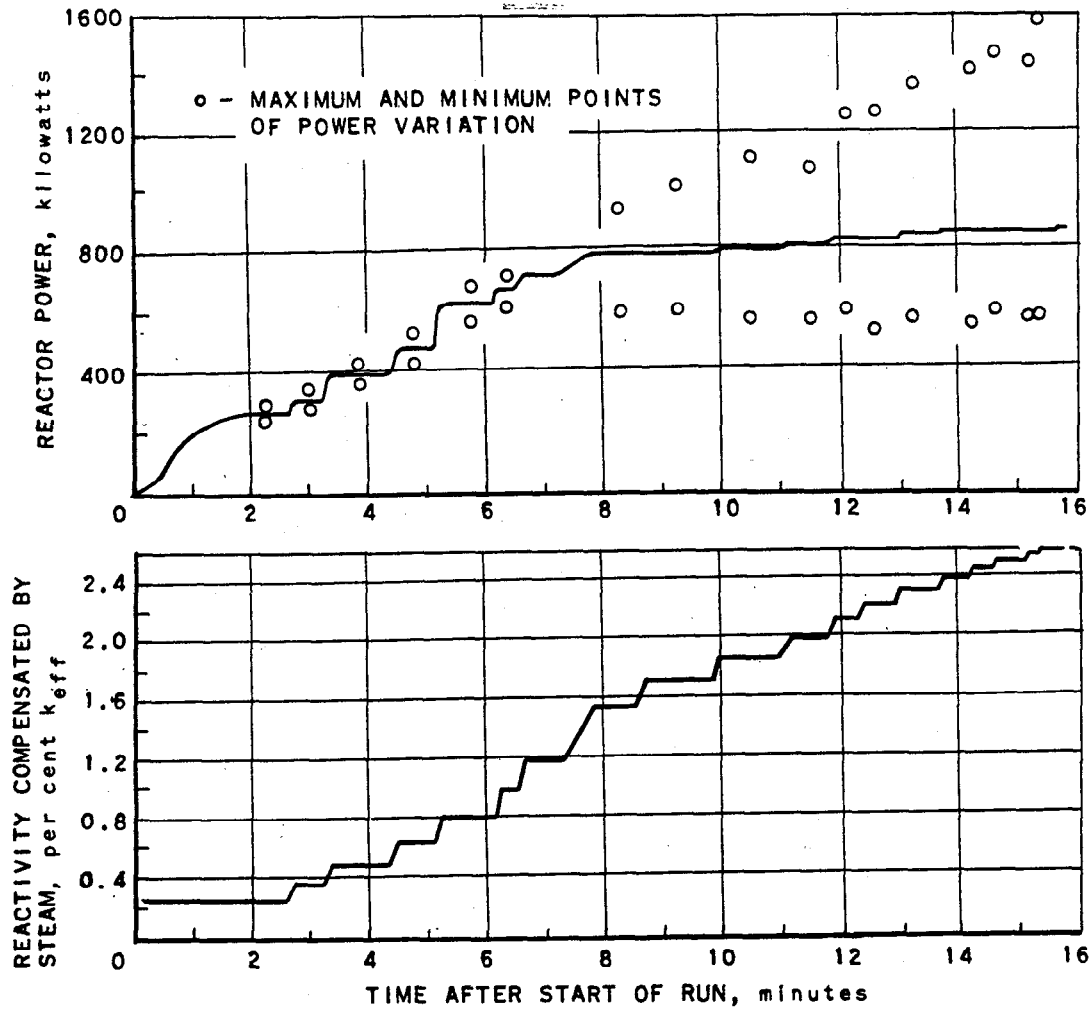


FIG. 53
 REACTOR POWER AND REACTIVITY COMPENSATED
 BY STEAM DURING A STEADY BOILING
 RUN AT ATMOSPHERIC PRESSURE

(RUN 2, 9/18/53)

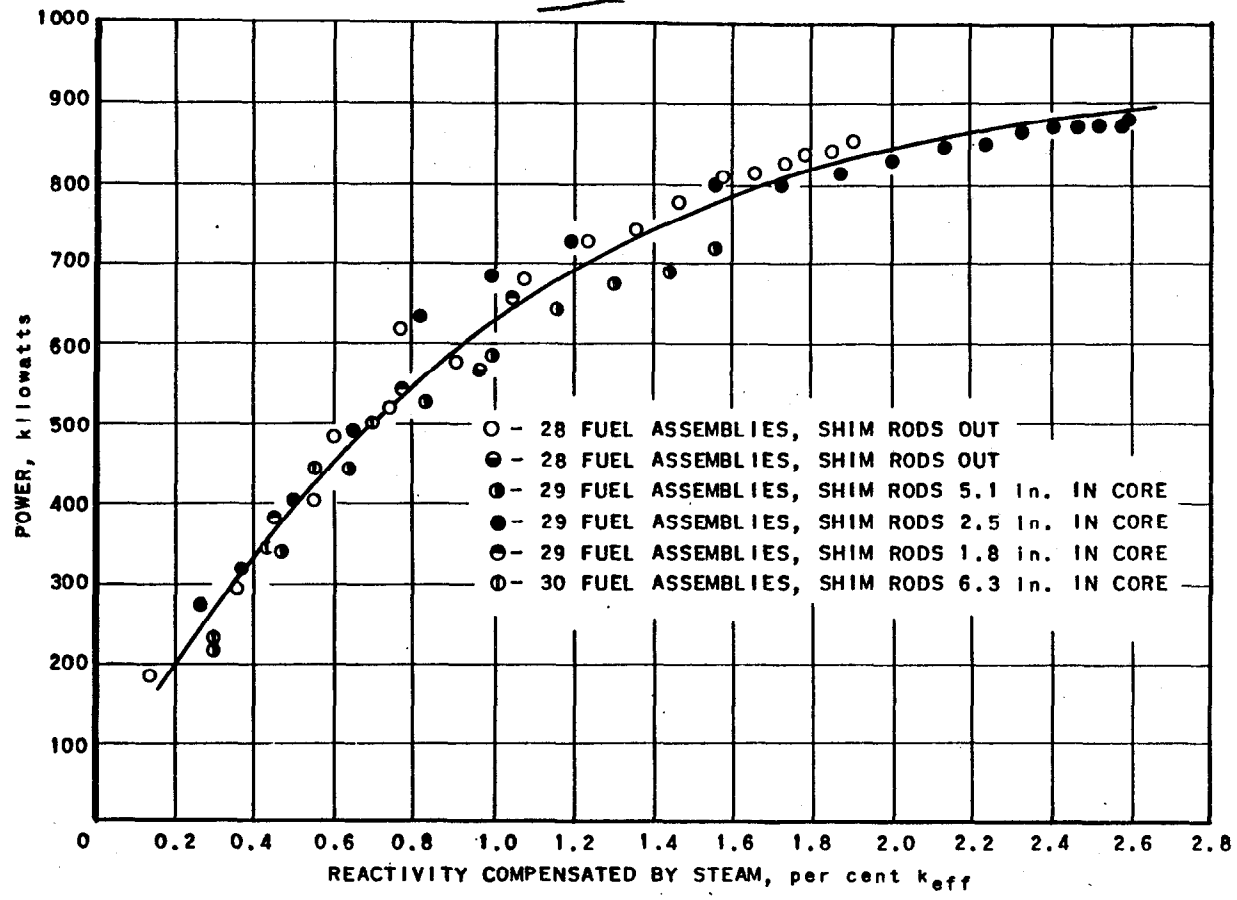


FIG. 54
REACTOR POWER AS A FUNCTION OF REACTIVITY
COMPENSATED BY STEAM FOR SEVERAL STEADY
BOILING RUNS AT ATMOSPHERIC PRESSURE

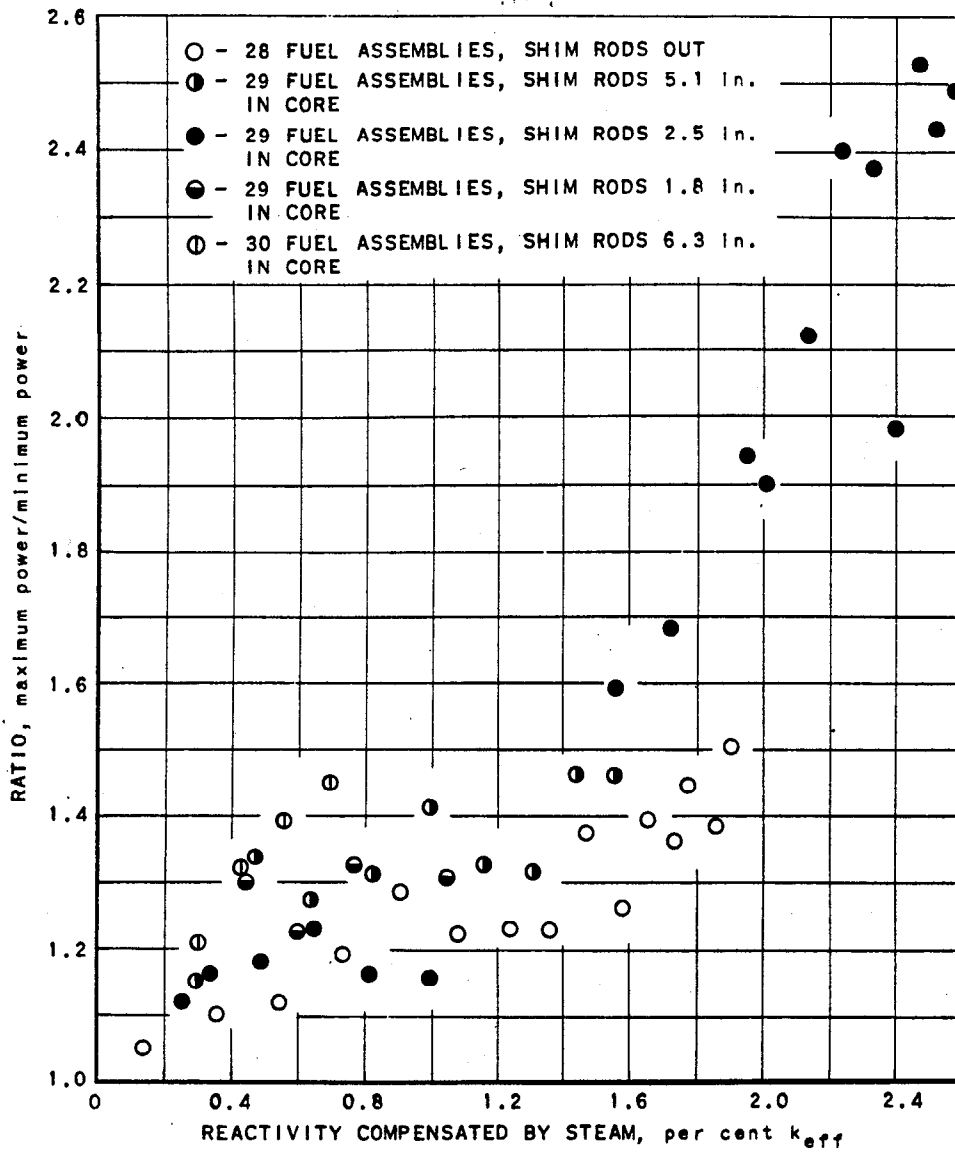


FIG. 55
 AMPLITUDE OF POWER VARIATION IN ATMOSPHERIC
 BOILING OPERATION AS A FUNCTION OF
 REACTIVITY COMPENSATED BY STEAM

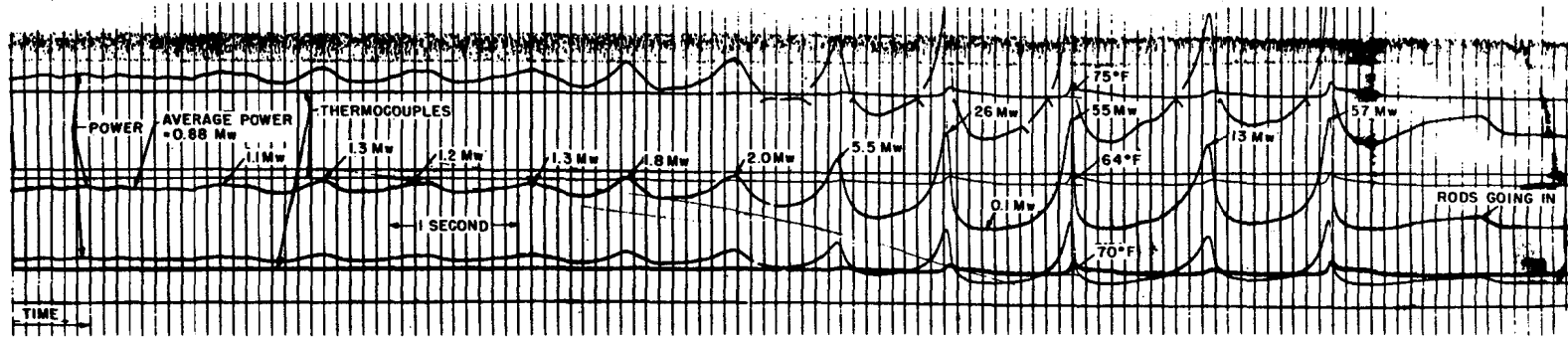


FIG. 56

FAST GALVANOMETER RECORDS SHOWING TRANSITION FROM OSCILLATORY BOILING TO "CHUGGING" AT ATMOSPHERIC PRESSURE. $2.6\% k_{off}$ COMPENSATED BY STEAM
(END OF RUN 2, 9/18/53)

THE THREE POWER RECORDS ARE FROM ION CHAMBERS OF DIFFERENT SENSITIVITIES, ON LOGARITHMIC SCALE. THE UPPERMOST TRACE IS UNRELIABLE BECAUSE OF A STICKING GALVANOMETER. THE TOP TEMPERATURE TRACE IS FROM THE CENTER OF FUEL PLATE 4. THE MIDDLE TRACE IS FROM THE CENTER OF PLATE 1, AND THE LOWEST TRACE FROM THE SURFACE OF PLATE 1.

123

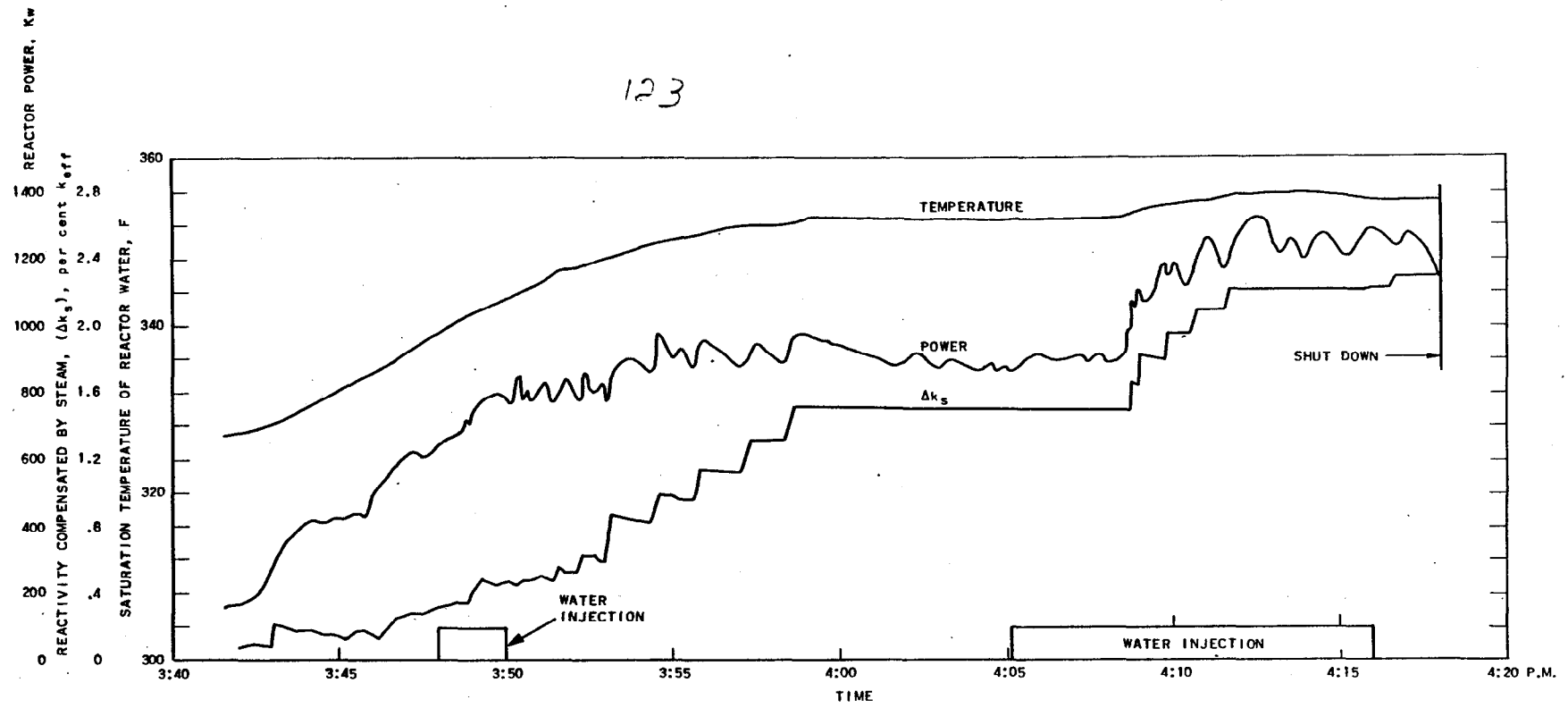


FIG. 57
RECORD OF PRESSURIZED BOILING RUN NO. 3, ON
OCT. 21, 1953, 32 FUEL ASSEMBLIES IN CORE

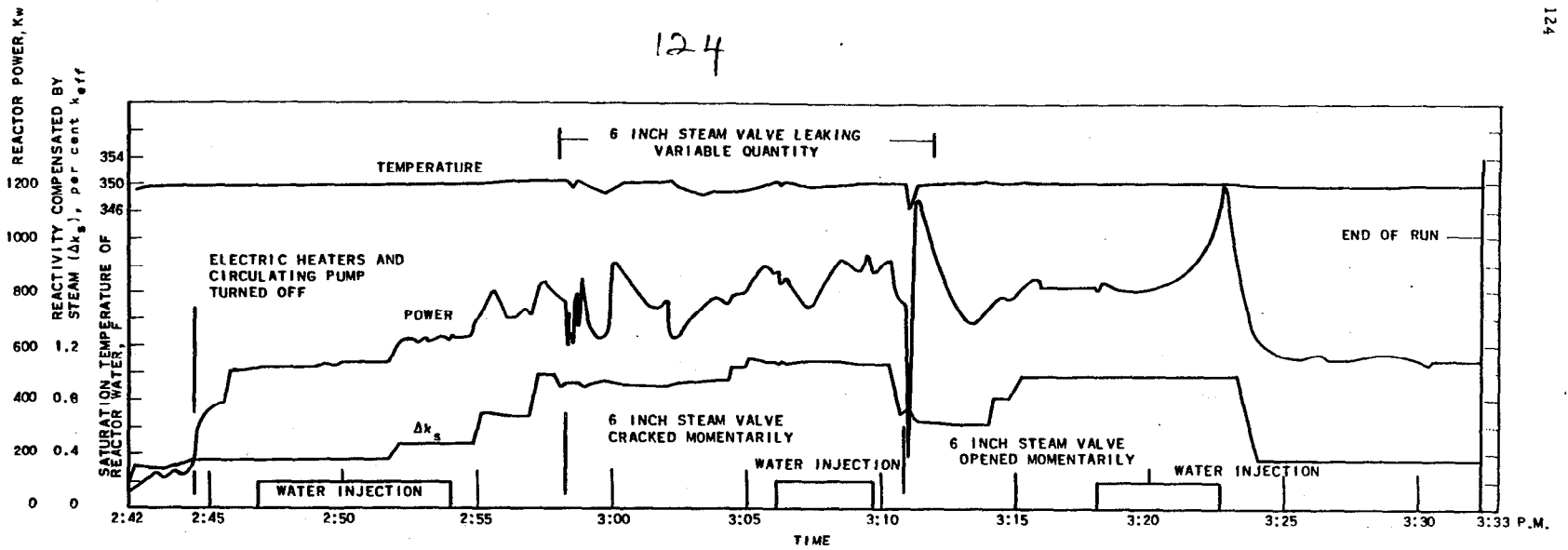


FIG. 58
 RECORD OF PRESSURIZED BOILING RUN NO. 3, ON
 OCT. 20, 1953, 32 FUEL ASSEMBLIES IN CORE

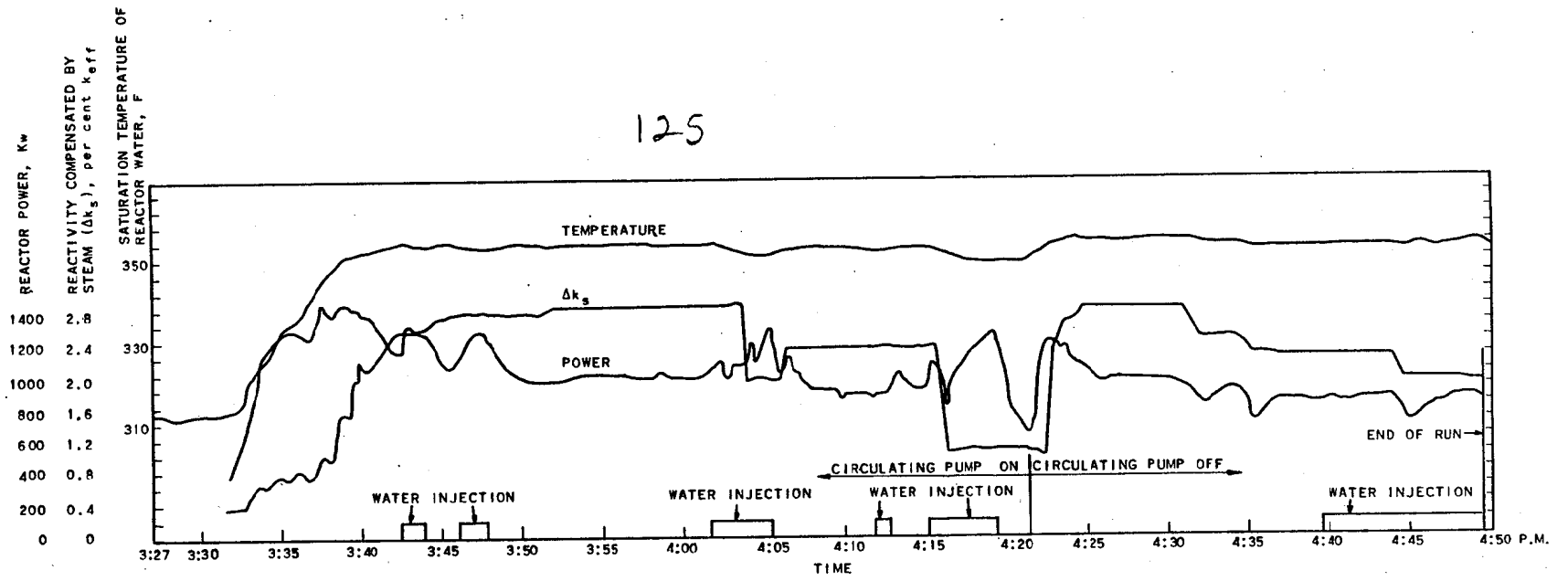


FIG. 59
 RECORD OF PRESSURIZED BOILING RUN NO. 3, ON
 OCT. 22, 1953, 32 FUEL ASSEMBLIES IN CORE

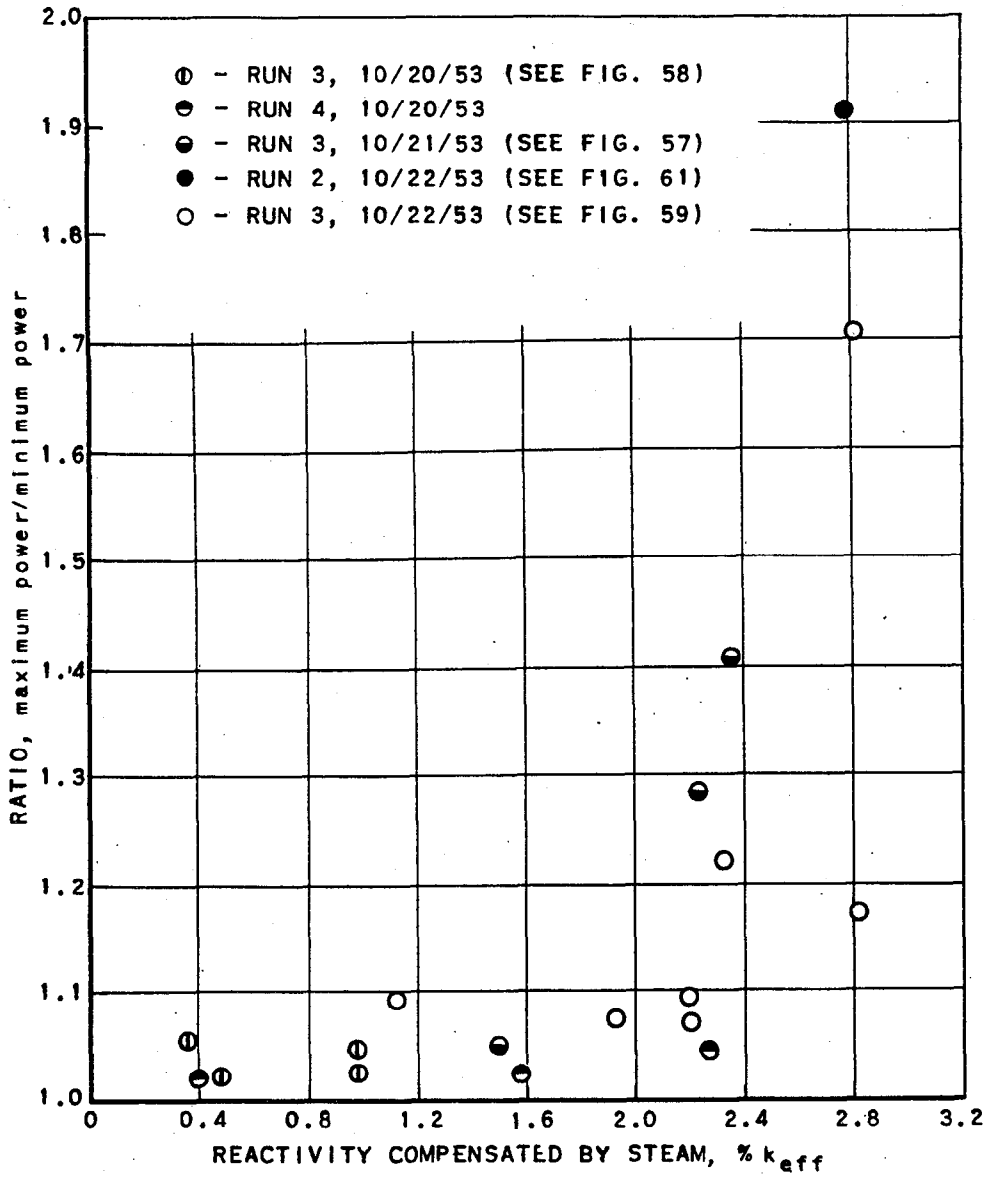


FIG. 60
AMPLITUDE OF RAPID POWER FLUCTUATION IN
PRESSURIZED BOILING OPERATION AS A
FUNCTION OF REACTIVITY COMPENSATED BY STEAM

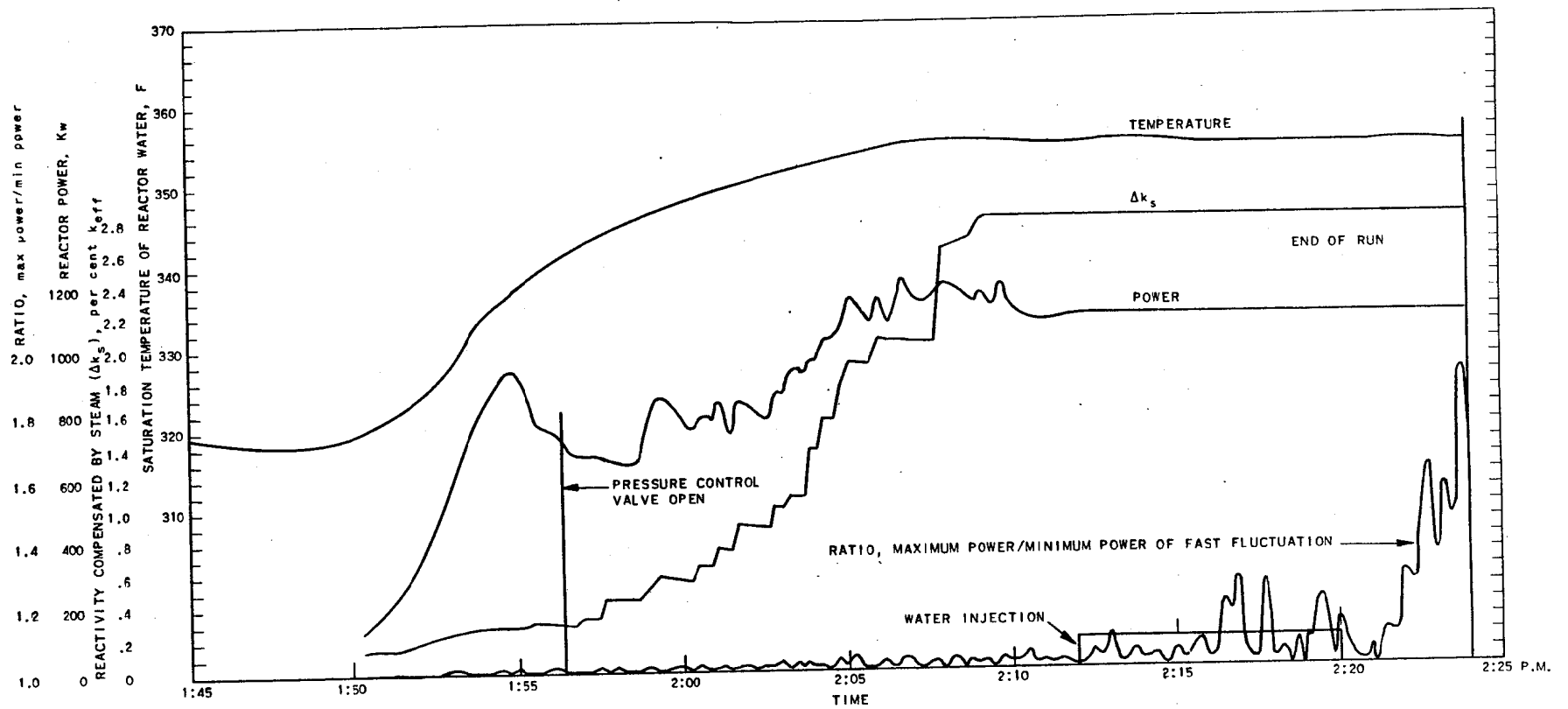


FIG. 61
 RECORD OF PRESSURIZED BOILING RUN NO. 2, ON
 OCT. 22, 1953, 32 FUEL ASSEMBLIES IN CORE

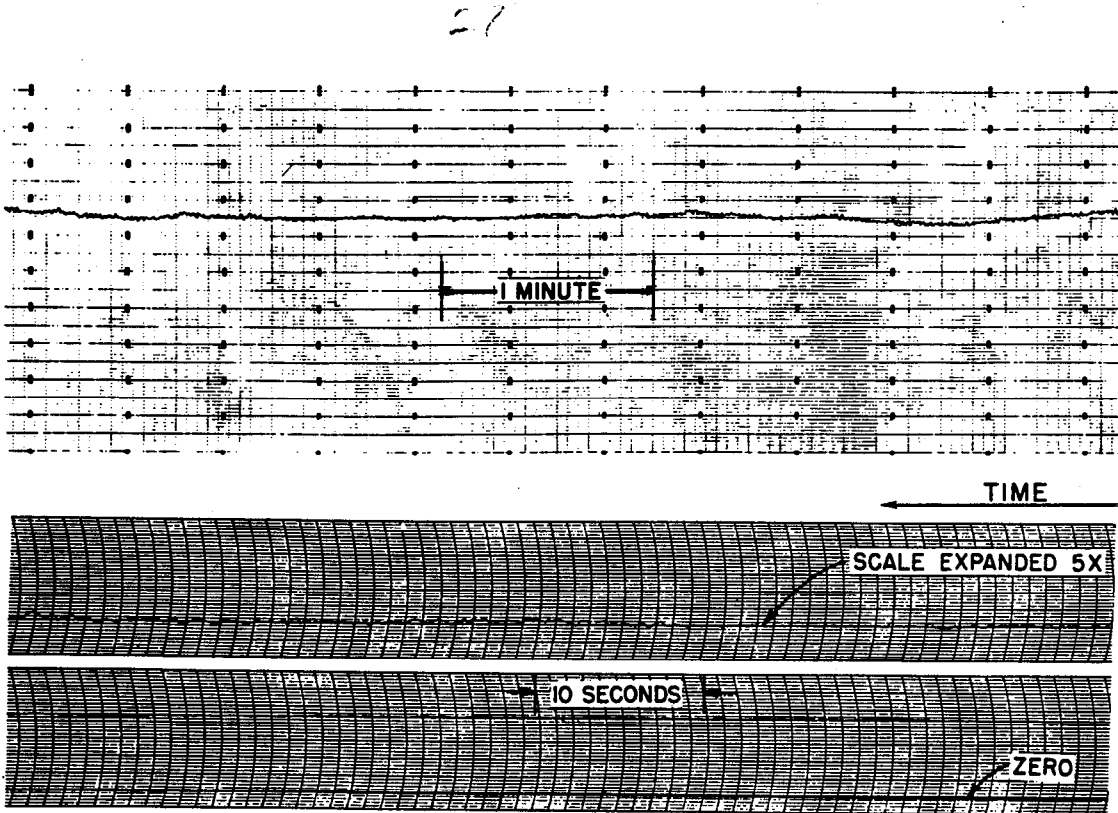


FIG. 62

POWER RECORDS OF STEADY BOILING FROM RUN 4, 10/20/53

THE REACTOR WAS OPERATING AT A POWER OF 970 kw AT 130 psig, WITH 1.6% k_{eff} COMPENSATED BY STEAM. FEEDWATER WAS BEING INJECTED DURING THIS RUN.

THE UPPER RECORD IS FROM A BROWN ELECTRONIK RECORDER SHOWING OUTPUT OF COMPENSATED ION CHAMBER; ZERO IS AT BOTTOM OF CHART.

THE LOWER RECORDS ARE FROM A DOUBLE PEN BRUSH RECORDER ON THE SAME ION CHAMBER, WITH EXPANDED TIME SCALE. THE LOWEST RECORD INCLUDES THE ZERO POWER LINE AS INDICATED. THE RECORD JUST ABOVE EXPANDS THE AMPLITUDE OF POWER VARIATION BY A FACTOR OF 5; THE ZERO FOR THIS RECORD IS OFF THE CHART.

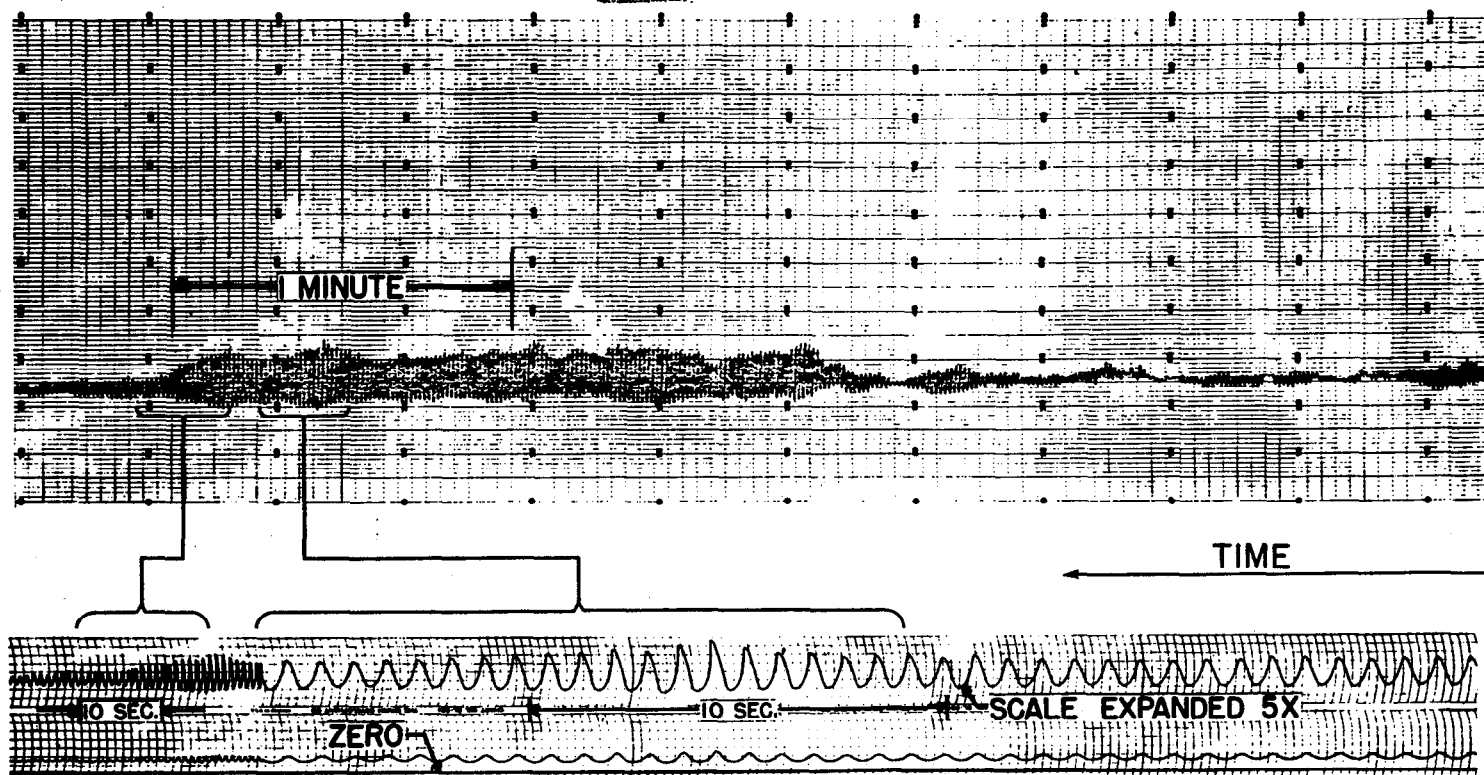


FIG. 63

POWER RECORDS OF OSCILLATORY BOILING FROM RUN 2, 10/22/53

THE REACTOR WAS OPERATING AT AN AVERAGE POWER OF 1100 kw AT 130 psig, WITH 2.8% k_{off} COMPENSATED BY STEAM.

THE UPPER RECORD IS FROM A BROWN ELECTRONIK RECORDER SHOWING OUTPUT OF COMPENSATED ION CHAMBER; ZERO IS AT BOTTOM OF CHART.

THE LOWER RECORDS ARE FROM A DOUBLE PEN BRUSH RECORDER, EXPANDING PORTIONS OF THE UPPER RECORD AS INDICATED. THE LOWEST RECORD INCLUDES THE ZERO POWER LINE AS INDICATED. THE RECORD JUST ABOVE EXPANDS THE AMPLITUDE OF OSCILLATION BY A FACTOR OF 5; THE ZERO FOR THIS RECORD IS OFF THE CHART.

35

----- LARGE AMPLITUDE OSCILLATION ($\frac{\max}{\min} = 1.88$)

----- SMALL AMPLITUDE OSCILLATION ($\frac{\max}{\min} = 1.16$)

———— SINE VARIATION

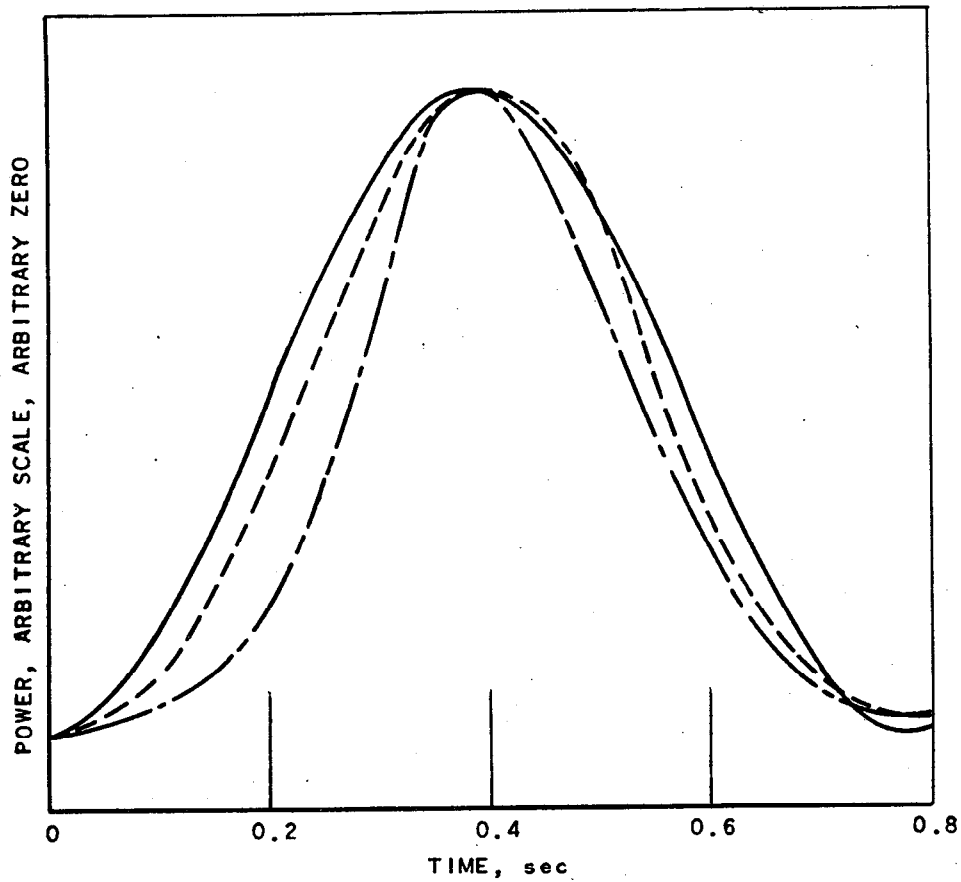


FIG. 64
REPRESENTATIVE SHAPES OF POWER OSCILLATIONS
IN PRESSURIZED BOILING

(FROM RUN 2, 10/22/53; 2.8% k COMPENSATED BY STEAM)

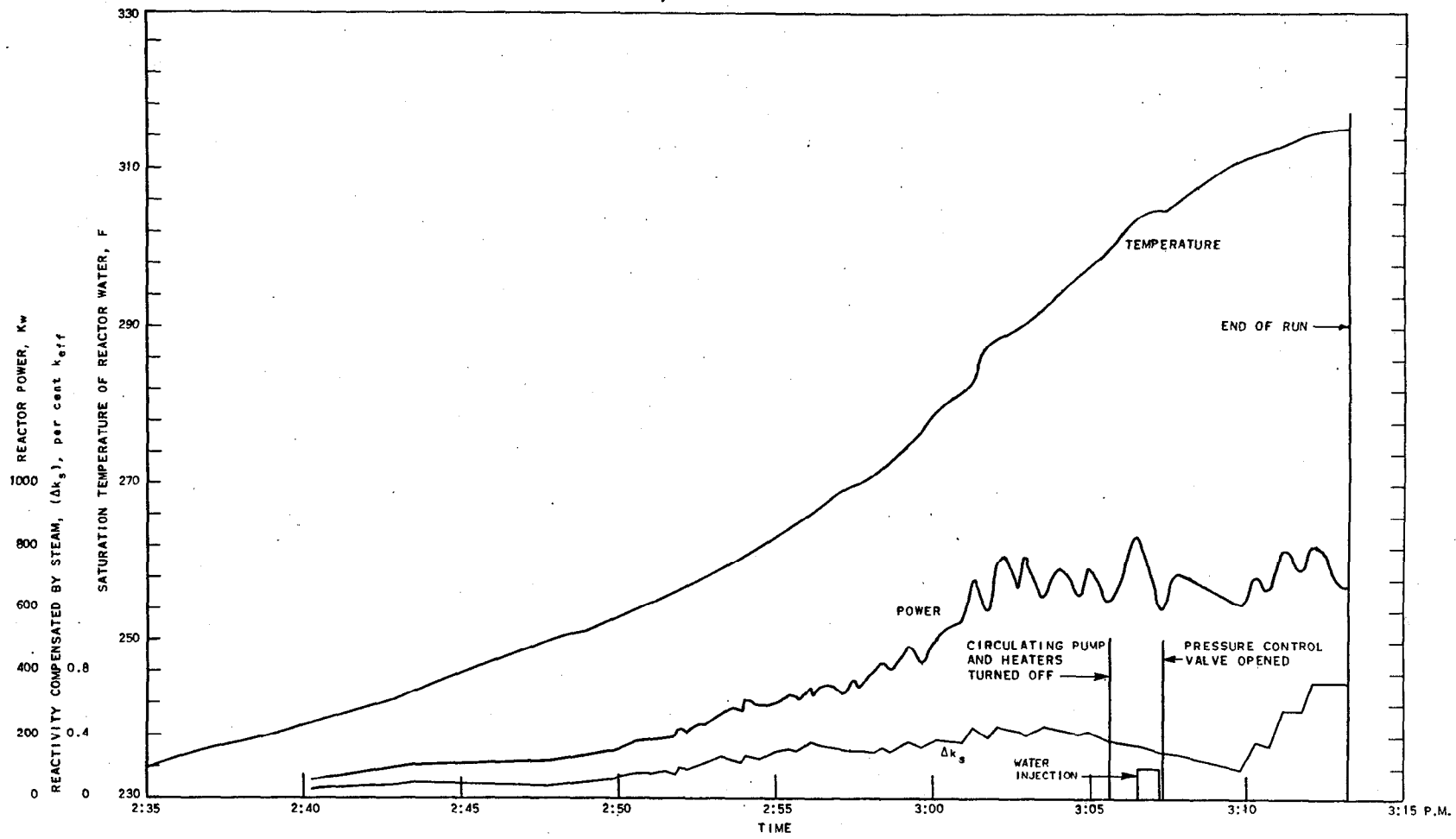


FIG. 65
RECORD OF PRESSURIZED OPERATION IN CLOSED VESSEL,
RUN 2, OCT. 15, 1953, 30 FUEL ASSEMBLIES IN CORE

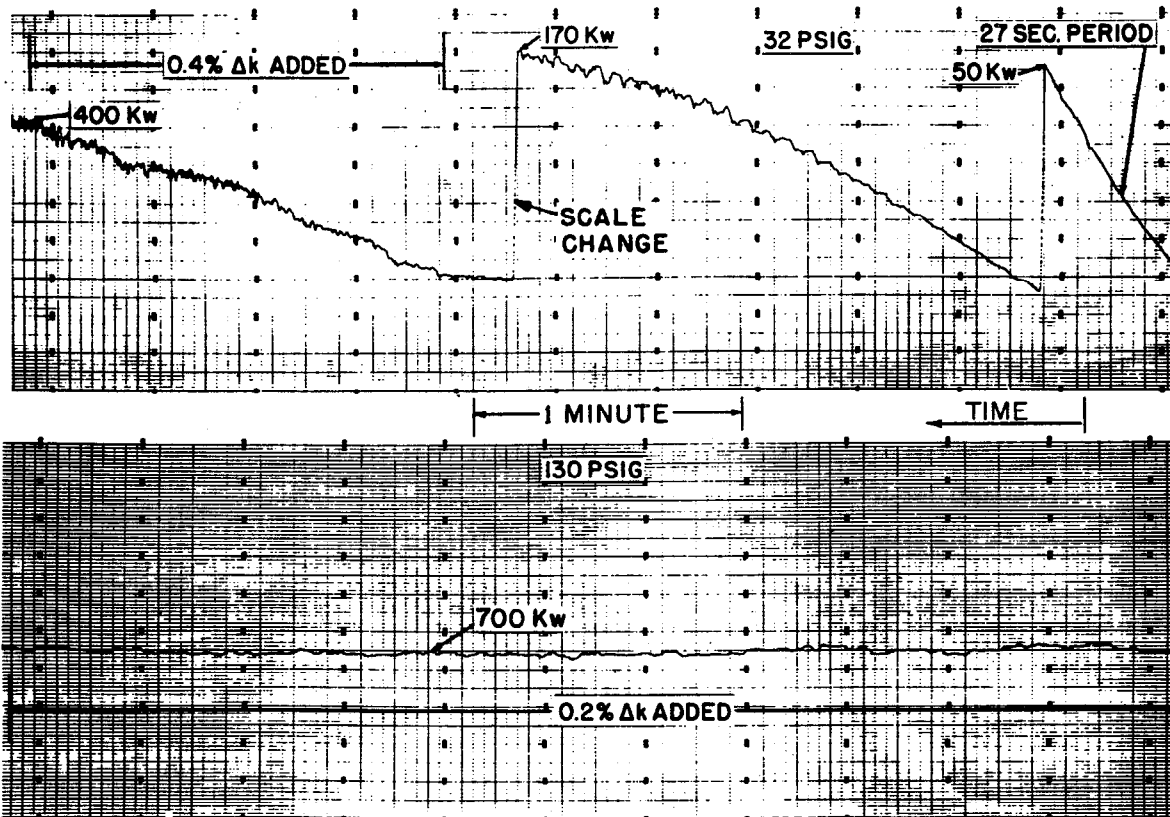


FIG. 66

POWER CHART SHOWING APPROACH TO POWER AND STEADY OPERATION IN CLOSED VESSEL

ZERO IS AT BOTTOM OF CHART.

THE REACTOR WAS BROUGHT UP TO POWER AT 32 psig BY PUTTING IT ON A 27-SECOND PERIOD AND ALLOWING THE POWER TO RISE UNTIL IT BEGAN TO LEVEL OFF OF ITS OWN ACCORD. FURTHER REACTIVITY WAS THEN ADDED FOR FURTHER POWER INCREASE. (TOP RECORD)

THE LOWER RECORD WAS MADE LATER AFTER THE POWER OPERATION HAD RAISED REACTOR PRESSURE TO 130 psig. REACTIVITY MUST BE ADDED SLOWLY TO COMPENSATE FOR TEMPERATURE COEFFICIENT IF POWER IS TO BE HELD CONSTANT.

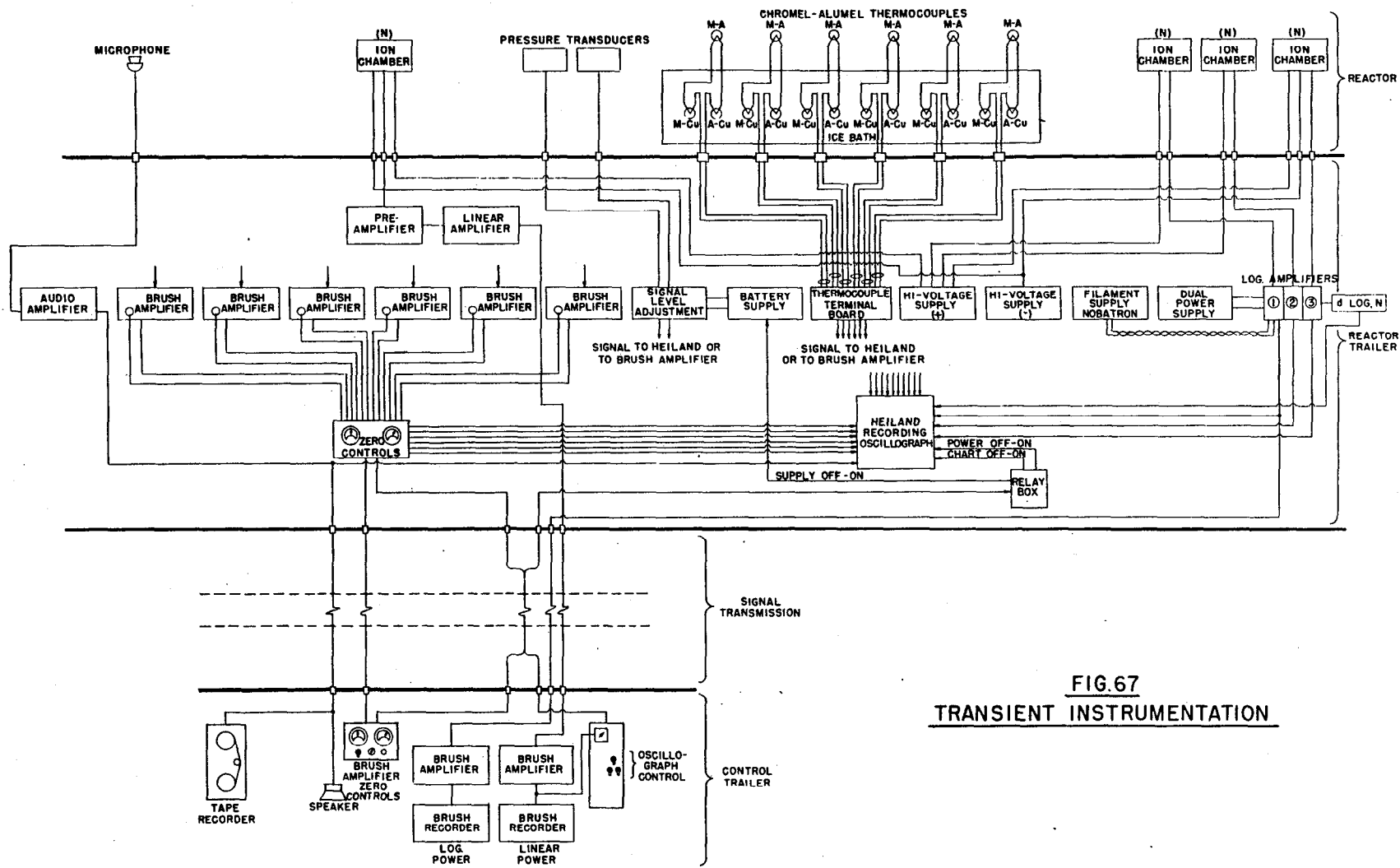


FIG. 67
TRANSIENT INSTRUMENTATION

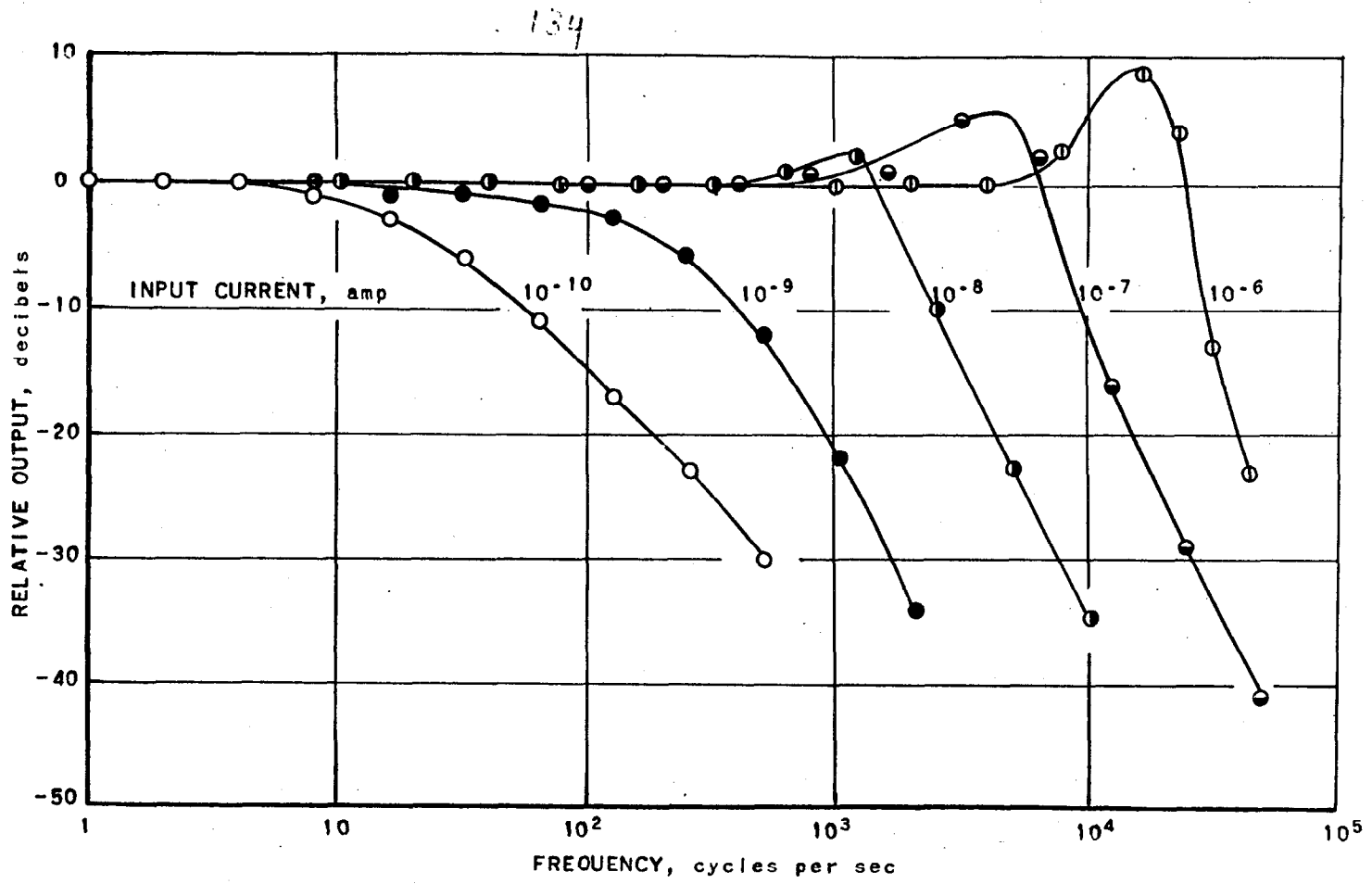


FIG. 68
FREQUENCY RESPONSE OF
LOGARITHMIC AMPLIFIER

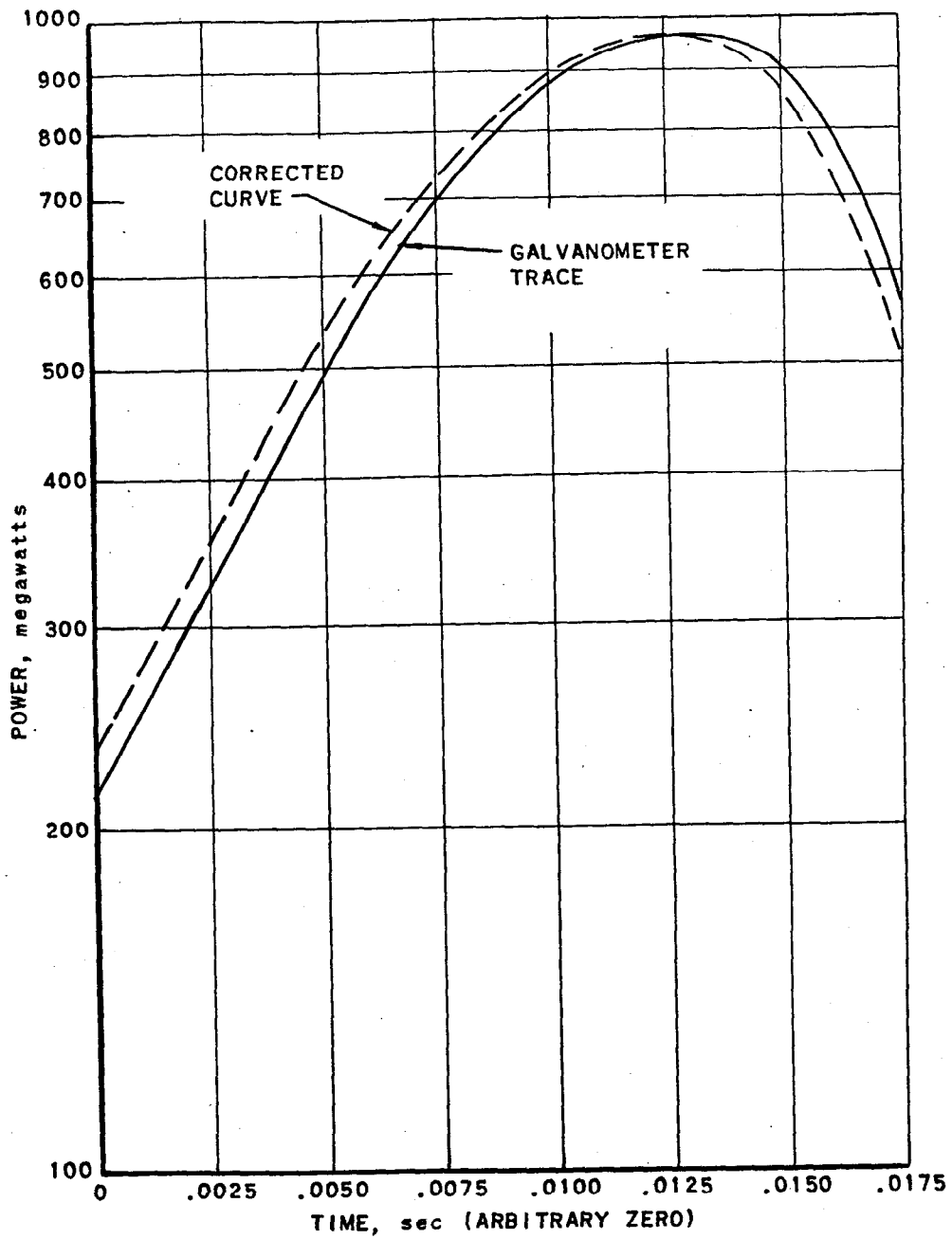


FIG. 69
CALCULATED CORRECTION TO POWER
TRANSIENT FOR GALVANOMETER LAG
PERIOD OF EXCURSION = 0.0062 sec

136

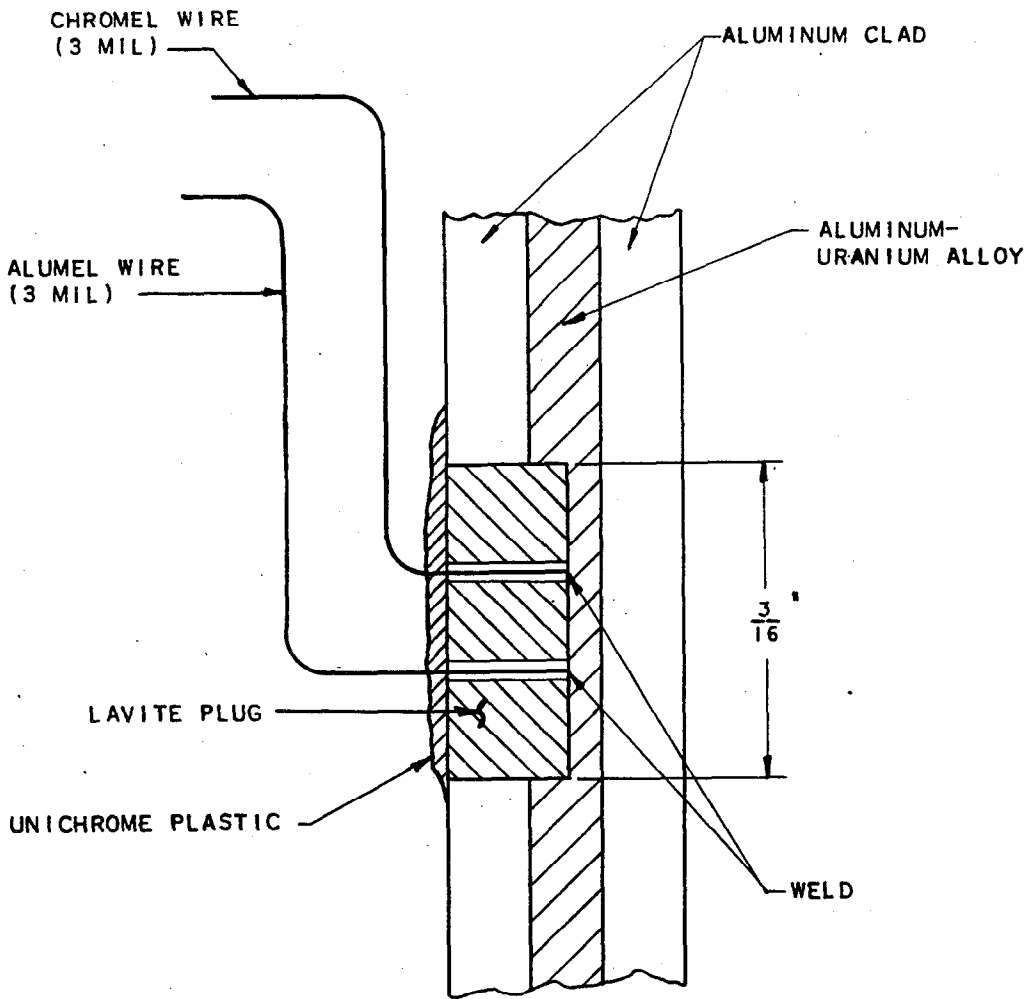


FIG. 70
INSTALLATION OF THERMOCOUPLE
AT CENTER OF FUEL PLATE

137

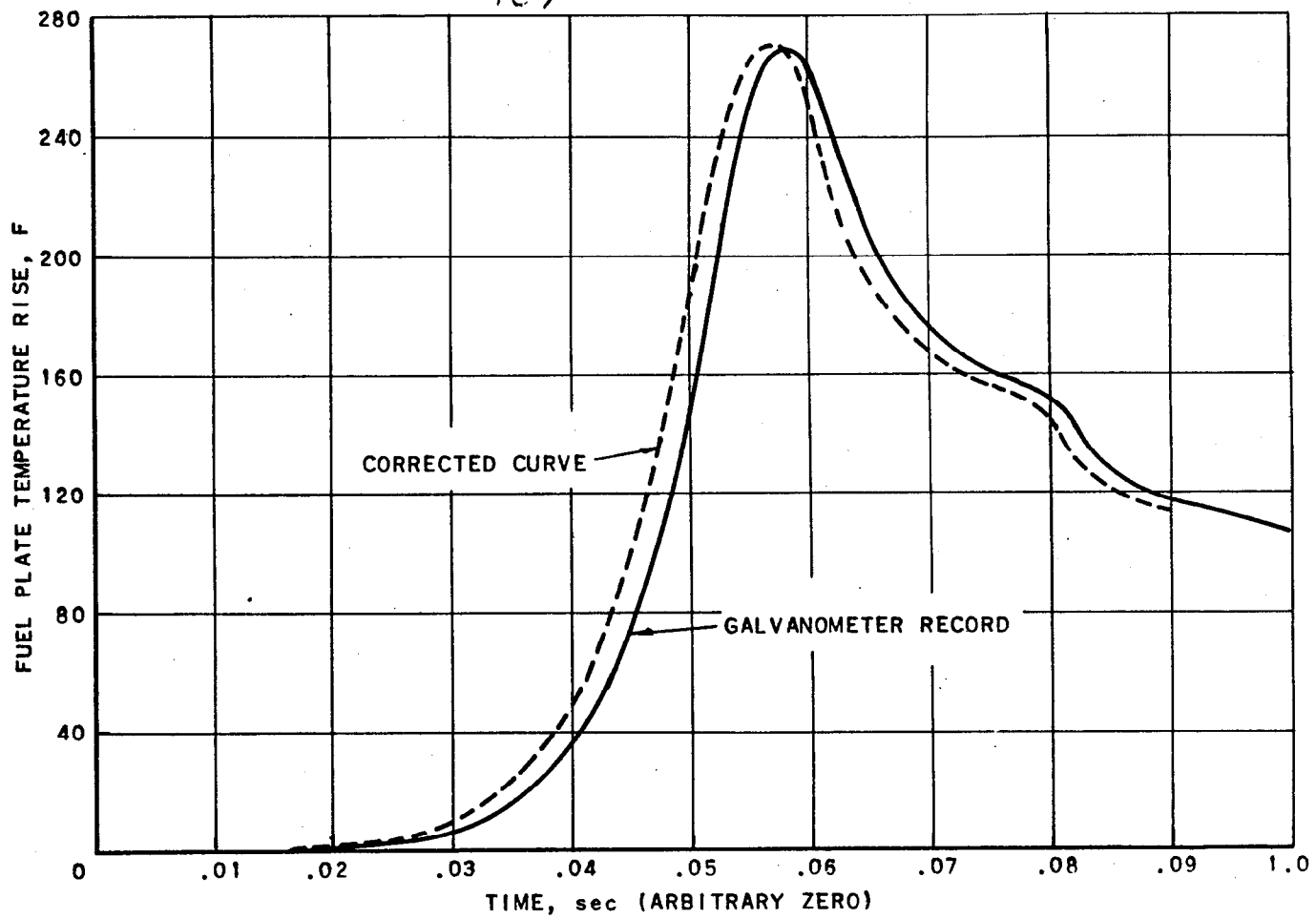


FIG. 71
CORRECTION TO TEMPERATURE CURVE
FOR GALVANOMETER TIME RESPONSE

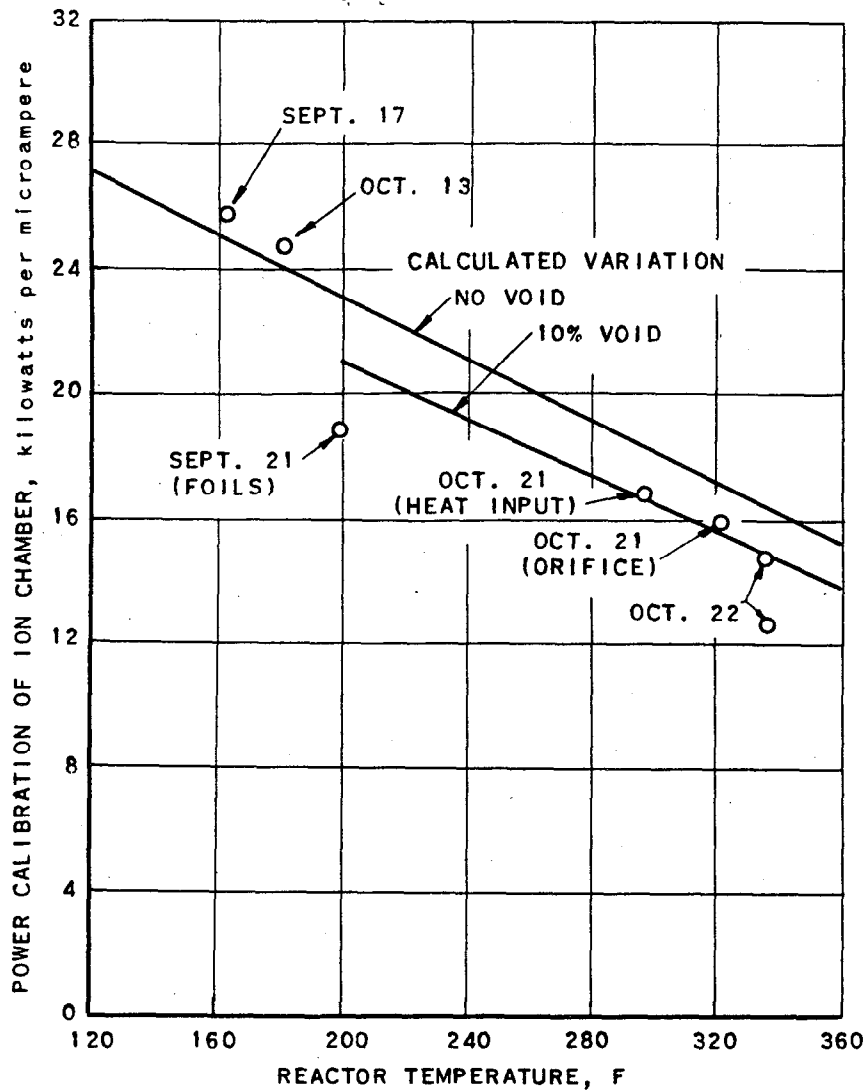


FIG. 72
CALIBRATIONS OF REACTOR POWER

140

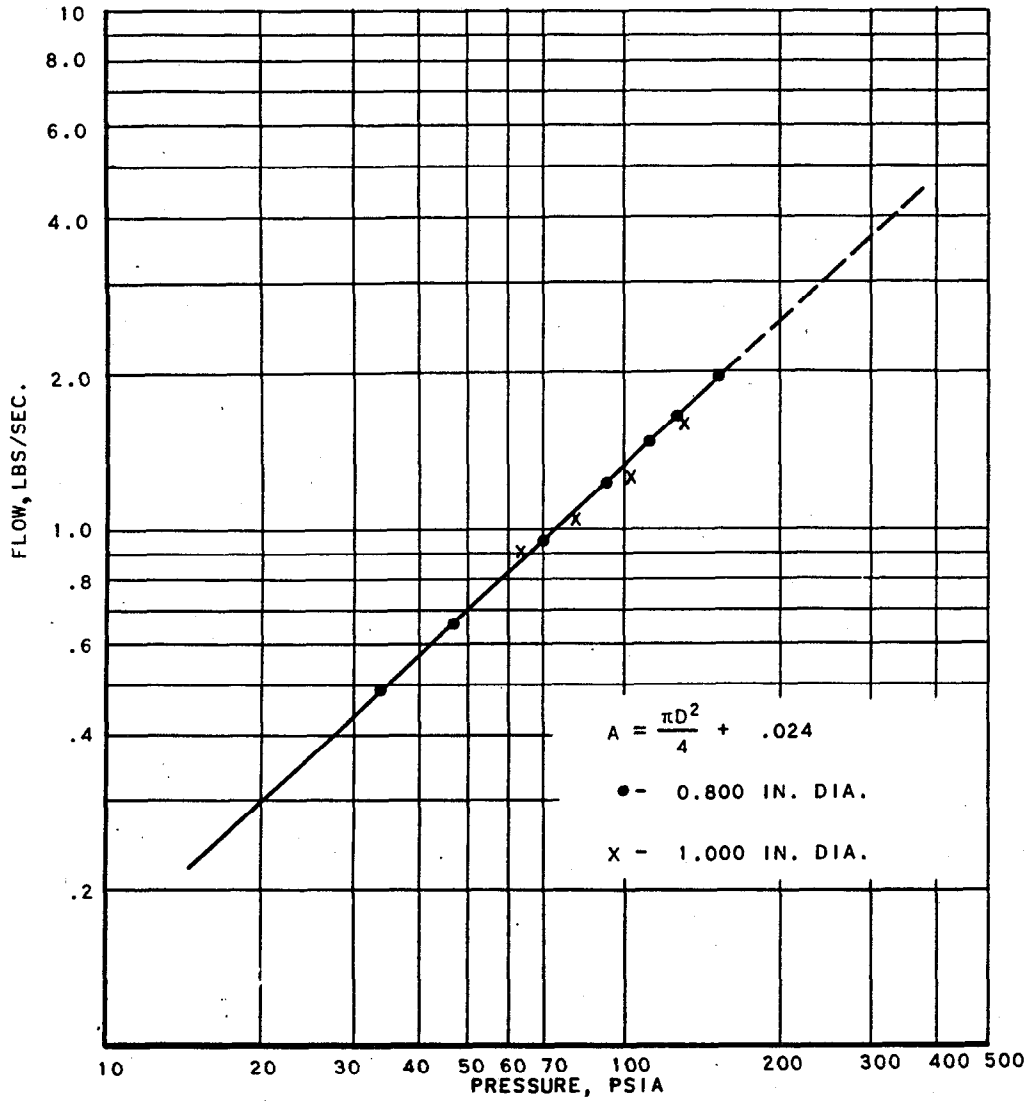
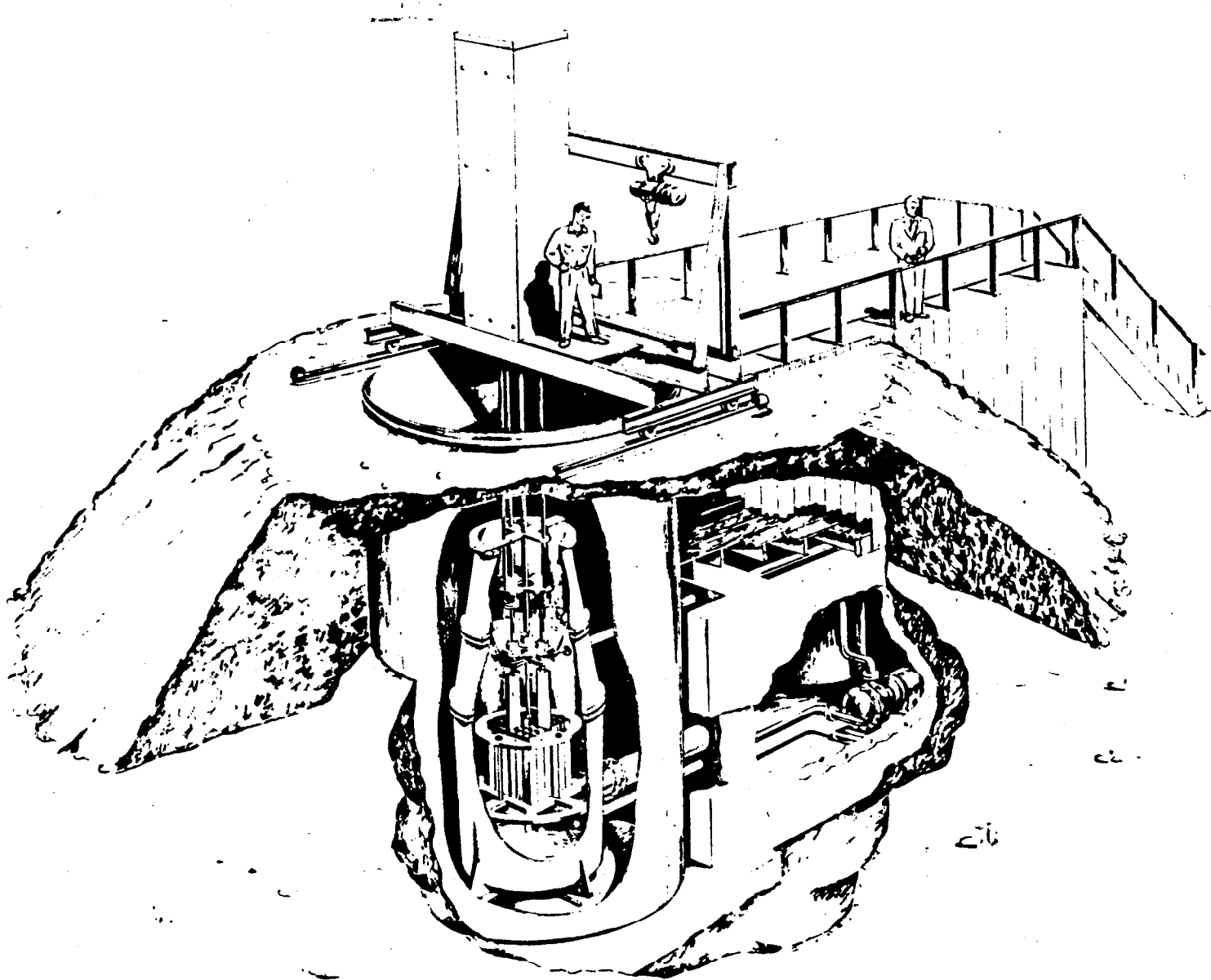


FIG. 74
 SATURATED STEAM FLOW
 THRU A SHARP EDGE ORIFICE
 $W = .0198 A(P)^{.91}$



★ U. S. GOVERNMENT PRINTING OFFICE: 1956 O-372346

FIG. 75
CUTAWAY DRAWING OF BORAX INSTALLATION